SolarDynamics LLC

Design Basis Document / Owner's Technical Specification for Nitrate Salt Systems in CSP Projects

DOE Grant Number: DE-EE0009810

Volume 3 - Narrative

Signatures:

	Name	Signature	Date
Prepared by	Bruce Kelly	Bruce Kelly	7/14/2025
Prepared by	Luca Imponenti	On file	7/14/2025
Checked by			
Approved by			

Rev.	Description	Signatures		
		Prepared	Approved	Date
A	Draft	BK	HP	3/22/2024
0	New text in: Section 2.2 Demonstration Facility Section 5.3.4 Leak Detection System Section 5.15.4 Subset of Creep Assessment in Weld Regions Section 5.16.3 Stress Relaxation Cracking in Type 316LNB with Lean Austenitic Weld Filler Section 5.15.6 Creep Assessment with Consideration of Residual Welding Stresses	BK, LI		7/14/2025

	Section 5.15.7 Relaxation of Residual Stresses Prior to Tank Commissioning Section 5.15.8 Required Relaxation of Residual Stresses to Achieve a 30-Year Creep Life Section 5.15.9 Code Interpretation of Residual Stresses Section 6.3 Salt-Side Pressure Relief Valves Section 6.7.3 Static Salt Mixers Section 8.5 Pipe Maintenance			

Table of Contents

List of Figures

List of Tables

1. Introduction, Report Format, Acknowledgements, and Disclaimer

1.1 Introduction

The work proposed concentrates on a Design Basis Documents / Owner's Technical Specification for parabolic trough and central receiver power plants using nitrate salt as the heat transport fluid and the thermal storage medium. The goals are to 1) distill the successful experience with nitrate salt systems from as many commercial projects as possible, 2) provide technical bases for equipment design/selection that an owner can impose on an EPC contractor, 3) compile this information in one location to provide guidance on salt systems that is as broadly applicable to as many projects as possible, and 4) work toward an industry consensus on a Design Basis Document.

1.2 Project Goal

The principal goal of the project is to develop a Design Basis Document for nitrate salt systems in CSP projects that reflects the lessons learned from earlier commercial projects. The document allows an owner to provide design guidance, and to impose a minimum set of requirements, above and beyond those in the normal Codes and Standards, on an EPC contractor in an effort to avoid a repeat of past mistakes. If successful, this would allow salt systems to achieve the same levels of reliability and availability as commercial parabolic trough plants using diphenyl oxide / biphenyl (i.e., Dowtherm A, Therminol VP-1) as the heat transfer fluid.

1.3 Report Format

The report consists of 3 volumes:

- Volume 1 - Specifications for Parabolic Trough Projects
- Volume 2 - Specifications for Central Receiver Projects
- Volume 3 - Narrative

Volumes 1 and 2 include discussions of the following topics:

- Plant functional requirements for the salt systems
- Plant operating states, and transitions between states, for the salt systems
- Risk analysis of the principal salt components

- Plant requirements for the salt systems to meet the functional and the operating requirements
- Type of specification for the principal salt components: functional; or prescriptive
- Current state of the art for salt systems.

Volume 3 discusses a number of cases in which the salt equipment at commercial parabolic trough and central receiver projects has not met the projected levels of reliability and availability. Possible reasons for the sources of the problems are discussed, as is a range of possible alternate designs that could avoid the known problems.

1.4 Acknowledgements

This material is based upon work supported by the U.S. Department of Energy's Office of Energy Efficiency and Renewable Energy (EERE) Solar Energy Technologies Office (SETO) submitted under DE-FOA-0002378 Topic Area 4a: CSP: PERFORM, Technical Specifications, Control No: 2378-1549, with Award Number DE-EE0009810.

The subrecipients on the project are the Electric Power Research Institute and Malta.

We would like to acknowledge the contributions provided by the following organizations for their review of the draft report: Alia Energy, Atlantica Yield, Contratos y Diseňos Industriales, Cerro Dominador, Crescent Dunes, Fichtner, High Temperature System Designs, National Renewable Energy Laboratory, Sandia National Laboratories, and Vast Energy. Finally, thanks to Shane Powers for his support and guidance on the project.

1.5 Disclaimer

2. Inorganic Heat Transport Fluids in Parabolic Trough Projects

2.1 Fluid Selection

A range of potential inorganic fluids can be considered as the working fluid, including the following:

- Binary, ternary, and quaternary nitrate salt mixtures
- Ternary nitrate / nitrite salt mixtures
- Quaternary nitrate / nitrite salt mixtures.

A review of the benefits and the liabilities of 6 candidate mixtures is presented in Section 10.3 of Volume 1 - Parabolic Trough Specifications.

The ideal salt would have 1) a high upper temperature limit in terms of thermal stability, 2) a low freezing point, 3) a high specific heat, and 4) be inexpensive. As one might expect, none of the candidate salts fulfills all of the ideal requirements.

As discussed in Section 10.3 of Volume 1, the mixture which best meets all of the requirements is the binary mixture of 60 weight percent sodium nitrate and 40 percent weight percent potassium nitrate. Although it has the highest melting point (a nominal 235 °C, depending on the mixture fractions and the nitrite concentration) of the candidate salts, the benefits of a high thermal stability and a low material cost typically offset the liability of a high cost for freeze protection system in the collector field.

2.2 Demonstration Facility

The German Aerospace Center and the University of Évora in Portugal operate a test facility for molten salt technologies near the city of Évora [1]. The platform has a parabolic trough solar field, a salt storage system, and a steam generator. The working fluid is the binary mixture of sodium nitrate and potassium nitrate.

In the solar field, HelioTrough 2.0 trough collectors form a circuit, that operates at outlet temperatures up to 565 °C. The collectors, with a total length of 684 meters, have a maximum thermal output of around 3.5 MWt.

The salt system comprises a hot and a cold storage tank, an underground dewatering tank, a salt melting system, in combination with pumps and valves to control the various operating modes.

[1] https://www.dlr.de/en/sf/research-and-transfer/research-infrastructure/evora-molten-salt-platform

The steam generator has a capacity of 1.8 MWt at 140 bar and 560 °C. Pressure and temperature reducing stations and an air-cooled condenser are installed instead of a steam turbine.

The focal points of the research include:

- Investigation of material wear due to corrosion and thermal cycles, and the evaluation of the thermal stability and the ageing of salt mixtures

- Demonstration of the reliability of critical components, such as flexible pipe connections in the solar field and the once-through steam generator

- Validation of the procedures to prevent salt freezing, to fill and drain the system, for blackout scenarios, and to remove blockages caused by freezing.

The technology demonstration characteristics of the work at Évora, together with the results of the salt component tests conducted by Solar Dynamics at Solar TAC [2], indicate that the use of nitrate salt as the working fluid in a commercial trough project is not imminent.

2.3 Temperature Control in the Collector Field During Non-Operating Periods

2.3.1 Introduction

Prior to filling with salt, the field piping, the receiver tubes, and the flex hose assemblies are preheated to a nominal temperature of 300 °C. This is to prevent thermally shocking the receiver tubes, and to prevent local freezing in the smaller lines. The field piping is preheated using the electric heat trace system (Section 2.3.2). The receiver tubes and the flex hose assemblies are preheated using a number of portable impedance heating systems (Section 2.3.3).

Once the system is filled, the primary means of temperature control is continuous circulation of cold salt during those periods in which the collector field is not in normal operation (Section 2.3.4).

Loss of Salt Circulation to the Solar Collector Assemblies

If salt circulation stops, then temperature control of the field piping is performed with the electric heat trace system. However, there is no permanent equipment to maintain control of the temperature of the receiver tubes and the flex hose assembles. Since it is not feasible to rapidly drain the equipment in the collector field (i.e., within hours), a loss of circulation necessarily results in salt freezing in the receiver

[2] Shininger, R. (Solar Dynamics, Broomfield, Colorado), SMART (Simplified Melting And Rotation-joint Technology) Final Report, DOE Contract DE-EE0008140, August 2022

tubes and in the flex hose assemblies. Conceptual methods to recover from freezing in the receiver tubes and in the flex hose assemblies is described in Section 2.3.6.

Loss of Site Electric Power to the Field Piping

At some point in the life of the project, electric power could be lost at the site. This could occur due to the simultaneous loss of imported electric power from the grid, the loss of emergency power from the standby Diesel generator, or the loss of the transformer supplying electric power to the emergency bus. Should this happen for a period of a few days, then salt will begin to freeze in the field piping. The process for recovering from freezing in the field piping is discussed in Section 2.3.8.

2.3.2 Heat Trace System

All of the fixed salt piping in the collector field will use electric heat tracing, for the following purposes:

- Preheating the equipment prior to filling with salt
- Temperature maintenance during periods when the salt is not circulating
- Freeze recovery.

The design of the heat trace system is identical to the systems described in Section 9.8 and Section 10.6 of Volume 1 - Parabolic Trough Specifications, and in Section 6.8 of Volume 3 - Central Receiver Specifications.

2.3.3 Impedance Heating System

Impedance heating system operates on "Joule heating," allowing electricity to flow through the pipe network, generating heat from the energy dissipated in the resistance of each component. The impedance heating system is intended for three primary functions:

1. Preheat a collector loop before initial filling with salt (in addition to subsequent filling operations following any maintenance tasks that require draining)
2. Freeze protection for a collector loop which has experienced a loss of flow
3. Freeze recovery of a collector loop which has experienced a loss of flow for an extended period.

The design of the impedance heating system is discussed in Section 10.9.2 of Volume 1, Specifications for Parabolic Trough Projects.

2.3.4 Continuous Salt Circulation

As with the Therminol in commercial trough projects, once the field piping and receiver tubes are filled, the system remains filled throughout the life of the project. This is the case because there is no on-site storage equipment with sufficient volume to hold the entire inventory of the working fluid.

It can be noted that the salt tanks in the storage system are in one of two conditions: one is empty, and the other is full; or both are partially filled. In principle, there is a large permanent volume to accept salt drained from the collector system. However, if collector system is being drained, then the temperature of the salt from the collector system is likely to be 'low'. Introducing low temperature salt into the hot tank, or transferring salt from the cold tank to the hot tank to make space available in the cold tank, has the potential to thermally shock, and permanently damage, the hot tank. As such, the volume available in the storage tanks is not available to drain the collector field.

The basis operating mode for the collector field is continuous circulation, for the following reasons:

- Since there are no provisions for draining the entire system, the principal means of freeze protection in the field piping and in the receiver tubes is continuous circulation during non-sunny periods [3]. Salt is circulated from the cold tank, through the collector field, and returned to the cold tank. Representative heat losses are on the order of 11 W/m^2 of collector aperture area.

- The inventory in the receiver tubes cools at a faster rate than the inventory in the field piping. Should the circulation stop for some period of time (say, hours), the temperature of the inventory in the field piping will be higher than the temperature of the inventory in the receiver tubes. When circulation resumes, there is the potential for thermally shocking the receiver tubes by introducing relatively warm salt from the field piping into the receiver tubes.

As such, the cold salt pumps must operate, essentially without interruption, for some 300,000 hours during the life of the project.

Thermal energy to compensate for the heat losses from the field piping and the receiver tubes is provided by the cold salt tank. If the temperature of the cold tank falls below a pre-determined value, then supplemental energy is supplied to the tank from external electric salt heaters. Electric power for the heaters is supplied from the grid, or should connection to the grid be lost, from standby Diesel generators.

[3] Salt can be drained from individual loops by 1) closing isolation valves at the ends of the loop, 2) connecting a vacuum tank, located on the bed of a truck, to one end of the loop, 3) opening a vent valve at the other end of the loop, and 4) pushing salt from the loop into the vacuum tank by means of air flowing into the vent valve. Salt can be returned to individual loops by 1) closing the vent valve, 2) connecting the loop to the vacuum tank, 3) drawing a vacuum in the loop, 4) opening a vent valve on the vacuum tank to push salt into the loop, and 5) opening the isolation valves at the ends of the loop to establish salt circulation.

2.3.5 Loss of Circulation Leading to Freezing in Receiver Tubes and Flex Hose Assemblies

In commercial projects, the reliability of the cold salt pumps, the electric salt heaters, and the standby Diesel generators is generally excellent, and the probability that continuous salt circulation can be maintained is regarded as high. Nonetheless, there are a number of conditions that could result in a loss of circulation, as follows:

- The switchgear supplying electric power to the cold salt pumps fails
- A crack develops, almost anywhere, in the headers of the field piping
- A defect in the insulation on the flex hose assemblies or the loop crossover piping leads to a frozen plug
- Salt isolation valves must be moved periodically to prevent sticking associated with corrosion. The isolation valve could move from open to closed, but then fails to re-open
- Operation of the salt pumps may require permissiveness from flow meters, pressure transmitters, or isolation valve positioners. If the signals from the flow meters, the pressure transmitters, or the valve positioners are lost, then the pump will trip. If it appears that repairs to the flow meters, pressure transmitters, or valve positioners will require a period that could challenge the freezing time of a receiver tube in the worst-case condition (broken glass envelope), then the DCS logic could be changed to bypass the permissive. At this time, the pumps could be restarted. However, having a qualified DCS engineer at the site to revise the logic is not a certainty, particularly at night, on the weekends, and during holiday periods
- The pumps develop a mechanical problem, such as a broken coupling, or there is a problem with the variable frequency drive for the motors
- An operator, in an attempt to reduce the auxiliary power demand of the salt circulation pumps, operates the pumps at too low of a flow (leading to overheating), too low of a speed (leading to vibration), or beyond the run-out point (leading to vibration). Overheating and vibration will damage a pump, which then requires the pump to be removed for repair.

It is difficult to quantify the above effects, but the probability that one of the above, or something similar to the above, will occur during the life of the plant is a value approaching 100 percent. Depending on the source of the problem, and depending on the number and the location of the isolation valves in the field piping, something in the range of $^{1}/_{16}$ to $^{16}/_{16}$ of the salt in the receiver tubes and flex hose assemblies could freeze.

2.3.6 Freeze Recovery in the Receiver Tubes and Flex Hose Assemblies

Impedance Heating of Receiver Tubes

Previous studies looking at impedance heating of molten salt parabolic trough plants considered power densities up to 250 W/m for freeze recovery of the solar field [4]. A recent set of computational fluid dynamics calculations of the melting process show a total melt time of 12.0 hours for heat collection elements in which the vacuum space is intact [5]. (Melt times for receiver tubes with a lost vacuum or a broken glass envelope are the subject of separate studies.) The difference in heat losses between the bellows and receiver tube results in an acceptable maximum difference in temperature of 12 °C along the length of the receiver. Finite element calculations from the same study show a heat input of 250 W/m produces stresses of 40 MPa in the receiver tube and 9.5 MPa in the glass envelope, which are well below the yield strength of the absorber tube (205 MPa) and the glass envelope (27 MPa), respectively. The calculated stress values noted above assume the salt is free to expand during melting, as noted in previous freeze-thaw tests [6].

Another recent study considers a reduced order modeling approach to model and optimize a freeze recovery system for a commercial molten salt parabolic trough plant. In this case, the impedance heating system is limited by the cost of electrical utilities required to switch the plant from a 240 MW source to a 150 MW sink [7]. Depending on the size of the project, the ambient conditions, and the capacities of the electric heating systems, the cost constraints resulted in estimated melt times for the entire solar field in the range of 100 to 300 days.

In order to avoid challenges with electrical infrastructure and reduce the capital cost of impedance heating systems for the plant, a mobile heating system has been proposed and evaluated [8]. The mobile concept can be completely housed in trailers that can be moved by vehicle, each trailer would have a diesel generator and several DC power supplies depending on the plant geometry. It is estimated such a mobile system could significantly reduce the capital cost compared to fixed impedance heating circuits permanently installed at every collector.

[4] D. Kearney, B. Kelly, and U. Herrmann, "Engineering aspects of a molten salt heat transfer fluid in a trough solar field," Energy, Vol. 29, No. 5-6, pp. 861-870, 2004
[5] Shininger, R., Imponenti, L., Kattke, K., and Marcotte, P. SMART: Simplified Melting And Rotation-joint Technology. United States: N. p., 2022. Web. doi:10.2172/1882508.
[6] G. Kolb, C. Ho, B. Iverson, T. Moss, and N. Siegel, "Freeze-thaw tests on trough receivers employing a molten salt working fluid", Proceedings of ASME Energy Sustainability, 2010
[7] C. Prieto, A. Rodríguez-Sánchez, F. J. Ruiz-Cabañas, and L. F. Cabeza, "Feasibility study of freeze recovery options in parabolic trough collector plants working with molten salt as heat transfer fluid," Energies, vol. 12, no. 12, 2019
[8] Shininger, Ryan, Imponenti, Luca, Kattke, Kyle, and Marcotte, Patrick. SMART: Simplified Melting And Rotation-joint Technology. United States: N. p., 2022. Web. doi:10.2172/1882508.

During freeze recovery, salt in the headers and the flex hose assemblies should be melted prior to solar heating of the receiver tubes to allow the salt to expand in the axial direction. In a commercial system, there are many factors that cause salt to melt unevenly in a receiver tube (damaged glass envelopes, lost vacuum, broken mirrors, etc.), so it is possible that sections of the solar field could experience constrained salt expansion during freeze recovery. Modeling this phenomenon is very difficult. In addition, the initial conditions after freezing, in terms of void space in the receiver tubes, are not necessarily known. For these reasons, any freeze recovery system will have to be demonstrated at full scale (i.e., a complete loop) before commercial application. To date, demonstrations of freeze protection using impedance heating have occurred with nitrate salts in 2-collector and loops operating with design temperatures of 500 °C [9], and freeze recovery has only been demonstrated on a smaller string of HCEs [3].

Solar Heating of Receiver Tubes

The solar heating method, or controllable solar flux heating, uses solar energy for freeze protection and recovery. Recent studies suggest it is possible to thaw frozen salt in the receiver tubes if the heat input is attenuated to reasonable levels [Imponenti et al, 2020]. One method to accomplish this is via a solar 'pass-through', i.e., cyclically moving the mirrors back and forth through the focal point of the collector. The heat input to the receiver tubes is adjusted by pausing the mirrors in the off-focus position before completing the next pass-through cycle. This method is attractive as it requires no additional hardware; however, additional testing is required before the technology can be considered commercially viable.

The main problems regarding solar heating involve local non-uniform heat inputs and losses from the following effects:

- Receiver tubes with lost vacuum or broken glass envelopes
- Non-illuminated portions of the receiver tubes at the end of a collector at low sun incidence angles
- Broken or missing mirrors.

Additional aspects include the time and the weather conditions required for a full freeze recovery, which may restrict the effectiveness to the summer months at many plant locations.
While modeling studies have shown the stress levels in the receiver tubes to be well below allowable values, no analyses have been performed on the collector drives to determine if the continuous back and forth motion effects the lifetime of this component.

[9] Gaggioli, W., Fabrizi, F., Rinaldi, L., D. Ascenzi, "Experimental tests about the cooling/freezing of the molten salts in the receiver tubes of a solar power plant with parabolic trough", AIP Conference Proceedings 1850, 2017

Since solar heating is only applicable for the illuminated portions of the receiver tubes, an impedance heating system will still be required for both the receiver tubes and the flex hose assemblies. Solar heating may be used to supplement the impedance heating systems, allowing capital and operational cost savings.

2.3.7 Loss of Site Electric Power Leading to Salt Freezing in the Field Piping

As noted above, salt freezing in the field piping requires the simultaneous loss of imported electric power from the grid and emergency power from the standby Diesel generator. The probability that both sources of electric power would be simultaneously lost is low. However, the project lenders will assign a non-zero probability to the condition, and the project will need to specify, and evaluate, a method for recovery.

2.3.8 Freeze Recovery in the Field Piping

Technical Considerations

In commercial solar projects, the electric heat tracing performs the following functions:

- Preheat an empty pipe from an initial temperature of about 25 °C to the required salt fill temperature of 275 °C. The preheat period, which determines the heat input to the pipe, ranges from 8 to perhaps 16 hours

- Once the pipe is filled, but there is no flow in the pipe, maintain the temperature of the line at a value of at least 275 °C to prevent freezing.

As one might imagine, the thermal input to the pipe to meet the preheat requirement can be fairly modest, as the thermal mass of the system is limited to the thermal mass of the metal, plus a nominal one-half of the thermal mass of the insulation. However, there will be instances in which the heat trace system will be required to thaw the salt in the field piping. In this case, the thermal mass of the system increases substantially; i.e., by the sum of the sensible heat required to increase the temperature of the salt from ambient to the melting point, plus the latent heat required to convert the solid salt to a liquid.

The time required to thaw a frozen line is a function of the diameter of the line. As the diameter of the line increases, the surface to volume ratio decreases, which generally increases the thawing period. In a commercial project, the largest line size is about DN 600 (24 in.). If the heat trace is designed to preheat an empty line in a period of 8 hours, then the required duty is a nominal 700 W/m. If the line, after filling, becomes frozen, then the time required to thaw the line is approximately 10 days.

If the heat trace system is operated with a duty cycle of 100 percent over a period of 10 days, then the pipe will reach a steady state temperature; in this case, a value of just over 600 °C. For a hot salt header, fabricated from stainless steel, this metal temperature is acceptable. However, for a cold salt header fabricated from carbon steel, the maximum metal temperature should be limited to 400 °C to prevent high metal corrosion rates. Doing so limits the allowable thermal input from the heat trace system to a nominal 400 W/m, which, in turn, increases the thawing period to about 20 days.

The 10 and 20 days thawing periods are based on 7 in. of calcium silicate insulation in an as-new condition. However, the quality of the insulation is expected to degrade over time due to 1) gaps developing in the insulation from daily thermal expansion and contraction cycles, 2) moisture intrusion, and 3) insulation compaction due to foot traffic. If the thermal conductivity of the insulation increases by 20 percent, then the thawing periods increase to about 12 days for the stainless steel lines and 24 days for the carbon steel lines.

A worst case condition be associated with local damage to the insulation which increased the thermal conductivity by a value of 50 percent. The damage could be due to personnel walking on the salt piping, incomplete repairs to the insulation, or salt leakage from a failed valve packing saturating the insulation. Should these conditions occur, the time to thaw a carbon steel header is on the order of 1 month.

As discussed in Section 6.4 (Risk Analysis) of Volume 1, Specification for Parabolic Trough Projects, the time to recover from a frozen collector field is in the range of 35 to 60 days. In practice, the time to recover may be longer, depending on the condition of the field piping insulation, the availability of the mobile impedance heating systems, and whether electric power to the field piping is interrupted during the freeze recovery process.

Financial Considerations

It is not unreasonable to expect that the first commercial projects will freeze salt in the collector field more often than expected, and the recovery times will be longer than expected. A potential, but not implausible, scenario might be one in which salt freezes in the field once in each of the first 5 years of commercial operation, and the recovery time in each case is 75 days. This would result in an availability in the first 5 years of commercial service of 70 to 75 percent, rather than the expected 90 percent. A worst case scenario might be on in which salt freezes twice in the first year of commercial service, and the recovery time in each case is 90 days. This would result in an availability of 50 percent in the first year of service.

Plant availabilities in this range, particularly early in the life of the project, will have a noticeable, and detrimental, effect on the return on investment to the equity providers. In principle, the equity providers can compensate for the availability risks by increasing the return on investment. However, this will increase the levelized cost of energy. At some point, the risk premium for the use of an inorganic heat transfer fluid will offset the benefits of using an inorganic fluid; i.e., a reduction in the unit cost of the storage system, and an increase in the gross Rankine cycle efficiency. The economics of a plant using an inorganic fluid may essentially be a on par with the economics of a plant using Therminol as the working fluid. In this case, the investment community would, in their own interests, continue with the current state of the art in trough technology, and the commercial potential of the advanced working fluid may not be realized.

3. Oil-to-Salt Heat Exchangers in Parabolic Trough Projects

3.1 Configuration

Shell and Tube

The industry has generally adopted shell-and-tube heat exchangers for oil-to-salt heat exchangers. The designs include 1) fixed tubesheet with U-tube bundles, 2) floating tubesheet with straight-tube bundles, and 3) header/coil arrangements with circular tubesheets.

The combination of the heat transfer properties of salt and the optimum approach temperatures require long heating lengths, which, in turn, often results in 3 to 6 heat exchangers in series. For the heat exchangers at the low temperature end of the series, the shell and tube materials can be carbon steel. For the heat exchangers at the high temperature end of the series, the tubes are stainless steel to provide the required corrosion resistance to the chlorides in the salt.

Flat Plate

Rather than shell and tube designs, two commercial projects selected a flat plate design. Stainless steel plates are stamped to provide the desired flow pattern. A group of plates are stacked, and then seal welded at the edges. Distribution boxes at each end of the exchanger align the salt flow and the oil flow in alternating, counterflow layers. An external steel box frame provides the required resistance to bowing of the plates generated by the fluid pressures.

The design offers a favorable combination a large heat transfer area in a small footprint, and low pressure drops on both the oil- and salt-sides. The principal liability is a significant difference in the low thermal inertia of the plates, and the relatively high thermal inertias of the perimeter plate welds and the external frame. To limit the stresses in the transitions between the thin metal sections and the thick metal sections, the allowable rate of temperature change is typically restricted to values (~ 1.5 to 2 °C/min) which are lower than values for shell and tube designs (~ 10 °C/min). Unfortunately, a rate of 2 °C/min is impractically restrictive for equipment that receives heat directly from the solar field. In commercial service, the heat exchangers developed cracks after only a few years in operation. The cracks allowed Therminol, at a pressure of 10 bar, to leak into the salt side, at a pressure of perhaps 2 bar. A pressure of 2 bar is less than the vapor pressure of Therminol at the design temperature. As a result, the Therminol flashes on the salt-side of the heat exchangers, carrying Therminol vapor into the ullage space of the storage tanks. Some of the Therminol eventually makes its way to the atmosphere, which represents both an emissions problem and a financial penalty to replace the lost Therminol.

On a point related to the leaks, it is difficult to access the portions of the heat exchangers where the cracks develop. The experience with leak repair has been decidedly mixed, and in some cases, the only method to repair the leak is to replace the heat exchanger.

3.2 Equipment Location

The heat exchangers are large and heavy pieces of equipment. The lowest cost approach to supporting the equipment is to place the heat exchangers at grade. However, commercial projects have located the equipment in one of the following two locations:

- On an elevated platform between the storage tanks, with a height slightly above the mid-point of the wall height of the tank

- On an elevated platform between the tanks, at a height above the top of the wall of the tanks.

These approaches are not inexpensive, as 1 to 1.5 kg of structural steel are required to support each kg of equipment. In addition, the wind loads on an elevated structure translate to higher foundation costs. Nonetheless, the benefits associated with elevating the equipment are judged to outweigh the costs, for the following reasons:

- With the heat exchangers located at grade, a drain tank, located below grade, is required. The drain tank requires a pit, electric heat tracing, thermal insulation, a range of instruments, and two drain pumps. This approach will incur a cost (but it will be less than the cost of an elevated structure)

- The drain pumps in the drain tank will have a certain capacity, which in turn, defines the time required to drain the heat exchangers. If the heat exchangers must be drained quickly in an emergency, then the drain pumps may not have the desired capacity unless large, and expensive, pumps are initially selected

- If the height of the elevated platform is at least the height of the mid-point of the tank walls, then the heat exchangers can be drained by opening a valve to the tank with the lowest inventory level. This passive drain approach is more reliable, and has a higher availability, than the active drain method associated with a drain tank and drain pumps. It can be noted that the mass of salt in the heat exchangers and in the associated piping is 'small' relative to the mass of salt in a storage tank, even with the tank at the minimum level. Assuming that adequate mixing occurs between the inventory in the tank and the salt entering the tank, then the thermal transient experienced by the tank during a drain sequence will be well within the limits set by the tank supplier.

- Most importantly, the heat exchangers, at some point in the life of the project, will need to be drained for inspection and maintenance. If the heat exchangers are located above the storage tanks, then there is no method by which salt can enter the heat exchangers after the equipment has been drained, and expose the maintenance personnel to potential harm. Similarly, if the heat exchangers are located at the mid-point of the tank wall height, and if the inventory levels in both tanks are set the same, then there is no method for salt to enter the heat exchangers. This is a subtle point regarding safety. There have been instances in which pipes were allowed to cool to ambient temperature, forming frozen plugs in the lines. The project staff knew, with certainty, that there was no danger to the personnel working downstream of the frozen equipment. In separate cases, the frozen plugs thawed, resulting in severe injury in one case and death in a second. Locating the equipment on an elevated platform is, in effect, a form of insurance. And like all insurance, it is a complete waste of money, until it is needed.

4. Salt Tanks in Parabolic Trough Projects

4.1 Material Selection

A range of corrosion studies have shown acceptable corrosion characteristics of carbon steel, at temperatures up to 400 °C, with chloride contents up to 0.6 percent [10,11]. As a result, all commercial parabolic trough projects fabricate the cold tank and the hot tank from carbon steel.

4.2 Corrosion Characteristics

At least one commercial project has experienced problems with significant corrosion in the salt tanks. The repairs involved suspending the tank on external supports, and replacing a portion of the bottom course in the tank wall.

An examination of the sections removed showed evidence of stress corrosion cracking. This form of corrosion is different than the uniform surface corrosion processes observed in the Abengoa and the Sandia studies.

Stress corrosion cracking is a combined mechanical and electro-chemical corrosion process which results in cracking of certain materials [12]. The mechanism is not simply an overlapping of corrosion and mechanical stresses, but an auto-catalytic, self-accelerating process leading to high metal dissolution rates. The process includes an oxidation reaction:

$$Fe \rightarrow Fe^{++} + 2\ e^-$$

The oxidation reaction is accompanied by a reduction reaction, typically involving the oxygen and water:

$$O_2 + 2\ H_2O + 4\ e^- \rightarrow 4\ OH^-$$

Further reactions can then occur, including:

$$Fe^{++} + 2\ OH^- \rightarrow Fe(OH)_2$$

$$2\ Fe(OH)_2 + H_2O + ½\ O_2 = 2\ Fe(OH)_3$$

[10] Sanchez, L., and Madina, V. (Abengoa Solar NT, Sevilla, Spain), 'Estudio de corrosion del acero A516Gr70 en tanques piloto. Tiemp 1', Documento 12-0106-IN-641-000, July 2009

[11] Bradshaw, R. W., and Clift, W. M. (Sandia National Laboratories, Livermore, California), 'Effect of Chloride Content of Molten Nitrate Salt on Corrosion of A516 Carbon Steel', Sandia Report SAND2010-7594, November 2010

[12] Corrosion in Carbon Steels – IspatGuru

The hydrated oxides can lose water during dry periods, and revert to anhydrous oxides, including ferrous oxide (FeO) and ferric oxide (Fe_2O_3, hematite).

Initially, a small pit is formed at the surface, and develops into a crack due to applied or residual stresses in the material. The crack formation opens up a new active (non-passive) metal surface, which corrodes very easily. This leads to further crack propagation and exposure of new highly active metal surfaces in the crack. Metal dissolution in the crack advances rapidly until mechanical failure occurs. Brittle failure can occur in normally ductile metals at stress levels which are less than the yield strength. Internal stresses in a material can be sufficient to initiate an attack of stress corrosion cracking.

Stress corrosion cracking of carbon steel is rare compared with stress corrosion cracking of stainless steel. One potential source of cracking in carbon steel is the exposure of the metal to liquid water in the presence of nitrates. One hypothetical failure mechanism is as follows:

- The outside of the tank is exposed to nitrate salt. The source of the salt could be 1) vapor condensation from ullage gases passing through a vacuum / pressure relief valve, or 2) salt leakage from pumps, valves, instruments, or piping above the tanks

- Water comes into contact with the outside of the tank. The source of the water could be 1) site flooding during a particularly heavy rain, 2) rainwater entering gaps in the tank insulation, or 3) maintenance personnel using wash water to remove the salt

- As noted above, process conditions (i.e., hydrostatic loads) can produce stresses, which are 1) within the ASME allowable values, but 2) high enough to initiate cracking. Additional stresses can be generated should water come into contact with the tank. Heat transfer will produce local temperature gradients, which, in turn, can generate local thermal stresses. Temperature gradients on the order of 45 °C can produce stresses equal to the ASME allowable value, and a gradient of approximately 115 °C can cause the material to yield.

Should the above combination of conditions occur, then a failure due to stress corrosion cracking may be the result.

To limit the potential for stress corrosion cracking, the following approaches can be adopted:

- If frozen salt is to be removed from the metal, methods should be limited to mechanical abrasion or media blasting

- To prevent runoff, following heavy rains, from coming into contact with the bottom of the tank, a comprehensive drainage system can be provided. Alternately, the tanks can be elevated above grade; however, this approach can be more expensive than a drainage system.

- Ensure that the metal jacket covering the insulation is always free of gaps and defects

- To the extent possible, locate equipment, such as pumps, valves, instruments, and fittings, away from the top of the tank

- Substitute a ferritic material, such as 2¼ Cr - 1 Mo, for the carbon steel. The chromium offers a more robust surface passivation layer than can be provided by carbon steel, and the absence of nickel in the alloy limits the potential for stress corrosion cracking. It can be noted that 1) the reliability of salt tanks fabricated from carbon steel has been excellent, and 2) the occurrences of stress corrosion cracking in carbon steel are rare, and the sources of the corrosion are both understood and preventable. Selecting a ferritic material would only apply to rare cases where carbon steel would be routinely, and unavoidably, exposed to combinations of salt and liquid water.

4.3 Survival Hypothesis for Carbon Steel Tanks

The cold tanks in central receiver projects, and the hot and the cold tanks in parabolic trough projects, are fabricated from carbon steel. Known failures in carbon steel tanks include weld defects (1 tank) and stress corrosion cracking from water/salt mixtures on the tank exterior (several tanks). However, in contrast to stainless steel tanks, there have been no known failures due to leaks in the floor.

The similarities between carbon steel tanks, and the stainless steel hot salt tanks in central receiver projects, are numerous. The common features include the following:

- The system geometries are essentially identical: flat bottom tank with a self-supporting domed roof; insulated foundation with cooling air passages; and inlet salt flow distribution by means of a distribution ring header

- The floors consist of a staggered array of thin (7 to 8 mm) rectangular plates. The plates are connected to one another by butt welds. The floor deforms during the welding process, producing an array of shallow domes

- Prior to filling with salt, the tanks are preheated using combustion gases. Less-than-perfect control over the flow distribution of the combustion gases can produce radial temperature gradients in the floor, which are of sufficient magnitude to potentially buckle the floor

- When the tank is filled, hydrostatic forces push the floor flat against the foundation

- Residual stresses due to welding and floor deformations tend to persist; i.e., stress relaxation is moderate due to the low operating temperatures

- Radial temperature gradients are an inherent characteristic of the tank and the foundation design, and the gradients have the potential to damage the floor

- Daily reversals in floor friction forces, due to daily thermal cycles, are also an inherent characteristic, and have the potential to damage the floor.

Nonetheless, there are important differences with the hot salt tanks in projects operating at design temperatures above 500 °C, as follows:

- The coefficient of thermal expansion for carbon steel (11 to 12 10^{-6} /°C) is approximately 70 percent of the coefficient of expansion for stainless steel (16 to 17 10^{-6} /°C). For a given temperature differential, the thermal stresses due to self-restraint in a carbon steel tank are about 30 percent lower than the thermal stress due to self-restraint in a stainless steel tank. This characteristic is important in reducing the effects of radial temperature gradients in the floor

- The thermal conductivity of carbon steel (40 to 45 W/m-°C) is at least a factor of 2 higher than the thermal conductivity of stainless steel (15 to 20 W/m-°C). The higher conductivity has a second-order, but useful, effect in terms of reducing thermal stresses during transient conditions

- For carbon steel, at 370 °C, the stress amplitude associated with a fatigue life of 40,000 cycles is 209 MPa. For stainless steel, at 540 °C, the stress amplitude associated with a fatigue life of 40,000 cycles, is 159 MPa. For a given stress amplitude, carbon steel accumulates fatigue damage at a lower rate than stainless steel

- In a central receiver project, during transient conditions, the salt flow enters the cold tank at a temperature that is higher than the bulk inventory. Due to density differences, the incoming flow rises, rather than sinks. This reduces the potential for local temperature gradients in the floor, and the associated thermal stresses

- The temperature gradients in the tank are a function of the inventory temperature, the thermal resistance of the insulation, and the degree to which the properties of the insulation have degraded over time. In a parabolic trough project, the inventory temperature in the hot tank is approximately 180 °C lower than the inventory temperature in the hot tank of a central receiver project. The lower temperatures reduce the potential to produce large temperature gradients, and thereby large thermal stresses, in the tank, particularly in cases in which the insulation has degraded or been subject to mechanical damage.

- The response time of the collector field in a trough project is longer than the response time of the heliostat field / receiver in a central receiver project. As such, the rates of temperature change in the hot tank of a trough project are relatively slow. This reduces the potential for non-isotropic temperatures in the bulk inventory, and reduces the magnitude of intra-tank thermal stresses due to self-restraint

- Both the cold tank and the hot tank in parabolic trough plants operate at temperatures below which creep damage can start to develop. The opposite applies to the hot tanks in central receiver projects

- The niobium in Type 347H generates niobium carbonitrides. The non-uniform precipitation of the carbonitrides, as discussed in Section 5.16.2, leads to non-uniform strength distributions, stain localization, internal cracks, internal voids, and eventually external cracks. The precipitation characteristics are the most pronounced in areas of high strains; i.e., the tops of buckles. The floors in carbon steel tanks likely experience similar deformations and areas of high strains. However, unlike Type 347H stainless steel, the strength and the ductility of carbon steel do not decay over time.

In general, if a carbon steel tank can survive the first 3 years of service, then it is likely to survive the full 30 years.

5. Hot Salt Tanks in Central Receiver Projects

5.1 Representative Commercial Design

5.1.1 Tank

A representative storage quantity for a commercial project is 30,000 to 40,000 metric tons of salt. Since the salt has an extremely low vapor pressure (< 1 kPa at 600 °C), the lowest cost storage approach is a vertical tank with a flat bottom and a self-supporting roof. Due to the chemical stability of the salt, the tank can be vented directly to the atmosphere.

Design standards for this type of tank, operating at temperatures up to 600 °C, have yet to be developed. In the interim, the closest design standard is American Petroleum Institute Standard 650, Welded Tanks for Oil Storage. However, the Standard only considers operating temperatures up to 260 °C, and low cycle fatigue conditions are not part of the Standard. As a result, a hybrid design approach has typically been adopted, as follows:

- For design temperatures above 260 °C, allowable material stresses are derived from Section II of the ASME Code
- For the evaluation of low cycle fatigue, the methods described in Section VIII, Division 2, of the Code are often adopted.

It can be noted that, in some project jurisdictions, an evaluation of the fatigue life using Section VIII Division 2 is not required. However, this can present a substantial risk to the project in terms of the reliability of the storage system. A discussion of the recommended design codes is presented in Section 5.14.1.

For design temperatures above 538 °C, the H grades of stainless steel, with a minimum carbon content of 0.04 percent, are required by the ASME Code. Candidate materials include Type 304H, Type 316H, and Type 347H stainless steel. At the 10 MWe Solar Two demonstration project, the hot tank was fabricated from Type 304H [13]. However, to avoid potential problems with intergranular stress corrosion cracking, the solar industry has adopted Type 347H, a stabilized stainless steel, in the current generation of projects.

5.1.2 Foundation

The foundation consists of the following elements, moving from the top down:

[13] Pacheco, James (Sandia National Laboratories, Albuquerque, New Mexico), 'Final Test and Evaluation Results from the Solar Two Project', Sandia report SAND2002-0120, January 2002

- A layer of solid lubricant; candidate materials include sand, perlite, and calcium silicate
- The primary tank support / insulating layer under the floor. Candidate materials include expanded clay, expanded glass, and refractory bricks
- A concrete base mat below the insulating layer
- A concrete ring wall to retain the insulating layer underneath the tank.

The foundation base mat has a series of cooling air pipes embedded in the concrete. Air flow in the cooling passages is established by fans or by natural convection. The air flow rate is set to maintain the soil temperature, directly beneath the foundation base mat, at values no higher than 75 °C. The goal is to limit the desiccation of the soil, and the oxidation of organic materials, to values that prevent unpredictable settlements of the tank.

5.2 Failure Patterns

The number of commercial central receiver projects in service, excluding those in China, is six: Gemasolar, Cerro Dominador, Crescent Dunes, Noor III, Redstone, and Noor Energy 1. The first four plants have been in service for some number of years, and the last two have recently entered service.

Among the first four, the hot salt tank at Gemasolar has failed, and a replacement tank has been built alongside the first tank. Also, the hot salt tank at Crescent Dunes has developed leaks in the floor on three occasions, and problems have developed with two other projects. For the plants which have been in service for more than 1 year, the failure rate, for all intents and purposes, is essentially 100 percent. Given the limited number of commercial projects the failure rate of hot salt tanks is not commercially sustainable.

With the limited number of cases, it is difficult to define a generic or a typical failure mechanism. Nonetheless, all of the tanks share a common set of characteristics which, when combined, are potential sources of future problems. The common design and operating characteristics include the following:

- The floor is fabricated from an array of rectangular plates. Welding the plates to one another generates residual welding stresses which are equal to, or higher, than the yield stress (see Section 5.5). Weld shrinkage establishes tensile stresses at the top of the plates, which are balanced by compressive stresses at the bottom of the plates. The stresses cause the plates to bow upward at the center, and the plates take on the shape of a shallow dome. The height of the dome is in the range of 50 to 150 mm. It can be noted that the floor is a large, thin sheet. The sheet, having been deformed by the welding process, has a low structural stability in terms of its ability to tolerate compressive stresses

- The tank is filled with water for the hydraulic tests. When the hydrostatic pressure reaches a value of about 7 kPa (approximately 1 m of water), the plates are pushed flat against the foundation (see Section 5.6). Changing the shape of the plates from domed to flat generates compressive stresses at the edge of the plates that are at, or above, the yield stress. When the water is removed at the end of the hydraulic tests, the plates revert from flat back toward the original domed shapes. However, the residual stresses and the shape of the floor after the hydraulic tests will be different than the residual stresses and the shape of the floor before the hydraulic tests

- Radial temperature gradients in the floor are an inherent characteristic of a flat bottom tank on an insulated foundation (See Section 5.7). Specifically, the conduction heat transfer into the foundation near the center of the tank is 'low' due to the long conduction heat path from the center of the foundation to the ambient. In contrast, the conduction heat transfer into the foundation, and to environment, near the perimeter of the tank is 'higher' due to the relatively short conduction heat paths to the ambient. A radial temperature gradient establishes a combination of radial and tangential stresses in the floor. At some value for the gradient (yet to be defined, but perhaps 30 to 40 °C), the combination of radial and tangential stresses can reach the yield value near the center, and at the perimeter, of the tank

- The tank is preheated using combustion gases from a fired air heater (see Section 5.8). The gas flow patterns inside the tank are determined by the arrangement of the inlet duct and the outlet chimney. However, high temperature air is a relatively poor mechanism for convection heat transfer, and the uniformity of the gas flow pattern inside the tank is determined by the sophistication of the duct and chimney arrangement. Further, the thermal inertia of the floor is lower than the thermal inertia of the wall, and the thermal inertia of the floor is several orders of magnitude lower than the thermal inertia of the foundation. This combination of features has the potential to establish radial temperature gradients in the floor which are high enough to establish compressive stresses at, and above, the yield point. Should this happen, the floor, due to its low structural stability in compression, has the potential to develop further deformations. Preliminary finite element calculations show that the floor can develop a set of orthogonal buckles, which span the diameter of the tank, during the preheating process

- Three items can be noted regarding a finite elements analysis of the floor after the preheating process:
    - Static analyses will not reproduce the buckles seen in the floor; a quasi-static or a dynamic analysis is needed
    - The shape and the dimensions of the buckles are highly influenced by the shape and the dimensions of the initial deformations produced during welding and following the hydraulic tests

  - The deformations produced in the floor during welding, and the associated residual stresses, vary across the floor. The characteristics follow a statistical pattern, but they also contain random elements. Since the shape and the dimensions of the buckles are a function of the welding deformations and the residual stresses, the characteristics of the buckles (length, height, width, residual stress, and residual strain) also contain random elements. As such, developing a generic, or a typical, analysis predicting the creep-fatigue properties of the buckled regions is difficult. Nonetheless, it is possible to state that the creep-fatigue life of the buckled regions will be considerably less than the life of the project.

- When the tank is filled with salt, hydrostatic loads are sufficient to push the plates down flat against the foundation (see Section 5.9) for a second time. This removes the domed deformations that exist after the hydraulic tests (but does not remove any buckles which may have formed during the hydrostatic tests and the preheating process). When the plates transition from a domed shape to a flat shape, the edges of the plates are again placed into compression. The radial stiffness of the wall is several orders of magnitude greater than the radial stiffness of the floor, and some fraction of the compressive loads on the plates can be translated into additional deformations at the buckles, if present

- The rectangular plates used to fabricate the floor do not all have the same dimensions, the plates are not perfectly square, and the plates have some level of curvature. To accommodate the variations in the horizontal and the vertical gaps between plates, weld backing strips are typically used. The backing plates are intentionally welded to the bottom of the floor, and become a permanent feature of the tank. When the tank is heated from ambient to the design temperature for the first time, the backing strips push the sand in the top layer of the foundation toward the edge of the tank. This leads to 1) local portions of the floor which are unsupported, which generates bending stresses in the floor, and 2) local variations in the friction forces generated between the floor and the foundation

- After the tank enters commercial service, the temperature of the inventory increases during the day, and decreases during the evening and during shutdown periods. The thermal expansion and contraction of the tank generates friction forces on the floor, and these forces oscillate between compression and tension (see Section 5.10). Under certain conditions, the tank can be close to full and the temperature of the inventory can increase. The calculated compression stresses near the center of the tank can exceed the yield value. This, in turn, can produce additional plastic deformations, particularly if the displacements occur near buckles in the floor. The difficulty of analyzing this effect is compounded by the non-uniform distribution of friction resulting from the use of weld backing strips

- The flow entering the tank is mixed with the bulk inventory by means of a distribution header located about 1 m above the floor (see Sections 5.11 and 5.12). However, the distance between the center of the tank and the distribution header, and the distance between the distribution header and the wall of the tank, is on the order of 8 to 12 m. As such, non-isotropic temperature distributions in the inventory, on the time scale of minutes, can develop during transient conditions. Further, daily transient conditions (i.e., receiver startup) consist of relatively cold salt entering the hot tank. The difference in temperature between the salt entering the tank and the bulk inventory is ideally small (< 10 °C). However, depending on decisions made by the operator, the difference can be as large as 100 °C. Under these conditions, cold salt will descend toward the floor due to density differences, which, in turn, can lead to local depressions in the temperature of the floor. Local variations in temperature on the order of 40 °C can generate thermal stresses at, or above, the yield point. The associated strains can add to, or subtract from, the strains already present in the floor

- The commercial hot salt tanks built to date use Type 347H stainless steel. This material is a stabilized stainless steel, which provides additional resistance to intergranular stress corrosion cracking compared to the H grades of Type 304 and Type 316. The stabilizing element added to the alloy is niobium. However, thermodynamic considerations lead to the precipitation of niobium carbonitrides (see Section 5.16.2). Within the grain boundaries, a fine-grained precipitate of niobium carbonitride forms; at the grain boundaries, a coarse-grained precipitate is formed. On a time scale of years, a precipitate-free zone can develop between the grain boundaries. The strength of the coarse-grained precipitate is lower than the strength of the fine-grained precipitate, and the strength in the precipitate-free zone is lower still. When the material is subjected to tensile stresses, the material develops strains, but the strains are concentrated in the area with the lowest strength (precipitate-free zones). This leads to internal cracking, micro-void formation, or a combination of the two. The defects eventually progress to the exterior. The process is known as stress relaxation cracking, and it is accelerated by temperature and strain

- Any section of the floor which has buckled is a region of high strain, with the highest strains occurring at the top of the buckle. The strains at these locations are also influenced by friction forces between the floor and the foundation. The friction forces, which are highest near the center and at the perimeter of the tank, reverse direction daily due to the cyclic thermal expansion and contraction of the tank

- Stress relaxation cracking will proceed most quickly in the regions of the highest strains; i.e., the tops of the buckles. Further, these sections of the tank are 1) subjected to cyclic loading, and 2) the fatigue life of material subjected to previous plastic strains is generally quite low. As such, the area of the tank most prone to failure, through a combination of stress relaxation cracking and low cycle fatigue, is the top of the buckles near the center of the tank. It can be noted that the cracks seen to date in the floors of commercial tanks have occurred at this location.

5.3 Consequences of a Leak in the Floor

Salt has a low surface tension, and as such, it is an effective wetting agent. Expanded clay is an effective thermal insulation due to its large number of extremely small internal cavities. These material characteristics lead to a situation in which salt, when in contact with clay, fills the internal cavities with salt. The saturation process requires a period of days to weeks; however, once the clay is saturated, there is no practical mechanism for removing the salt from the clay.

5.3.1 Heat Losses

The thermal conductivity of salt (0.55 W/m-°C) is about 2.5 times the thermal conductivity of expanded clay (0.22 W/m-°C). As such, exposing the clay to salt increases the thermal conductivity of the clay, with the increase a function of the degree of saturation. However, there are little, and often conflicting, data on the increase. A representative value for the increase is on the order of 1.5.

If exposure of the expanded clay to salt increases in the thermal conductivity of the foundation insulation by a factor of 1.5, then the heat transfer through the foundation will increase by a similar factor. As a consequence, the temperature of the soil can rise above the design value of 75 °C. To limit the possibility of unpredictable tank settlements, the capacity of the foundation cooling fans will need to be increased. If higher fan capacities are insufficient to maintain soil temperatures below 75 °C, air chillers can be added at the inlet to the cooling fans.

5.3.2 Floor Stresses

As discussed in Section 5.7, even moderate radial temperature gradients in the floor can produce stresses at, or above, the allowable values in Section II of the ASME Code.

Should the tank develop a leak, the heat flux into the foundation will increase. An increase in the heat flux will change the radial temperature gradient in the floor. This, in turn, has the potential to either decrease or increase the radial and tangential stresses in the floor. Further, the distribution of the salt in the foundation may be random and change over time. As a result, the heat flux into the foundation, the temperature distribution in the floor, and the stress distribution in the floor could also be random and change over time. As such, the potential exists for new, and unexpected, radial and circumferential temperature distributions to develop in the floor.

In principle, an estimate could be made of the changes in the stress distribution in the floor due to a leak if the radial and the circumferential temperature distributions in the floor were known. However, there are typically a limited number of thermocouples installed on the floor; perhaps 8 to 12. This number of temperature readings may not be enough to accurately predict a stress distribution in the floor. If so, it may not be possible to estimate the potential for plastic collapse, or the remaining creep and fatigue life, of the floor. The Owner may decide that the risks associated with this situation are not acceptable. Unfortunately, the only solution is to remove the foundation material exposed to salt, and replace with foundation with new material. However, due to the size of the tank, replacing the foundation requires that the floor be removed, the tank elevated by means of a jacking system, the foundation excavated, and the floor replaced with a new floor.

5.3.3 NOx Production

A more significant problem is the chemical reaction of expanded clay with salt. Nitrate salt is an oxidizing agent. The expanded clay, during its production, is fired at temperatures high enough to form an oxide. However, one oxide species can react with an oxidizing agent to form another oxide species. At the temperatures seen in the foundation of a hot tank, clay can undergo the second oxidation step. The oxidation is accompanied by a series of reduction reaction in the salt, as follows:

$$NO_3^- \rightarrow NO_2^- + \frac{1}{2} O_2$$
$$NO_2^- \rightarrow NO + O^-$$

The NO leaves the clay in the form of a gas, and, upon exposure to the atmosphere, can react with oxygen to form NO_2.

The oxidation / reduction reactions are not particularly fast. However, due to the large quantities of clay in a tank foundation, and due to the large surface-to-volume ratios inside the clay structure, the NOx emitted from a foundation can be on the order of kg/day. Emission rates this high can present a health hazard to maintenance personnel, and may cause the project to exceed allowable emissions. Further, the NOx production should, in principle, continue until either all of the clay has been oxidized to its new oxidation state, or all of the salt has been reduced to NOx. Given the dimensions of the foundation in a commercial plant, this process could involve decades.

5.3.4 Leak Detection System

Identification of Leak Location

At the Solar Two demonstration project, the perimeter of the foundation used hard refractory bricks to support the concentrated load of the roof and the wall. However, the strength of the selected refractory would be reduced if the bricks were exposed to nitrate salt. To help ensure the integrity of the foundation following a leak, a continuous metal sheet was installed between the solid sand lubricant and the refractory. A leak would percolate horizontally through the sand layer, and then fall onto the soil outside of the foundation.

As might be imagined, a leak would percolate through the sand in essentially all directions, and the point on the soil where the leak accumulated may not be a good indication of the radial location of the leak. To help identify the source of the leak, an array of collection troughs or channels could be located at the top of the foundation.

One potential arrangement is an array of orthogonal channels. The channels would slope down from the center of the foundation to the perimeter; i.e., similar to that of the floor. A leak would flow primarily into 2 channels, and cross-correlating the positions on the perimeter where the leak appeared would provide an indication of the leak in the floor.

A second potential arrangement is an array of radial and tangential channels. A leak entering a radial channel would be directed to the perimeter of the foundation. However, some portion of the leak could enter a tangential channel, and then flow to one or more of the associated radial channels. This collection arrangement would provide information on the circumferential location of the leak, but only limited information on the radial location.

It should be noted that the effectiveness of the leak detection system requires that the foundation directly beneath the floor be as impervious to salt as possible. Specifically, if the material beneath the floor is pervious (i.e., sand), then the leak would flow horizontally as well vertically, and the leak would not be confined to only one or two channels. This, in turn, implies the following:

- The material at the top of the foundation is either a metal slide plate or a hard refractory

- If the material is a refractory, then the selected material must be chemically and structurally stable if exposed to salt. In addition, the coefficient of friction between the floor and the refractory will be different, and perhaps higher, than the coefficient of friction between steel and sand

- If the material is a metal plate, then the following applies:
    - The selected plate material must be resistant to galling with the stainless steel floor in the hot tank
    - A common approach to welding the floor is to tack weld a backing strip along the bottom edge of a plate, locate the adjacent plate, and perform a root pass in the space defined by the edges of the adjacent plates and the backing plate. The backing plate will be lower than the bottom of the floor; however, space for the backing plate is provided by movement of the sand beneath the floor. In contrast, with a metal plate beneath the floor, backing strips can no longer be used. This may require modifications to the floor welding procedure to ensure that the root pass only fuses with the floor plates and not with the plate beneath the tank
    - The floor, after welding, will have depressed sections at the weld seams and elevated sections near the centers of the plates. This will produce non-uniform contact between

the floor and the slide plate, which will produce 1) regions of locally high friction forces, and 2) friction forces which vary radially and tangentially in a non-uniform manner. To what extent this influences the stresses in the floor, and the consequent effect on the creep lifetime, will require FEA analyses

- After the tank enters commercial service, the residual welding stresses in the floor will start to relax. The will change the dimensions of the depressed and the elevated sections, which will change the distribution of the friction forces between the floor and the sliding plate.

Isolation of Foundation Insulation

Even if the collection channels can provide only a qualitative location of a leak, the collection equipment provides an important secondary function. Specifically, some fraction, and perhaps a majority, of the leak will be captured by the collection system. This will reduce the net flow rate of salt into the foundation insulation, which will 1) provide the operators with additional time to drain the tank, and 2) reduce the increase in the heat losses through the foundation due to adding salt (with a relatively high conductivity) to the foundation insulation (with a relatively low conductivity).

5.4 Foundation Perimeter Stiffness

The vertical loads on the foundation are a function of the radial location in the foundation. The highest loads occur at the perimeter of the tank, where the weight of the wall and the weight of the roof must be supported.

At the Solar Two demonstration project, the nominal diameters of the storage tanks were 12 m. The perimeters of the tank foundations were constructed by stacking, and mortaring, a group of refractory bricks. The bricks formed a ring wall, which carried the vertical loads of the wall and the roof down into the concrete mat foundation below. During the 3-year life of the project, no differential or unexpected settlements in either the hot tank or the cold tank were observed. A postmortem examination of the inside of both tanks showed no unexpected deformations of the floors or the walls [14].

Not too surprisingly, the construction of a ring wall using refractory bricks is a labor intensive exercise. Further, refractory bricks are expensive relative to other potential foundation materials. Commercial projects, both parabolic trough and central receiver, after the Solar Two project pursued less expensive approaches to the foundation design. A common approach used expanded clay, such as Utelite, as the primary foundation material under the entire tank. The expanded clay both supported the tank and provided the primary thermal insulation under the floor.

---

[14] Pacheco, James (Sandia National Laboratories, Albuquerque, New Mexico), 'Final Test and Evaluation Results from the Solar Two Project', Sandia report SAND2002-0120, January 2002

Allowable stress values for the expanded clay showed that the material could safely support the vertical loads at the tank perimeter due to the weight of the wall and the roof. However, during tank fabrication at one commercial project, depressions in the foundation were observed at the perimeter of the tanks even before the tanks were filled with salt. At another commercial project, depressions in the perimeter foundation were observed after the tanks were filled with salt, and then exposed to a number of thermal expansions and contractions. The depressions were produced by the movement of clay particles relative to one other, and the inability of the particles to remain in fixed positions over an extended period of time when exposed to cyclic loads. An hypothesis for this effect is based on the following:

- Finite element calculations of the foundation show that compressive loads at the perimeter of the tank can safely be accommodated by the foundation insulation. However, at a distance slightly beyond the edge of the floor, the compression loads drop to zero

- The foundation, by definition, does not move. As such, compressive forces in the foundation at the edge of the floor must be balanced by tensile forces in the foundation just outside the edge of the floor. The tensile forces are established by friction between adjacent particles in the expanded clay. However, the tank fills and drains daily, which results in a pattern of cyclic compressive loads on the foundations. This, in turn, results in cyclic tensile loads on the expanded clay. However, the clay particles are not bonded to one another, and cyclic loadings can result in particles moving relative to one another. The path of least resistance is a movement of particles out, up, and away from the zone immediately below the edge of the tank.

- The movement of the clay particles leaves the perimeter of the floor unsupported. The floor is not designed to withstand the bending loads generated by the weight of the wall and the roof, and the floor plastically deforms down in response.

The plastic deformations at the perimeter of the floor produce two undesirable effects:

- The high strains associated with plastic deformations significantly reduce the low cycle fatigue life of the floor at this location

- As the tank expands and contracts, the curved perimeter of the tank tends to push the expanded clay, rather than slide over the expanded clay. This increases the depth of the depression, which 1) increases the effective coefficient of friction between the floor and the foundation, and 2) promotes further plastic deformation of the annular floor plate.

In general, the use of expanded clay as the foundation material near the perimeter of the tank has been shown to not be an acceptable approach. Some form of a rigid material, such as refractory bricks or refractory castings, at the perimeter is required.

For existing tanks with clay foundations, inserting metal plates, between the bottom of the tank and the top of the clay, at the tank perimeter has been adopted as a corrective measure. However, the long term effectiveness of this approach is something of an unknown.

5.5 Floor Welding

In commercial salt tanks, the floor is typically fabricated from large rectangular plates. The plates are arranged on the foundation, and then butt welded along each face.

The plates, as supplied by the mill, are not all exactly the same dimensions and are not all exactly the same shape. This results in a variation in the gaps between plates. To assist in the welding process, weld backing strips are attached to the bottom of alternating plates. The backing strips also help to control the gas chemistry in the weld region.

The floor plates have a thickness in the range of 6 to 11 mm, depending on the tank vendor. The number of welding passes ranges from 1 to 3.

5.5.1 Residual Stresses

For a floor plate weld requiring 2 passes, the residual welding stresses are a function of the weld length, as illustrated by the red line in Figure 5-1 [15]. Residual stresses in the range of 300 to 700 MPa are well above the yield stress, which leads to plastic strains in the vicinity of the weld [16].

[15] Osorio, J. (National Renewable Energy Laboratory, Golden, Colorado), Failure Analysis for Molten Salt Thermal Energy Tanks for In-Service CSP Plants, DOE Award Number DE-EE00038475

[16] Huang, Hui, (Oak Ridge National Laboratory, Oak Ridge, Tennessee), 'Finite Element Analysis and In-Situ Measurement of Out-of-Plane Distortion in Thin Plate TIG Welding', UT-Battelle, LLC, under DOE Contract DE-AC05-00OR22725, January 2019

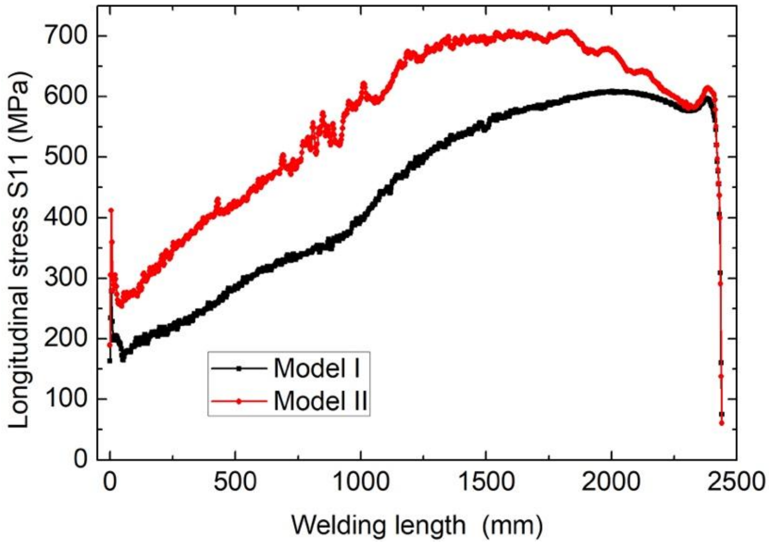

Figure 5-1 Longitudinal Residual Welding Stress

As the weld cools, the metal shrinks, which establishes tensile stress at the top of the weld. This is matched by compressive stresses at the bottom of the weld.

5.5.2 Plate Deformations

The deformation associated with the residual stresses for a subset of the floor welds is illustrated in Figure 5-2. The view shows the edge of two adjacent plates, with the weld located at the mid-point of the curve; i.e., at the lowest point. The overall displacement between the ends of the two plates and the low point at the weld zone is 86 mm.

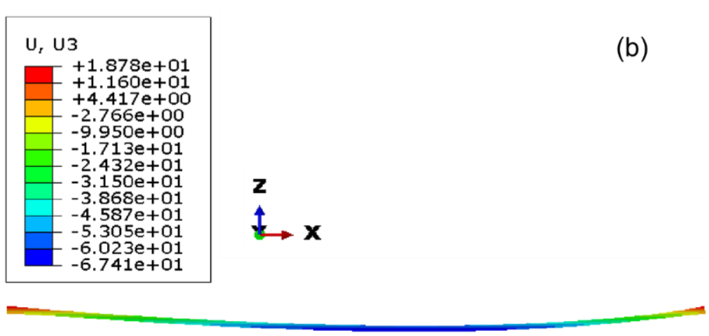

Figure 5-2 Plate Deformations due to Residual Welding Stresses

When all of the welding for the floor plates is completed, each plate takes on the shape of the top of a shallow sphere with a large radius. The low points in the floor are along the weld seams, and the high points in the floor are the centers of the plates.

It can be noted that the floor, after welding, is no longer flat; i.e., the floor has, in effect, buckled at each of the plate seams. This has important implications for the stability of the floor once the tank has been commissioned and is placed into commercial service.

5.5.3 Stress Relaxation

Stresses in the weld region, either due to welding or due to plate deformations, have values at or above the yield stress. This would normally result in creep lifetimes on the order of 2 to 3 years. However, the stresses do not persist due to stress relief. The effect is illustrated in Table 5-1 for 300-series stainless steels [17].

Table 5-1 Stress Relief as a Function of Temperature

Temperature, °C	Stress relief, percent
200 to 400	40 (peak)
550 to 650	35
850 to 900	55
950 to 1,050	95

Several months after the start of commercial service, the residual stresses have relaxed to a steady state value of about 125 MPa, as described in Section 5.15.8. This stress is permanent, and other stresses due to friction, radial temperature gradients, and transient thermal stresses can add to, or subtract, from this value.

It can be noted that stainless steels typically have sufficient uniaxial ductility to accommodate the plastic strains associated with the level of stress relaxation above. However, if the material is constrained, then strains can develop in multiple axes of the heat affected zones. Stainless steels with a high carbon content have a multiaxial failure ductility as low as 1 percent. The creep strain that occurs during the relaxation of the weld residual stresses could be sufficiently large to exceed the multiaxial failure ductility, and cracks could develop in the weld zone.

To a first order, the potential to damage the tank is perhaps the largest at the start of commercial service. As the weld and the plate stresses relax over the first 100 hours or so of operation at the design

[17] Peckner, D. and Bernstein, I., Handbook of Stainless Steel, Chapter 4, Table 25, ISBN 0-07049147-X, 1977

temperature, the residual stresses approach a lower, steady state value. To this end, it may be beneficial to heat treat the tank, at a nominal temperature of at least 550 °C for 100 to 200 hours, to remove some fraction of the residual stresses.

On a related point, the salt inventory at the Solar Two project was melted and then placed in the hot tank. In the hot tank, the inventory was heated to 540 °C over a period of 10 days, and then maintained at that temperature for 20 days. The purpose of the heating phase was to promote the thermal decomposition of the magnesium nitrate in the salt to magnesium oxide and various nitrogen oxides; i.e.,

$$Mg(NO_3)_2 \rightarrow MgO + 2\ NO_2 + \tfrac{1}{2}\ O_2$$

The decomposition process, which was a one-time event, released the NOx gas in the hot tank. This avoided potential problems with releasing the gas in the receiver, which may have had a detrimental effect on the heat transfer rates. Interestingly, the 20-day decomposition period may have had an inadvertent, but beneficial, effect of relaxing a portion of the residual welding stresses prior to the start of the test and evaluation program. In new commercial projects, it may be worthwhile to give some consideration to a similar process in which the hot tank is heated to a temperature close to the design temperature, and then held at that temperature for a period which is long enough to relax some portion of the stresses associated with fabrication, preheating, and the initial filling.

5.5.4 Post Weld Heat Treatment

One method for reducing residual welding stresses is a post weld heat treatment. A representative process is described in Section 8.3.2. The heat treatment process requires accurate control over heating rates, hold times, and cooling rates to achieve the desired combination of metal chemistry and stress reduction.

There are specialty contractors who provide heat treating services for large field equipment, such as the wall of a salt tank. However, the floor of the tank is more problematic. Specifically, 1) the floor can only be heated from one side, and 2) the floor is in contact with the foundation. The floor is relatively thin, and achieving the required heating rates and hold times should be feasible. However, with a hold time on the order of 1 hour, the temperature of the foundation directly beneath the weld will increase to a value approaching the treatment temperature. During the cooling period, the foundation will return some of this heat back to the weld, and it may not be possible to achieve the required cooling rate.

Further, should the tank develop a leak, the foundation will absorb some of the salt. Repairs could be made to the floor by draining the tank, removing the damaged sections, and welding in new sections. If the original floor required a post weld heat treatment, then the replacement sections should also receive a post weld heat treatment. However, the heat treatment temperatures are high enough to thermally decompose the salt absorbed by the foundation. The decomposition process releases NOx, which can be a hazard to plant personnel, and the decomposition also generates a range of oxide species. The oxides will produce very high corrosion rates, both during the heat treatment period and after the tank returns to commercial service.

In summary, it may not be feasible to conduct a post weld heat treatment on the tank floor, either during construction or following a repair. As such, the creep and fatigue life assessment of the floor will need to be based on the following:

- The metal properties and the metal chemistry at the boundaries of the plates in the as-welded condition

- A limited relaxation of residual stresses due to metal temperatures no higher than the design tank temperature.

5.6 Hydraulic Tests

A common commercial plate dimension is 2.44 m by 9.75 m (8 ft. by 32 ft.). A representative tank diameter in a commercial project is 42 m. As such, a nominal 13 rows of plates are required to span the diameter of the tank.

As discussed in Section 5.5, the plates in the floor are forced into the shape of the top of a sphere with a large radius. The deformations noted in Figure 5-2 are consistent with evidence from tanks in commercial projects which show deformation at the center of the plate on the order of 50 to 100 mm.

5.6.1 Plate Stresses

When the tank is filled with water for the hydraulic tests, hydrostatic loads on the plates push the plates down toward a flat shape. The deformation at the center of a flat plate, with a uniform loading and fixed at the edges, is given by the following equation from Roark:

$$y_{max} = \frac{\alpha q b^4}{E t^3}$$

where σ is a coefficient based on the length-to-width ratio of the plate [ ] (i.e., dimensionless), q is the pressure loading [MPa], b is the width of the plate [m], E is the modulus of elasticity [MPa], and t is the thickness of the plate [m]. The floor plates in commercial projects have a representative length of 10.0 m, a width of 2.50 m, and a thickness of 0.00715 m. The length-to-width ratio is 4, which results in a value for σ of 0.0284.

To reach a displacement of 100 mm for y_{max}, the required static pressure is 6,800 Pa, which corresponds to a water depth of 0.8 m. As such, soon after the tank begins to fill, the floor goes from a domed shape to a flat shape.

The peak stress in the plate occurs at the center of the long edge, and is given by the following equation from Roark:

$$\sigma_{max} = \frac{\beta q b^2}{t^2}$$

where β is a coefficient based on the length-to-width ratio of the plate [ ], q is the pressure loading calculated in the equation above [0.0068 MPa], b is the width of the plate [m], and t is the thickness of the plate [m]. For a plate with a length-to-width ratio of 4, β has a value of 0.5, and the peak stress is calculated to be 416 MPa. This value exceeds the yield stress at ambient temperature, which means that yielding occurs in a section of the weld region near the center of the plate, which relieves some portion of the imposed stress.

When the plate changes shape from domed to flat, the stress in the center of the plate can be estimated using the following equation from Roark:

$$\sigma_{max} = -\frac{\beta q b^2}{t^2}$$

where β is a coefficient based on the length-to-width ratio of the plate [ ], q is the pressure loading calculated in the equation above [0.0068 MPa], b is the width of the plate [m], and t is the thickness of the plate [m]. For a plate with a length-to-width ratio of 4, β has a value of 0.25, and the compressive stress is estimated to be 208 MPa.

5.6.2 Plate Deformations

If the center of the plate is raised by 100 mm, then the width of each plate is reduced by about 4 mm. When the tank is filled, hydrostatic loads push down on the plates, and change the shape of the plates from curved to flat. As such, the width of each plate will increase by 4 mm. Across the diameter of the tank, the total change in the width of the plates is 13 * 4 mm = 52 mm.

The radial stiffness of the wall is several orders of magnitude greater than the radial stiffness of the floor, particularly if the plates have already buckled due to welding. As such, the 52 mm increase in plate dimensions is converted into some combination of elastic and inelastic deformations. The deformations will be determined, in part, by the residual stresses produced during welding. Since the residual stress distribution is difficult to predict, and somewhat random, the additional plate deformations will also be difficult to predict and somewhat random.

When the water is removed at the end of the hydraulic tests, the hydrostatic loads are also removed. Residual stresses in the plates will cause the plate to return toward the domed shapes produced during the welding process. However, any plastic deformations produced in the plates when the tank was full will result in a different floor shape after the hydraulic tests than before the hydraulic tests.

To support a finite element calculation of the stresses in the floor, measurements can be taken of the floor shape before and after the hydraulic tests.

5.7 Radial Temperature Distributions in the Floor

Commercial salt storage tanks are placed on a foundation, which typically consists of the following elements:

- A concrete base mat, which is the lowest level of the foundation. A series of parallel cooling air pipes is located in the mat, and a flow of air is forced through the pipes by means of a fan. The air flow removes the majority of the heat flux (> 90 percent) passing from the tank into the foundation. The heat removal from the base mat maintains the soil temperature beneath the base mat to a maximum temperature of about 75 °C. This temperature ensures that the desiccation of the soil, and the oxidation of organic materials in the soil, do not reach levels which could cause settlement of the tank.

- A primary insulating layer, beneath the majority of the floor. The insulating material can be an expanded clay, such as Utelite®, or an expanded glass, such as FoamGlas®.

- A ring wall, composed of a hard refractory material, at the perimeter of the tank. The refractory provides the foundation stiffness needed to support the concentrated weight of the wall and the roof.

- A solid lubricant, such as sand, on top of the primary insulating layer and the refractory ring wall.

Near the center of the tank, conduction heat transfer from the floor into the foundation is primarily one-dimensional; i.e., straight down. The thermal resistance to conduction heat transfer is largely the thermal resistance of the primary insulating material. The overall thermal resistance in this direction is 'large'. Conversely, near the perimeter of the tank, conduction heat transfer from the floor is a combination of vertical heat transfer through the refractory material and horizontal heat transfer through the soil surrounding the refractory ring wall. The thermal conductivity of many refractories is about double the thermal conductivity of expanded clay, and the thermal conductivity of soil is a factor of 4 to 5 times the thermal conductivity of expanded clay. As such, the heat flux from the floor to the environment is a function of the radial position in the floor, as illustrated in Figure 5-3.

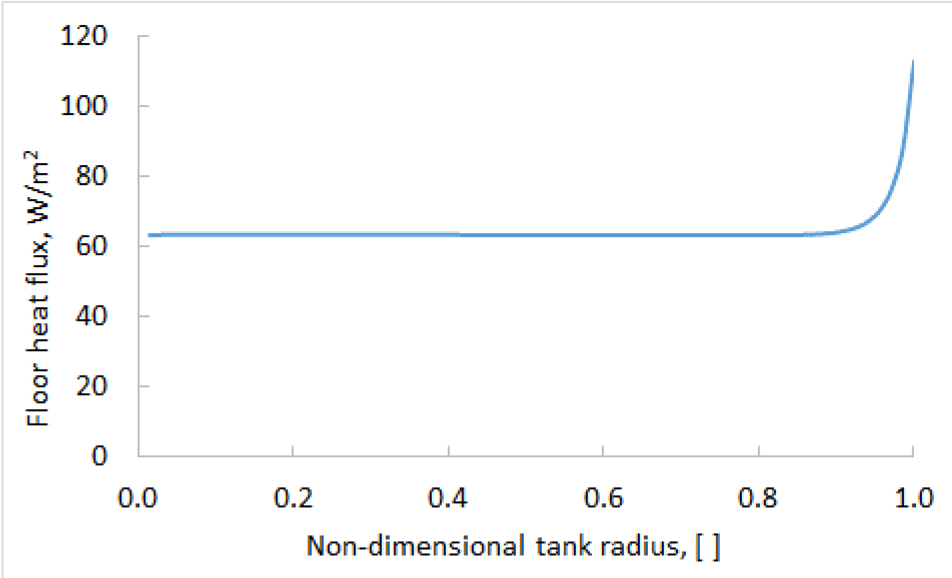

Figure 5-3 Radial Distribution of Heat Flux from the Floor in a Hot Salt Tank

Due to mixing within the tank inventory, the temperature of the inventory is largely isotropic. As such, if the heat flux from the floor to the foundation is a function of the radial position, then the temperature of the floor must also be a function of the radial position.

A two-dimensional, steady-state conduction heat transfer model of the foundation was developed to explore this effect. The model is simplified by simulating the convection heat transfer within the inventory as follows:

- Case 1 - The convection heat transfer is simulated by multiplying the thermal conductivity of the salt by a factor of 100

- Case 2 - The convection heat transfer is simulated by multiplying the thermal conductivity of the salt by a factor of 10

- Case 3 - The convection heat transfer is simulated by multiplying the thermal conductivity of the salt by a factor of 1. This represents a case in which the salt is completely stagnant. Such a condition can occur when 1) the temperature of the inventory is, say, 500 °C, 2) the plant starts an extended shutdown, and 3) the electric salt heaters do not start operation until the temperature of the inventory has decayed to, say, 300 °C.

In each of the three Cases, the depth of the salt inventory is taken to be 3.5 m, and the temperature at the top of the inventory is assumed to be a constant value of 560 °C.

In Case 1, the radial temperature gradient in the floor (blue line) is illustrated in Figure 5-4. The radial gradient is a modest 4 °C.

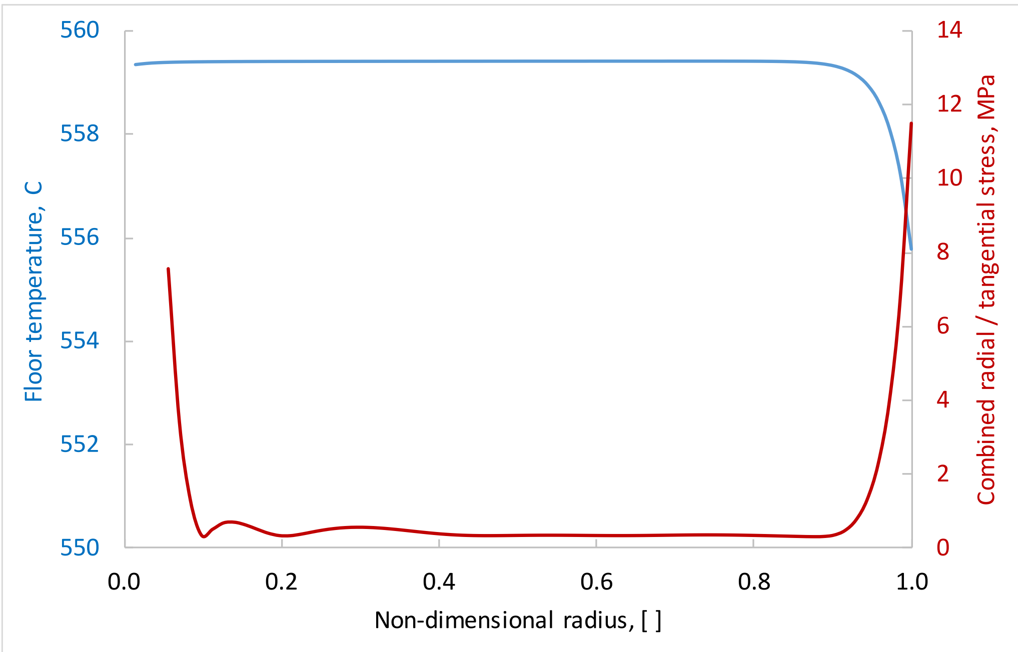

Figure 5-4 Case 1 - Radial Distribution of Floor Temperature and Floor Stress

For an unconstrained circular plate, subject to a radial temperature gradient, the radial stress and the tangential stress are given by the following formula in Roark [18]:

$$\sigma_r = \gamma E \left(\frac{1}{R^2} \int_0^R Tr\, dr - \frac{1}{r^2} \int_0^r Tr\, dr \right)$$
$$\sigma_t = \gamma E \left(-T + \frac{1}{R^2} \int_0^R Tr\, dr - \frac{1}{r^2} \int_0^r Tr\, dr \right)$$

where γ is the coefficient of thermal expansion (1/°C), E is the modulus of elasticity (kg/m-sec^2), R is the radius of the disc (m), and T is the temperature at any point a distance *r* from the center minus the temperature of the coldest part of the disc (°C). The radial and the tangential stresses are combined using the following formula:

$$\sigma_{Combined} = \sqrt{\sigma_r^2 - \sigma_r * \sigma_t + \sigma_t^2}$$

[18] Young, W. C., and Budynas, R. G., 'Roark's Formulas for Stress and Strain', Seventh Addition, 2002

In Case 1, with the convection modeled as 100 times the thermal conductivity of the salt, the peak stress in the floor is 12 MPa and it occurs at the perimeter (the calculated stress at the center is infinite, as the equation involves a division by zero). This value is approximately 11 percent of the allowable stress listed in Section II of the ASME Code for Type 347H stainless steel at 560 °C, and approximately 10 percent of the allowable stress associated with a creep lifetime of 300,000 hours as defined in API 579-1 / ASME FFS-1 (see Section 5.15.3).

Repeating the calculations for Case 2, in which the convection is modeled as 10 times the thermal conductivity of the salt, produces the temperature and the stress curves shown in Figure 5-5.

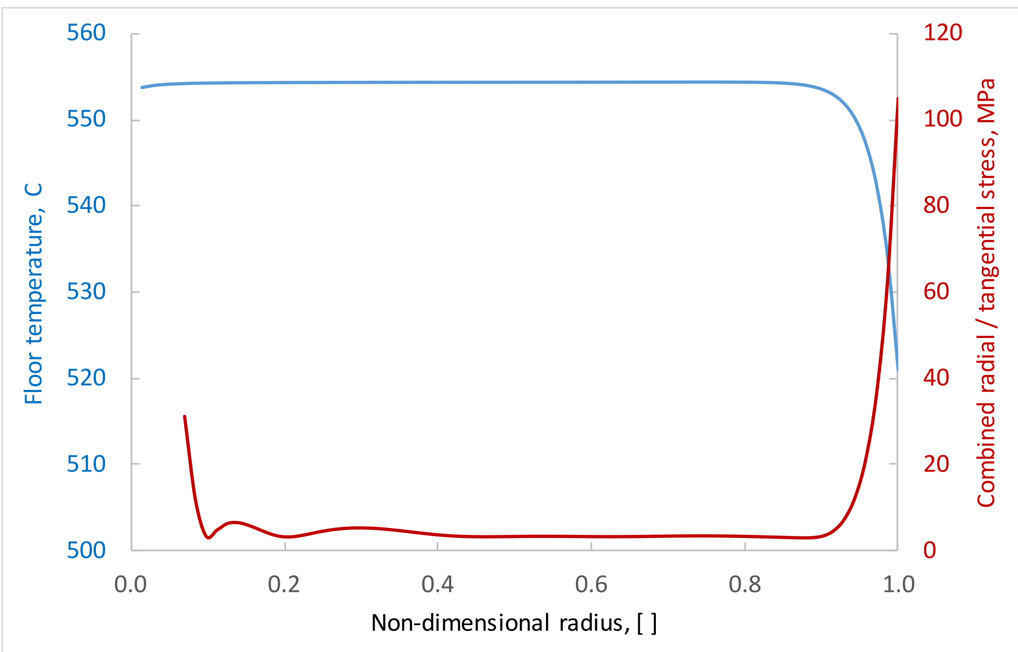

Figure 5-5 Case 2 - Radial Distribution of Floor Temperature and Floor Stress

The radial temperature gradient has increased to 33 °C, and the peak stress has increased to 107 MPa. This value is nominally equal to the ASME allowable stress, and approximately 85 percent of the allowable stress associated with a creep lifetime of 300,000 hours. Informal discussions with other organizations developing finite element models of the floor have reached similar results.

Repeating the calculations for Case 3, in which the inventory is assumed to be stagnant, produces the temperature and the stress curves shown in Figure 5-6. Due to the relatively low thermal conductivity of salt, a radial temperature gradient on the order of 175 °C is established.

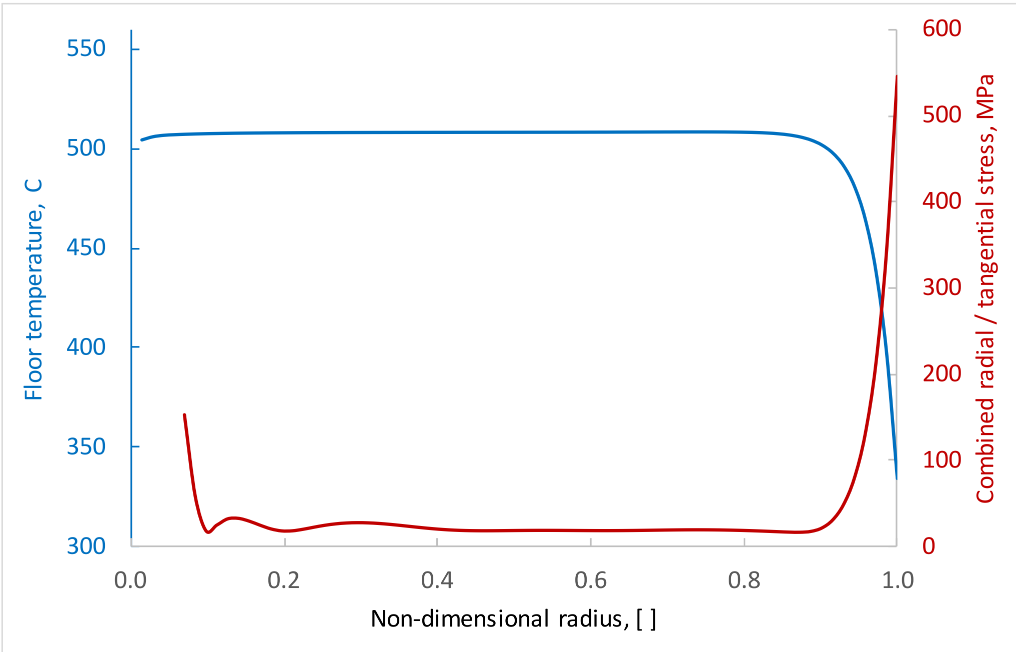

Figure 5-6 Case 3 - Radial Distribution of Floor Temperature and Floor Stress

Clearly, Case 3 represents something of a worst case condition, as 1) the time required to develop the steady-state temperature profile shown in Figure 5-6 could be several weeks, and 2) the operators are likely to recognize the problem, and establish some form of circulation in the tank, before salt temperatures reach values this low. Nonetheless, the calculated temperature profile indicates the potential for two significant problems:

1. The calculated stresses at the perimeter are the same order of magnitude as the tensile strength, and rupture of the floor cannot be discounted.

2. The temperature of the metal at the perimeter of the tank (330 °C) is perhaps 100 °C above the freezing point of the salt. Nonetheless, there is the potential for salt to freeze 1) if there are local defects in the insulation, 2) if the insulation has become wetted by salt due to leakage from the pumps, valves, and instruments above the tank, or 3) if water has infiltrated the insulation due, for example, to heavy rains. If frozen salt develops in the floor near the perimeter of the tank, then the salt will be thawed by recirculating the inventory within the tank. In the regions beneath the frozen salt, the heat flux into the metal will be defined by the thermal conductivity of the solid salt. However, in the regions adjacent to the frozen salt, the heat flux into the metal will be defined by the convection heat transfer coefficients of the circulating salt. The two heat fluxes

could differ by an order of magnitude, which, in turn, could produce local temperature gradients large enough to damage the tank. Unfortunately, the freeze / thaw progression would be largely random and beyond the control of the project. As such, it may be impossible to assess the potential damage to the tank from a freeze / thaw cycle.

Clearly, the steady-state model only mimics the effect of convection within the salt inventory. Nonetheless, the calculations show that a radial temperature gradient about 35 °C establishes stresses equal to the ASME allowable value, and a gradient of approximately 50 °C produces stresses at the yield value. Further, should the inventory becomes stagnant for even a moderate period of time (i.e., days), then permanent damage to the floor may be inevitable.

Should the floor plastically deform due to a radial temperature gradient, and the gradient is then removed, the stress distribution in the floor will be a combination of the new temperature gradient, plus a hysteresis effect from the plastic deformation. Further, the magnitude of the hysteresis effect will be difficult to both calculate and verify.

5.8 Tank Preheating

Prior to filling the tank with salt, the tank and the top of the foundation are preheated to a nominal temperature of 320 °C to prevent a thermal shock to the tank. The heating medium is hot air from a propane- or a natural gas-fired direct air heater. The hot air is directed through a manway in the roof, flows down a short (2 m) temporary gas duct suspended from the roof, enters the tank with the flow directed nominally toward the center, and then exits through a second manway in the roof.

The preheating period ranges from 7 to 20 days. The allowable rate of temperature change is limited; values in the range of 1.5 to 2 °C/hr are typical. Limits are also placed on the intra-tank temperature differential; however, the allowable differentials are relatively high. In one commercial project, differences in temperature as high as 33 °C between the center of the tank and any wall location are permitted.

The preheating process is one in which damage could occur to the tank, as follows:

- Due to non-uniform heat losses from the tank, radial temperature gradients of 25+ °C can be established in the floor

- The flow of preheating air enters the tank at only one location, and the air flow path is dictated by the location and the shape of the inlet duct. As such, the air flow path is known on a gross basis, but is largely beyond the control of the operators. Further, air at high temperatures has a low density, and is generally a poor mechanism for heat transfer. The combination of inexact control over the air flow and the low heat transfer coefficients can result in unavoidable non-uniform temperature distributions in the tank

- The allowable measured intra-tank temperature differentials are the same order of magnitude as the radial temperature gradient (35 °C in Case 2 above). A radial gradient of 35 °C, particularly in combination with the friction forces between the floor and the foundation, has the potential to plastically deform the floor

- The thermocouples located in the tank may not be in the exact locations required to measure the maximum intra-tank temperature differentials. As such, the measured maximum differential might be 33 °C, but the actual maximum differential could be in excess of 33 °C. (One method to avoid this limitation would be to monitor the temperature of the floor and the wall using an infrared thermometer. The measuring portions of the instrument will need to tolerate temperatures as high as 400 °C.)

The floor, at the start of the preheating phase, has already deformed due to the welding processes. During preheating, a radial temperature gradient in the floor will develop, with the highest temperature near the center and the lowest temperature at the perimeter. If the gradient exceeds some threshold value, probably on the order of 35 to 50 °C, then compression stresses near the center of the tank can exceed the yield value. The buckling resistance of the floor will be very low due to 1) the preexisting plate deformations, and 2) the absence of stabilizing hydrostatic forces from the salt. As such, the floor could develop permanent buckles (ridges) even prior to the start of commercial service. As with every metal, the stresses associated with plastic deformation will have a significant detrimental effect on the creep life and the low cycle fatigue life.

As noted above in Section 5.2, the characteristics of the buckled regions (length, height, width, residual stress, and residual strain) are functions of the welding deformations and residual stresses. These characteristics will have some random features, and it is difficult to develop a generic analysis which applies to all buckled regions. However, the creep-fatigue life of a buckled region is always expected to be less than the 30-year life of the project.

5.9 Tank Filling

Following the completion of the tank preheating, the shape of the floor will consist of a combination of domed sections (generated at the end of the hydraulic tests) and perhaps some buckled regions. The salt melting process begins, as described in Section 9.4, Nitrate Salt Handling and Melting Specification, in Volume 1 - Specifications for Parabolic Trough Projects. As the tank is filled with salt, hydrostatic loads will push the floor plates down against the foundation for a second time. The required hydrostatic pressure is on the order of 7 kPa, which corresponds to a salt depth of about 0.4 m. Since the minimum salt level in the tank is 1.0 m during commercial operation, the floor remains flat against the foundation for the life of the tank.

Changing the shape of the plates from domed to flat will generate stresses at both the edges and at the center of the plates. The deflection of the plates will depend on the shape of the floor at the completion of both the hydrostatic tests and the preheating. However, the shape of the floor at the end of preheating may not be known, or it may be difficult to measure. As such, estimating the stresses at the edges of the plates, and at the centers of the plates, after the fill process is likely to involve large uncertainties. Nonetheless, some portions of the plate edge and the plate center stresses will remain as permanent stresses. Under various conditions, the permanent stresses could add to, or subtract from, other stresses generated by friction, radial temperature gradients, and transient temperature conditions.

From a review of the plate deformations, two observations can be made:

- The vertical dimensions of the buckles seen in commercial tanks are larger than the cumulative changes in the plate widths discussed above. However, there are a number of mechanisms, discussed in the Sections below, which can produce ratcheting, the starting point of which are the buckles produced during filling (and likely preheating)

- Buckles, once produced, are permanent. Specifically, there are only 2 mechanisms that could, in principle, remove a buckle:
    - Hydrostatic forces. The maximum hydrostatic load of approximately 250 kPa occurs when the tank is full. However, the stiffness of a triangular, or a semi-circular, buckle is such that a load of 250 kPa produces vertical deflections in the buckle that are much smaller than the height of the buckle
    - Inverted radial temperature gradients. If the floor is placed in tension, the tensile forces will pull on the sides of the buckles, which causes the height of a buckle to decrease. However, for the buckles to permanently deform, the tensile stresses on the buckle must exceed the yield value. This can occur if the temperature of the floor at the perimeter of the tank is 40 °C, or more, above the temperature of the floor at the center of the tank. However, the heat loss pattern in the tank, plus the flow distribution inside the tank, will not allow this condition to occur. Further, to remove the buckle, the height of the buckle would need to be converted into a linear, plastic, compression of the floor. But it is not possible to simultaneously subject local portions of the floor to compression stresses and other portions of the floor (i.e., the buckles) to tensile stresses.

5.10 Friction Between the Floor and the Foundation

5.10.1 Daily Thermal Cycles

Over the course of a typical operating day, the hot tank undergoes the following cycle:

- In the afternoon, the inventory level and the inventory temperature reach their maximum values
- Early in the evening, the inventory level reaches its minimum value. Heat losses from the tank cause the temperature of the inventory to decay.
- Early in the morning, the receiver is started. Over the next 20 minutes or so, both the flow rate and the outlet temperature from the receiver increase. At a pre-defined downcomer temperature, salt flow is directed to the hot tank. The crossover temperature is on the order of 30 to 60 °C lower than inventory temperature. The goal is to capture as much useful thermal energy from the receiver as possible for electric power production. Note that this phase of the receiver startup results in a decay in the inventory temperature.
- Once the receiver reaches its normal design temperature, the temperature of the hot tank inventory starts to increase.
- The continuous heat losses from the tank, in combination with a maximum salt inlet temperature of 565 °C, mean that 1) the temperature of the inventory ranges daily between a minimum value of about 540 °C and a maximum value of about 560 °C, and 2) the inventory temperature never reaches the design receiver outlet temperature of 565 °C.

As such, the tank is subjected to a daily condition, typically in the afternoon, in which the level and the temperature of the inventory both increase. If the temperature of the inventory increases, then the tank will expand. Friction between the tank and the foundation, in turn, places the floor into compression. As discussed in the sections above, the floor has a low buckling resistance due to the plate deformations associated with welding, and due (potentially) to the plate deformations associated with preheating.

5.10.2 Initial Thermal Expansion

As an example of the thermal expansion, a hot salt tank in a representative commercial project has a nominal diameter, at ambient temperature, of 42 m. As the temperature of the tank is increased from ambient conditions to the normal design temperature of 565 °C, the radius of the tank increases by $\delta = R * \gamma * \Delta T = 0.219$ m, where R is the tank radius [m], γ is the coefficient of thermal expansion [1/°K], and ΔT is the change in metal temperature [°K]. Thus, at the design temperature, the radius of the tank is 21.219 m.

5.10.3 Maximum Friction Deflections

As noted above, the tank experiences daily thermal cycles, and the movement of the tank is constrained by friction forces between the floor and the foundation. The maximum amount which the floor can be radially deflected by static friction (i.e., before the tank starts to slide) is given by the following expression:

$$\delta = \frac{(1-\nu)\,\mu\,\rho\,H\,g\,R^2}{3\,E\,t_p}$$

where δ is the deflection of the floor, m
ν is Poisson's ratio, [ ]
μ is the coefficient of friction, [ ]
ρ is the density of the salt, kg/m^3
H is the depth of the salt, m
g is the acceleration due to gravity, m/sec^2
R is the outer radius of the tank, m
E is the modulus of elasticity for stainless steel, MPa
t_p is the thickness of the floor, m

With a representative maximum salt height of 11.5 m, and assuming that the coefficient of friction is 0.3, then the maximum deflection is 0.0055 m.

Along this line of thought, if the tank is at a condition where the friction loads are zero, and the temperature of the inventory increases, then the tank will expand by an amount equal to R * γ * ΔT. If the expansion amount is set equal to the maximum deflection possible due to static friction, then the associated change in inventory temperature is 15 °C. Stated another way, if the tank is full, and if the temperature of the inventory increases by 15 °C, then the maximum friction force will be applied to the foundation.

Operating experience from commercial plants shows that the hot tank experiences multiple cycles each year in which the tank is full, or nearly full, and the temperature of the inventory increases by at least 15 °C. One such situation in which this can occur is as follows:

- The receiver starts in the morning, but the skies are partially cloudy, and the receiver outlet temperature is set to a value less than 565 °C to prevent temperature overshoots during cloud transients
- The steam generator is not started until noon, which means that the inventory level in the hot tank is rising throughout the morning
- In the afternoon, the steam generator demand is close to the receiver output, and the level in the hot tank remains essentially constant
- The weather clears, and the receiver outlet temperature is increased to the design value of 565 °C.

As such, the floor is exposed to some number of cycles in each year in which the floor starts in a state with a low stress (i.e., close to empty) and then the stress in the floor reaches the maximum value possible due to friction.

5.10.4 Analytical Solution for Floor Stresses due to Friction

The tank expands and contracts due to daily changes in the temperature of the inventory. The friction force, kg-m/sec^2 (i.e., N), which can be applied by the tank to the foundation is as follows:

$$\tau_{Friction} = -\,\mu\,\rho\,H\,g\,A$$

where μ is the coefficient of friction, [ ]
ρ is the density of the salt, kg/m^3
H is the depth of the salt, m
g is the acceleration due to gravity, m/sec^2
A is the floor area, m^2

The shear force, kg-m/sec^2, that the foundation applies to the tank is given by the following:

$$\tau_{Foundation} = \frac{G * u * A}{t_{\,Foundation}}$$

where G is the shear modulus of the foundation, kg/m-sec^2
u is the deflection of the foundation, m
A is the floor area, m^2
$t_{Foundation}$ is the thickness of the foundation, m

A differential element of the floor is illustrated in Figure 5-7.

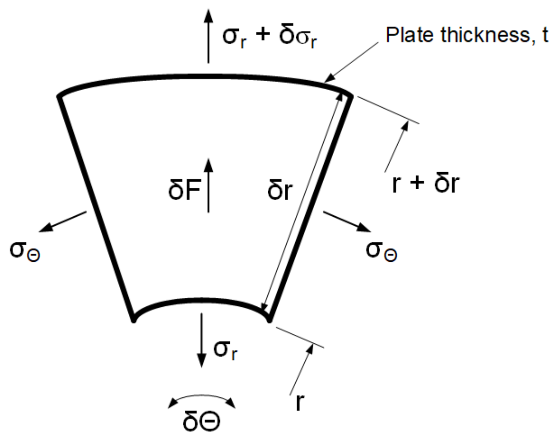

Figure 5-7 Differential Element of the Floor

Setting the force balance to zero yields the following:

$$2\ \sigma_\Theta \sin(\frac{\delta\vartheta}{2})\ \delta r\ t - \sigma_r\ \delta\Theta\ r\ t + (\sigma_r + \delta\sigma_r)\ (r + \delta r)\ \delta\Theta\ t + \delta F = 0$$

Using a small angle approximation $\sin(\frac{\delta\vartheta}{2}) \approx \frac{\delta\vartheta}{2}$, setting $\delta A = \delta r\ r\ \delta\Theta$, dividing by δA / t, and setting $\tau = \frac{\delta F}{\delta A}$ yields:

$$\frac{\delta\sigma_r}{\delta r} + \frac{1}{r}(\sigma_r - \sigma_\Theta) = -\frac{\tau}{t_p}$$

where σ_r is the radial stress, kg/m-sec^2 (i.e., Pa)
r is the radius, m
σ_Θ is the tangential stress, kg/m-sec^2
τ is the unit shear force between the floor and the foundation, kg/m-sec^2
t_p is the thickness of the floor, m

In an axisymmetric plate, the radial strain, [ ], is:

$$\varepsilon_r = \frac{\delta u}{\delta r}$$

the tangential strain, [ ], is:

$$\varepsilon_\theta = \frac{u}{r}$$

the radial stress, kg/m-sec^2, is:

$$\sigma_r = \frac{E}{(1-\nu^2)}(\varepsilon_r + \nu\varepsilon_\theta)$$

where ν is Poisson's Ratio, [ ]

and the tangential stress, kg/m-sec^2, is:

$$\sigma_\theta = \frac{E}{(1-\nu^2)}(\varepsilon_\theta + \nu\varepsilon_r)$$

Substituting in the equations above results in a second order differential equation for the deflection:

$$\frac{d^2u}{dr^2} + \frac{1}{r}\frac{du}{dr} - \frac{1}{r^2}u + \frac{(1-\nu^2)}{E}\frac{\tau}{t_P} = 0$$

The solution involves a number of terms, including the following:

- Concentrated vertical load of the wall and the roof, carried down to the perimeter of the floor
- Coefficients of friction, which can have different values for area under the majority of the floor and the area under the annular plate beneath the wall
- Thermal expansion and contraction of the tank due to daily changes in the temperature of the inventory
- Shear stiffness of the foundation
- Radial location in the floor where the shear force reaches a maximum.

The solution is subject to a boundary condition, in which the radial stress at the center of the floor is equal to the tangential stress at the center of the floor.

The location in the floor where the shear force reaches a maximum is designated r_2. For radial locations greater than r_2, the radial stress in the floor is given by:

$$\sigma_r = \frac{W_{Wall}\, g\, C_{F_{Perimeter}}}{2\,\pi\, R\, t_P} + \frac{(3+\nu)}{3}\frac{(\,C_{F_{Floor}}\rho\, g\, H)}{t_P}\,(R-r)$$

where W is the weight of the wall and the roof, kg
$C_{F_{Perimeter}}$ is the coefficient of friction beneath the annular plate, [ ]
$C_{F_{Floor}}$ is the coefficient of friction beneath the majority of the floor, [ ]
R is the tank radius, m
r is the radius at which the stress is calculated, m

and the tangential stress is given by:

$$\sigma_\Theta = \frac{W_{Wall}\, g\, C_{F_{Perimeter}}}{2\,\pi\, R\, t_P} + \frac{1}{3}\frac{(\,C_{F_{Floor}}\rho\, g\, H)}{t_P}\,((3+\nu)R - (1+3\nu)r)$$

For radial locations less than r_2, the expressions for the radial and the tangential stresses are as follows:

$$\sigma_r = \frac{W_{Wall}\, g\, C_F}{2\,\pi\, R\, t_P} + \frac{(3+\nu)}{3}\frac{(C_F\,\rho\, g\, H\, R)}{t_P} - \left(\frac{5}{24}\right)\frac{(3+\nu)\,(C_F\,\rho\, g\, H)^2}{(t_P\, g_F\,\alpha\,\Delta T)} - \left(\frac{1}{8}\right)\frac{(3+\nu)\,(g_F\,\alpha\,\Delta T)\,r^2}{t_P}$$

$$\sigma_\theta = \frac{W_{Wall}\, g\, C_F}{2\,\pi\, R\, t_P} + \frac{(3+\nu)}{3}\frac{(C_F\,\rho\, g\, H\, R)}{t_P} - \left(\frac{5}{24}\right)\frac{(3+\nu)\,(C_F\,\rho\, g\, H)^2}{(t_P\, g_F\,\alpha\,\Delta T)} - \left(\frac{1}{8}\right)\frac{(1+3\nu)\,(g_F\,\alpha\,\Delta T)\,r^2}{t_P}$$

Coefficient of Friction Values

A common solid lubricant used under the floors of commercial tanks is sand. A paper by Uesugi [19] summarizes the results of experiments to measure the coefficient of friction between a steel plate and sand.

The coefficient is a function of the surface roughness of the plate, the size of the sand particles, the vertical loading on the sand, and the number of strain reversals. However, the coefficients generally fall within a fairly narrow range of 0.5 to 0.7.

Representative Results for a Commercial Tank

For the purposes of the discussion, stresses due to friction were calculated using the following parameters:

[19] Uesugi, Morimichi, et. al., (Department of Architectural Engineering, Chiba University, Japan), 'Friction Between Sand and Steel under Repeated Loading', Soils and Foundation Volume 29, No. 3, 127-137, September 1989, Japanese Society of Soils Mechanics and Foundation Engineering

- Tank radius of 21.0 m at ambient temperature
- Coefficient of friction of 0.6 between the floor and the sand
- Coefficient of friction of 1.0 between the perimeter of the floor and refractory bricks beneath the perimeter of the floor
- Floor thickness of 7.14 mm
- Foundation shear stiffness of 320,000,000 kg/m^2-sec^2.

Case 0

Case 0 corresponds to the following transition: 1) the tank is empty, at a temperature of 20 °C, followed by 2) the tank is preheated to a temperature of 320 °C over the course of several days.

A plot of the radial and the tangential stresses is shown in Figure 5-8. Negative values correspond to compressive stresses; i.e., the expansion of the floor is resisted by the shear stiffness of the foundation.

Since the tank is empty, the vertical loads on the floor are largely determined by the weight of the floor; i.e., close to zero. The radial and the tangential stresses, which are determined by the friction forces at the perimeter of the tank due to the weight of the wall, the roof, and the insulation, have nominally the same values.

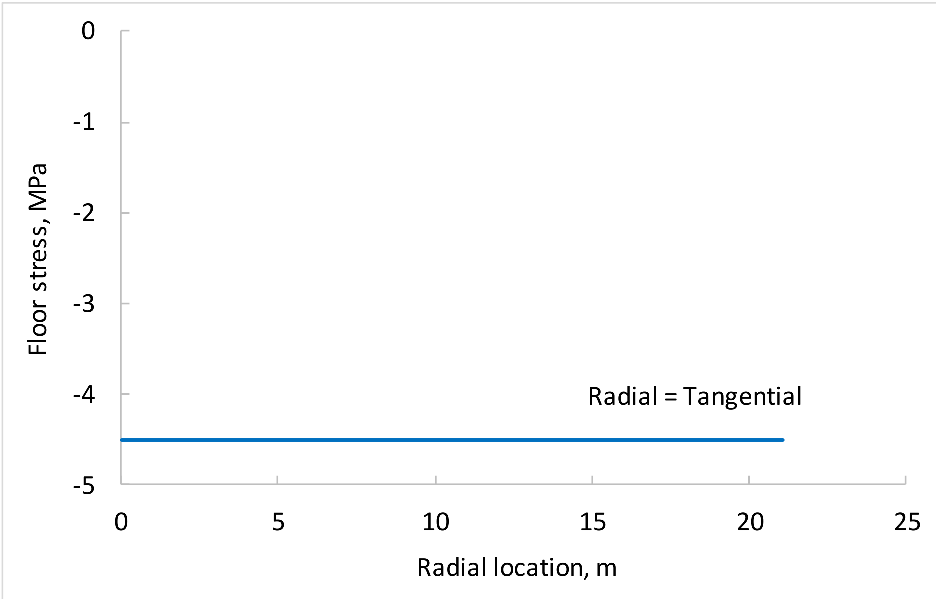

Figure 5-8 Radial and Tangential Floor Stresses for Case 0

Case 1

Case 1 corresponds to a condition in which 1) salt, at a nominal temperature of 320 °C, is loaded into the tank to a depth of 1.5 m after the tank has been preheated, followed by 2) the inventory temperature is raised to a value of 565 °C over the course of several days. The inventory depth remains at 1.5 m during this multi-day process to minimize the friction loads between the floor and the foundation.

With the inventory depth at the minimum, the radial and the tangential stresses in the floor, as a function of the radial location, are shown in Figure 5-9. Negative values for the stresses correspond to compressive loads.

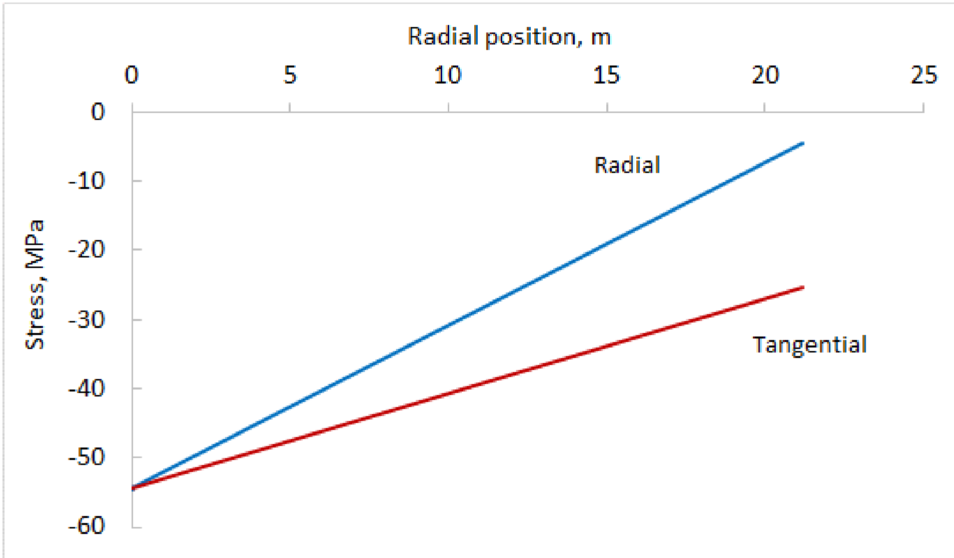

Figure 5-9 Floor Stresses for Case 1: 21 m Tank Radius; 7 mm Floor Thickness

The radial stress at the perimeter of the tank is not equal to zero due to the friction forces generated at the perimeter by the weight of the wall, the roof, and the insulation.

<u>Case 2</u>

In Case 2, the plant is in normal commercial service. At the beginning of the day, the inventory depth is 1.5 m. Over the course of the day, the inventory depth increases to 10.5 m. The inventory temperature remains constant at 565 °C. Since the tank neither expands nor contracts, the stresses in the floor remain constant at the profiles shown in Figure 5-9.

The project decides to postpone the startup of the turbine for a period of 8 hours to take advantage of higher energy sales prices. During this period, the tank cools from an initial temperature of 565.0 °C to a new temperature of 562.9 °C (ΔT = -2.1 °C). The temperature decays causes the tank to contract, and a ΔT of -2.1 °C represents the largest temperature change which can occur before the tank begins to slide on the foundation.

The floor stresses generated by this condition are shown in Figure 5-10. Positive values correspond to tensile loads.

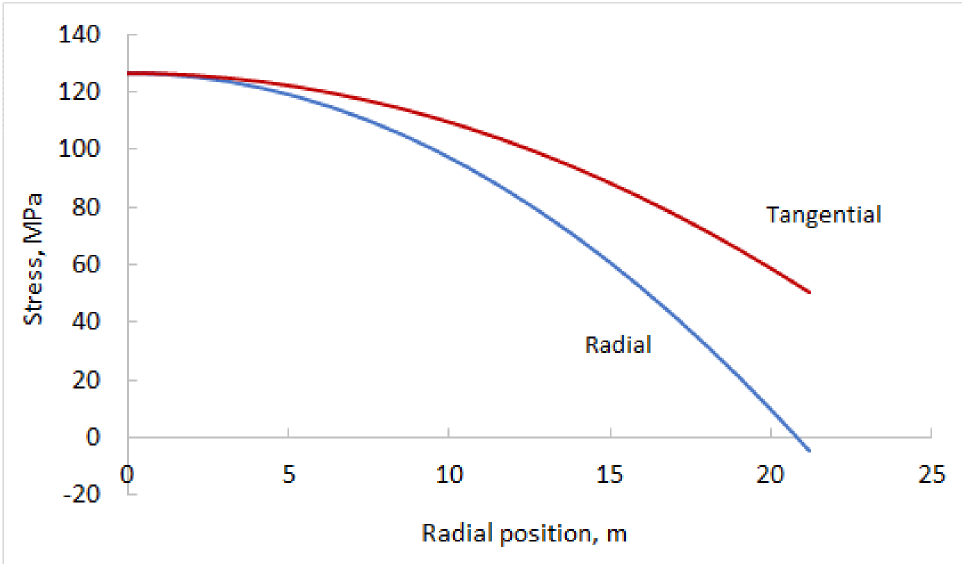

Figure 5-10 Initial Floor Stresses for Case 2: 21 m Tank Radius; 7 mm Floor Thickness

The stresses shown in Figure 5-10 assume that the floor starts in an unstressed condition. However, this is not the case, as the floor starts with the stress distribution shown in Figure 5-9. The stresses shown in Figure 5-9 can be combined with the stresses shown in Figure 5-10 if the change in shear stress with radius is a constant value; i.e., the tank has not yet started to slide. The linear superposition of stresses (i.e., Figure 5-9 + Figure 5-10) is shown in Figure 5-11.

Of note in Figure 5-11 are 1) the stress values, and 2) a situation in which a change in the inventory temperature of small as 2 °C can produce stresses within 80 percent of the allowable stresses listed in Section II of the Code.

Case 3

In Case 3, the tank begins the day with an assumed inventory temperature of 550 °C and an inventory level of 10.5 m. The inventory level in the morning is initially a high value in anticipation of meeting a high demand for electric energy during the day.

In the morning, the steam turbine is placed in service. Over the course of the day, the thermal power supplied by the receiver is nominally similar to the thermal power demand of the steam generator. As such, the inventory level in the hot tank largely remains constant at 10.5 m. However, the inventory temperature can increase above 550 °C if the solar radiation conditions are favorable and the receiver can operate for several hours at the design temperature of 565 °C.

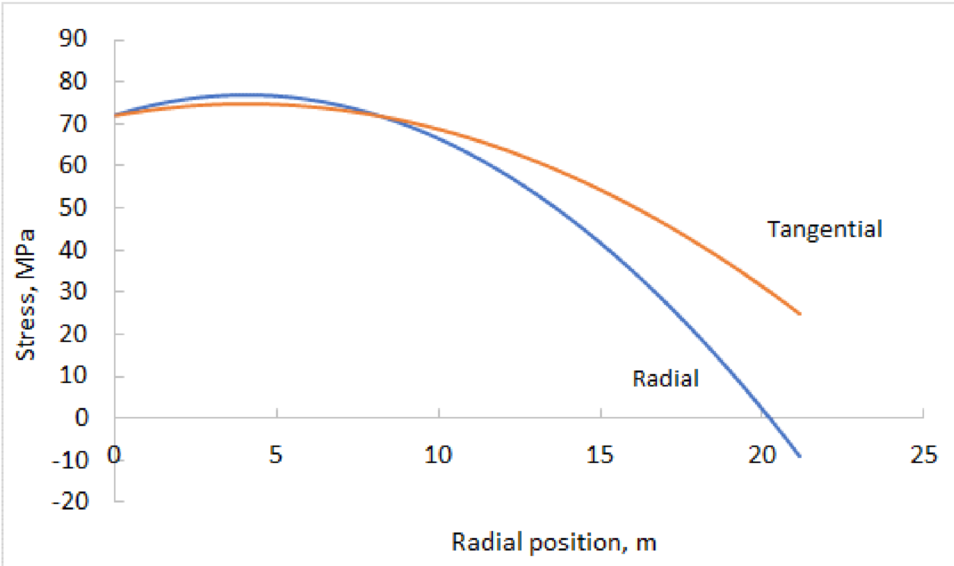

Figure 5-11 Final Floor Stresses for Case 2: 21 m Tank Radius; 7 mm Floor Thickness

Assuming that the inventory temperature reaches the design value of 565 °C, the stresses produced in the floor due to the expansion of the tank are shown in Figure 5-12. The combination of a high inventory level (10.5 m) and an increase in the inventory temperature (15 °C) places compressive loads on the floor near the center of the tank, and these stresses exceed the yield value. Similarly, if the tank has a high inventory level, but cools by 15 °C, then the tank will contract, generating a mirror image (tensile, rather than compressive) of the floor stresses.

Several items can be noted in this discussion:

- The combination of a high inventory level and an increase in the inventory temperature is not a hypothetical condition. It has been observed in commercial projects, when the project is trying to tailor electric energy deliveries to the needs of the local utility

- Similarly, the combination of a high inventory level and a decrease in the inventory temperature can occur if an afternoon with intermittent clouds results in a series of receiver start / stop cycles, each of which adds relatively cold salt to the hot tank

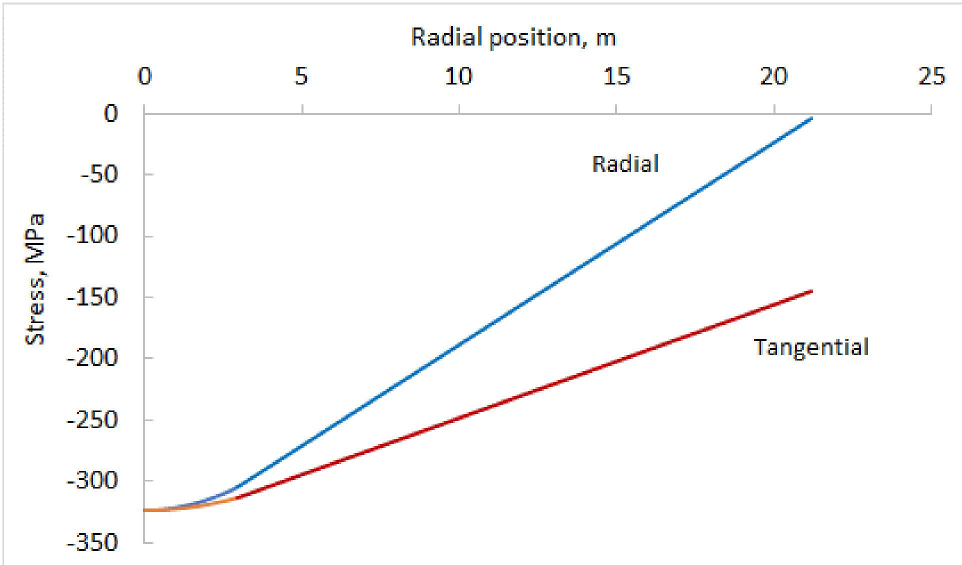

Figure 5-12 Floor Stresses for Case 3: 21 m Tank Diameter; 7 mm Floor Thickness

- The stresses shown in Figure 5-12 assume that the tank starts in condition with zero initial stress. Clearly, this will not be the case, as the stresses at any particular time will be determined by the temperature / level history of the tank up to that point. As might be imagined, 1) the history of the tank will largely be unknown, or 2) even if the history was known, it's unlikely that the project could develop a running calculation of the floor stresses which had a meaningful accuracy. To bound the problem, the stresses shown in Figure 5-9 (Case 1) represent a case in which 1) the inventory is at, or near, the minimum level (1.5 m), and 2) the tank has been sliding over the entire floor area, except for a small area near the center of the tank. This, in turn, should produce, in essence, a baseline stress at an inventory level of 1.5 m. As such, with inventory depths at or near the minimum, the stresses at the center of the tank should oscillate between two baseline values: -55 MPa (tank expanding); and +55 MPa (tank contracting). To a zeroth-order, the 55 MPa baseline stresses at the center of the tank will either add to, or subtract from, the stresses at the center of the tank developed at other combinations of level and temperature; i.e., those shown in Figure 5-12. The exact value for the stress at the center of the tank will require a more sophisticated calculation than the analytical solution noted above. Nonetheless, stresses well above the yield value are expected, particularly if compressive (tensile) stresses developed during the day add to baseline compressive (tensile) stresses carried over from when the tank was last at the minimum level.

Parametric Tank Designs

The friction stresses in a representative tank (21.0 m radius; 7 mm floor thickness), operating through typical daily and annual thermal cycles, are likely to be well above values which could be considered consistent with a creep lifetime of 30+ years.

To prevent potentially damaging stresses in the floor, the temperature of the inventory must be controlled to values in the range of perhaps ±2 °C of a reference value. However, the transient nature of the plant operations, plus conditions outside the project's control (i.e., forced outages), are likely to exceed the ±2 °C operating constraint on a regular basis.

One possible method for reducing the friction stresses in the floor is to make change changes to the tank design. As an example, one 100-percent capacity hot tank could be replaced by two 50-percent capacity tanks, and the thickness of the floor could be doubled from the minimum specified in API 650 (i.e., 2 x (6.35 mm + corrosion allowance)). This would result in a tank radius of 14.9 m and a floor thickness of 14.3 mm.

For this analysis, the balance of the design parameters, including the coefficient of friction between the floor and the foundation (0.6), the coefficient of friction between the annular perimeter plate and the foundation (1.0), and the shear modulus of the foundation (320,000,000 kg/m^2-sec^2), are assumed to remain unchanged.

<u>Case 1</u>

As in the previous section, Case 1 corresponds to a condition in which 1) the tank is preheated to 300 °C, 2) salt, at a nominal temperature of 320 °C, is loaded into the tank to a depth of 1.5 m, and 3) the inventory temperature is raised to 565 °C over the course of several days.

With the inventory at the minimum depth, the radial and the tangential stresses in the floor, as a function of the radial location, are shown in Figure 5-13. Negative values correspond to compressive loads.

To a first order, reducing the tank radius from 21 m to 15 m, and doubling the floor thickness from 7 mm to 14 mm, reduces the peak stresses at the center of the tank by about 60 percent (55 MPa down to 21 MPa).

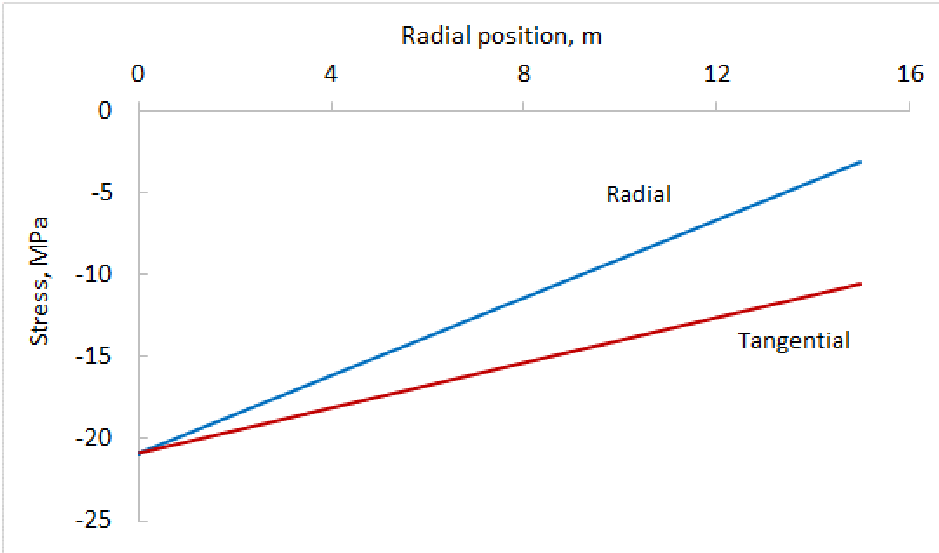

Figure 5-13 Floor Stresses for Case 1: 15 m Tank Radius; 14 mm Floor Thickness

Case 2

Similar to Case 2 above, the tank cools from an initial temperature of 565.0 °C down to a new temperature of 562.0 °C (ΔT = -3.0 °C). The temperature decays causes the tank to contract, and a ΔT of -3.0 °C represents the largest temperature change which can occur before the tank begins to slide on the foundation. The associated stresses are shown in Figure 5-14. Positive values represent tensile stresses.

As above, the compressive stresses shown in Figure 5-13 can be combined with the tensile stresses shown in Figure 5-14 using linear superposition. The results are shown in Figure 5-15. To a first order, reducing the tank diameter by a factor of 2 and doubling the floor thickness reduces the peak stresses at the center of the tank by a nominal 65 percent (78 MPa down to 25 MPa).

Case 3

Similar to Case 3, the tank begins the day with an assumed inventory temperature of 550 °C and an inventory level of 10.5 m. The inventory level remains constant during the day; however, the inventory temperature rises by 15 °C to a value of 565 °C by late in the afternoon. The associated stresses are shown in Figure 5-16.

Reducing the tank diameter by a factor of $\sqrt{2}$ and doubling the floor thickness reduces the peak stresses at the center of the tank by a nominal 65 percent (320 MPa down to 115 MPa). Importantly, the values are now the same order of magnitude as the allowable stresses listed in Section II of the Code.

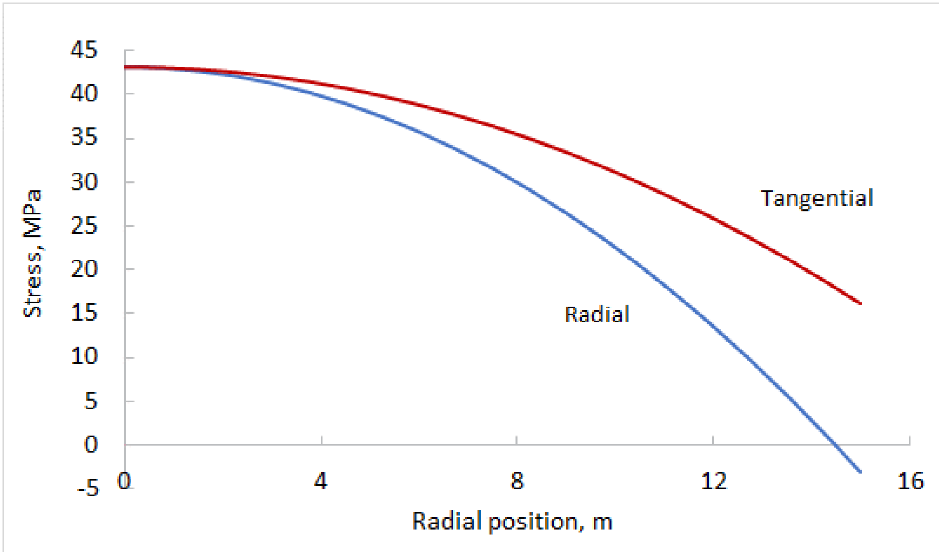

Figure 5-14 Initial Floor Stresses for Case 2: 15 m Tank Radius; 14 mm Floor Thickness

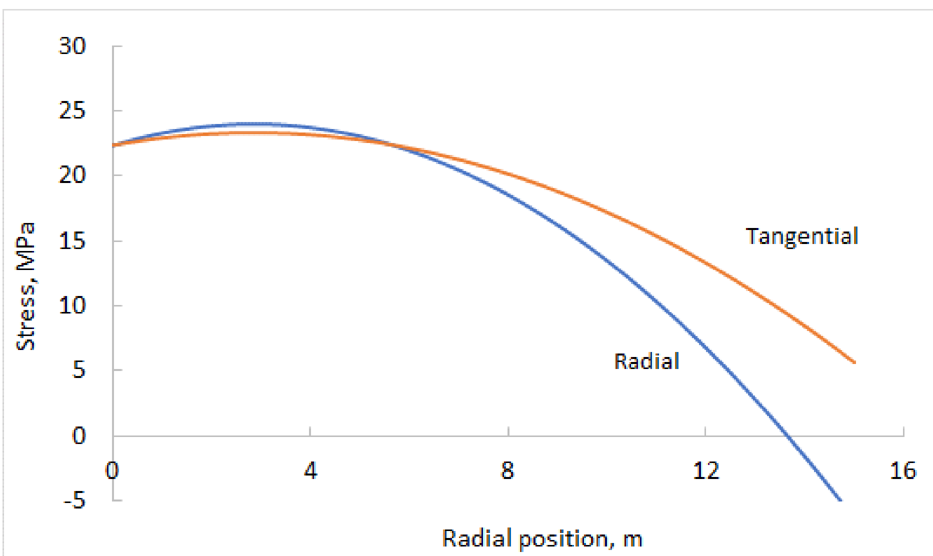

Figure 5-15 Final Floor Stresses for Case 2: 15 m Tank Radius; 14 mm Floor Thickness

As noted above in the discussion for the 21 m tank, an accurate estimate of the floor stresses for the 15 m tank will require 1) a more sophisticated approach than an analytical solution, and 2) analyzing the history of the floor stresses prior to the condition of interest. As such, it's not possible to state that the floor stresses for the 15 m tank will always be less than the allowable stresses listed in Section II of the Code. Nonetheless, it is apparent that there is likely a combination of tank diameters and floor thicknesses that result in stresses due to friction, in combination with stresses due to temperature gradients (Section 5.7), that satisfy the allowable limits discussed in Section 5.14.1, Changes in the Tank Design Codes.

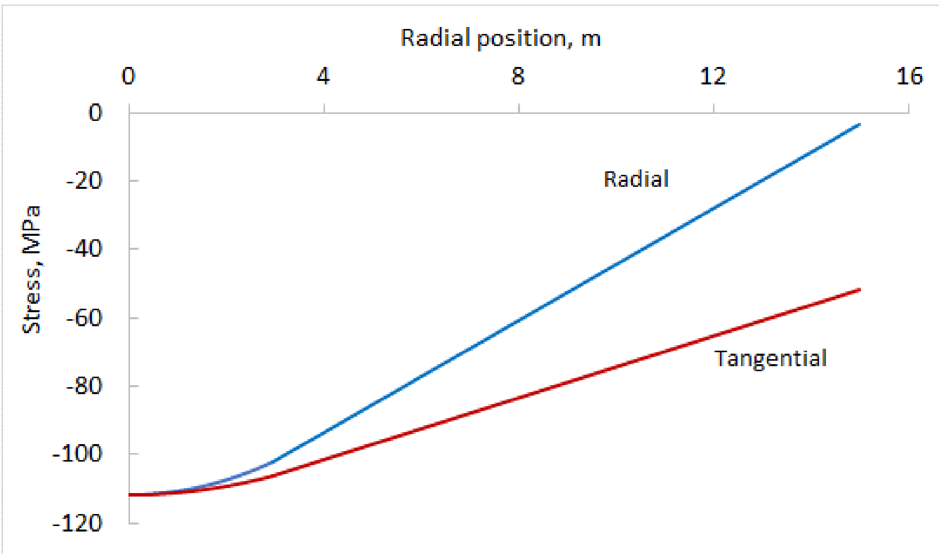

Figure 5-16 Floor Stresses for Case 3: 15 m Tank Radius; 14 mm Floor Thickness

5.11 Salt Inlet Flow Distribution

The salt flow entering the tank is typically distributed by means of a single ring header. The circumference of the header is in the range of 40 to 60 percent of the circumference of the tank. The header has either a series of holes or a group of eductors to distribute the incoming flow with the main inventory.

The distribution arrangement is simple and offers a low cost. However, it can suffer various performance liabilities, as follows:

1. The effectiveness of the mixing is dependent on the velocity of the salt leaving the distribution ring. At low receiver flow rates, the salt velocities in the header will be low, and the extent of the mixing will be limited. Imperfect mixing can either add to, or subtract from, the existing radial temperature gradient in the floor. Any operating condition which increases the radial temperature gradient carries the risk of adding creep or fatigue damage to the floor.

2. During receiver startup, or following a trip of the receiver, both the temperature and the flow rate of the salt can be well below design values. A condition can occur in which relatively cold salt

leaves the distribution ring, and the salt sinks to the floor due to buoyancy effects. This, in turn, can lead to a non-uniform temperature distribution in the floor immediately below the distribution ring.

5.11.1 Stresses Calculated from Analytical Expressions in Roark

The stresses associated with this flow condition can be estimated using the following expression from Roark:

> A thin circular disk at uniform temperature has the temperature changed ΔT throughout a comparatively small central circular portion of radius a. Within the heated part there are radial and tangential compressive stresses $\sigma_r = \sigma_t = \frac{1}{2} \Delta T \gamma E$. At points outside the heated part, a distance r from the center of the disk but still close to the central portion, the stresses are $\sigma_r = \frac{1}{2} \Delta T \gamma E a^2/r^2$ (compression) and $\sigma_t = \frac{1}{2} \Delta T \gamma E a^2/r^2$ (tension); at the edge of the heated portion, there is a maximum shear stress $\sigma_r = \frac{1}{2} \Delta T \gamma E$.

Using representative values for the modulus of elasticity, E, and the coefficient of thermal expansion, γ, for stainless steel, a local temperature depression of 54 °C results in a stress equal to the allowable stress for stainless steel at 560 °C. A local temperature depression of 87 °C produces stresses equal to the yield stress. The local stresses can either add to, or subtract from, the stresses normally present in the floor.

It can be noted that differences between the temperature of the salt in the distribution ring and the temperature of the bulk inventory can differ, during transient conditions, by values up to at least 90 °C.

5.11.2 Stresses Calculated from Finite Element Models

A computational fluid dynamics / finite element model has been developed for a hot salt tank at a commercial project. Using historical operating data from the project for inventory temperatures, flow conditions into the tank (flow rate, temperature), and flow conditions out of the tank (flow rate, temperature), floor temperatures have been calculated for a number of radial and circumferential locations as a function of time.

Using data from one particular day, which included a number of cloud transients, the differences in floor temperatures at two radial locations are shown in Figure 5-17. The two locations are as follows:

- Between Node 2 (17 percent of the tank radius) and Node 3 (33 percent of the tank radius)
- Between Node 5 (67 percent of the tank radius) and Node 6 (85 percent of the tank radius)

The circumferential location is 90° clockwise from North.

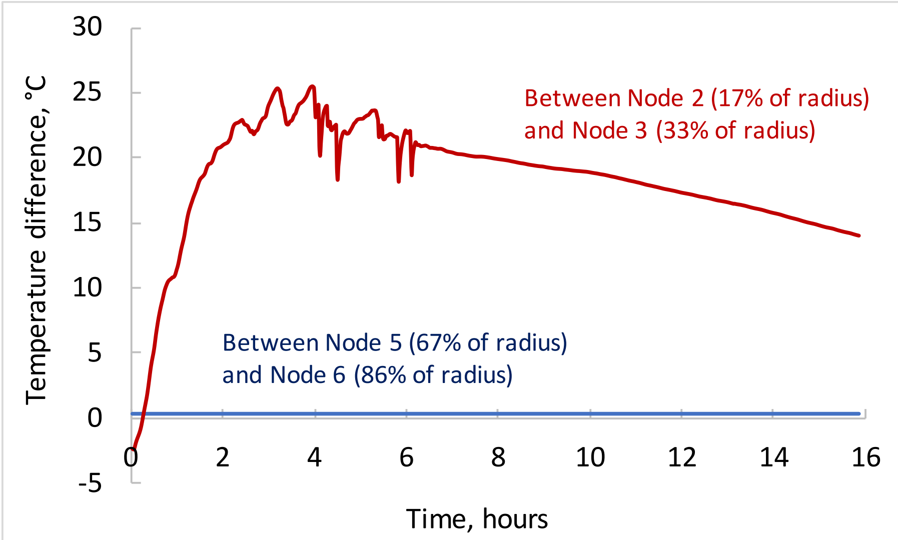

Figure 5-17 Differences in Floor Temperatures as a Function of Time; 90° Circumferential Location

The radial temperature difference is concentrated near, and somewhat inside, the location of the distribution header (between Nodes 2 and 3). Near the perimeter of the tank (between Nodes 5 and 6), the radial gradient has decayed to about 0.5 °C.

A plot of the circumferential temperature differences at Node 6, as a function of time, is shown in Figure 5-18. The temperature differences are calculated between circumferential locations of 45° and 90°.

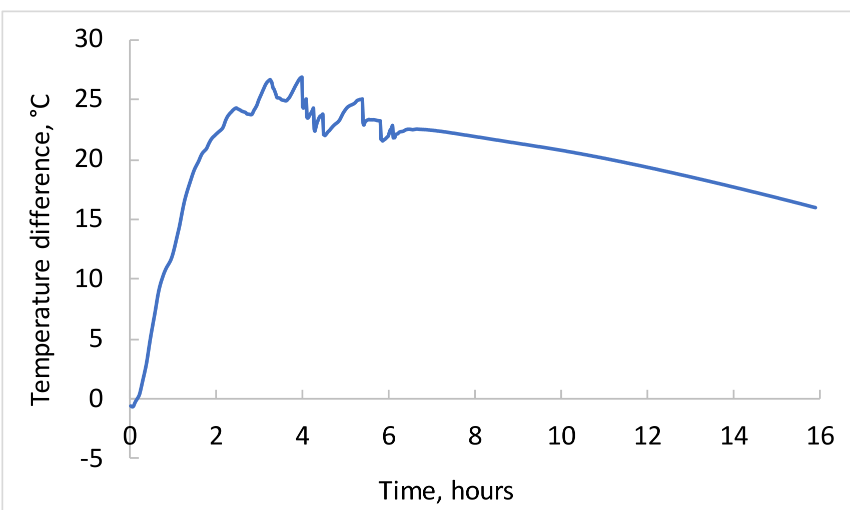

Figure 5-18 Differences in Floor Temperatures as a Function of Time; Node 6 Between 45° and 90°

With reference to Figure 5-17, the radial temperature difference at Node 6 is less than 1 °C during the 16 hour time span of interest. However, the circumferential temperature difference at Node 6 is greater than 20 °C for most of the duration.

Similar to Figure 5-18, a plot of the circumferential temperature differences at Node 6, for circumferential locations of 90° and 135°, is shown in Figure 5-19.

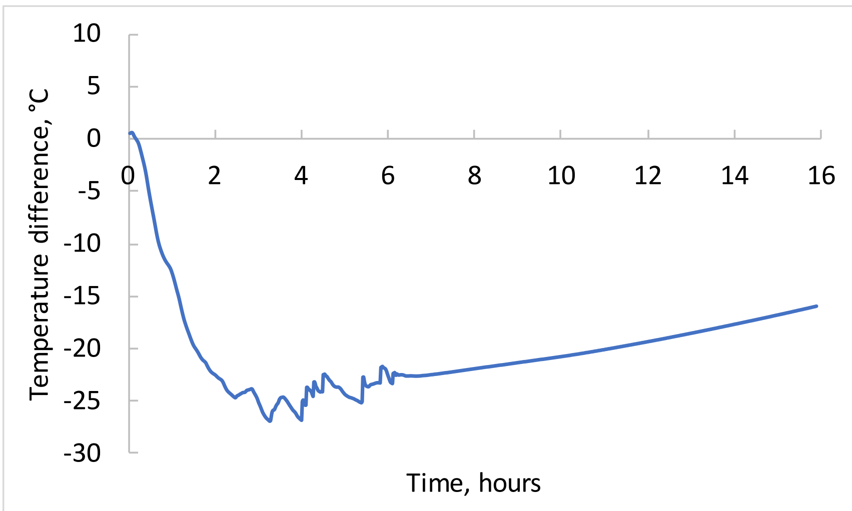

Figure 5-19 Differences in Floor Temperatures as a Function of Time; Node 6 Between 90° and 135°

The temperature differences in Figure 5-18 are essentially the mirror image of the temperature differences in Figure 5-19, which means that temperature differences between the 45° location and the 135° location are only a few °C.

The von Mises stresses in the floor at Node 6, generated by the circumferential temperature differences noted above, are shown in Figure 5-20. Throughout the calculation period, the stresses exceed the yield stress. If the material is routinely operating at or above the yield stress, then the creep life of the floor will be less than the 30-year life of the project.

Several items can be noted from the discussion above:

- The analysis was conducted for only one day from the multiple days of operating data supplied to the study by the commercial project. Only one day of data were analyzed due to the lengthy computational time required (several weeks on a high performance computer)

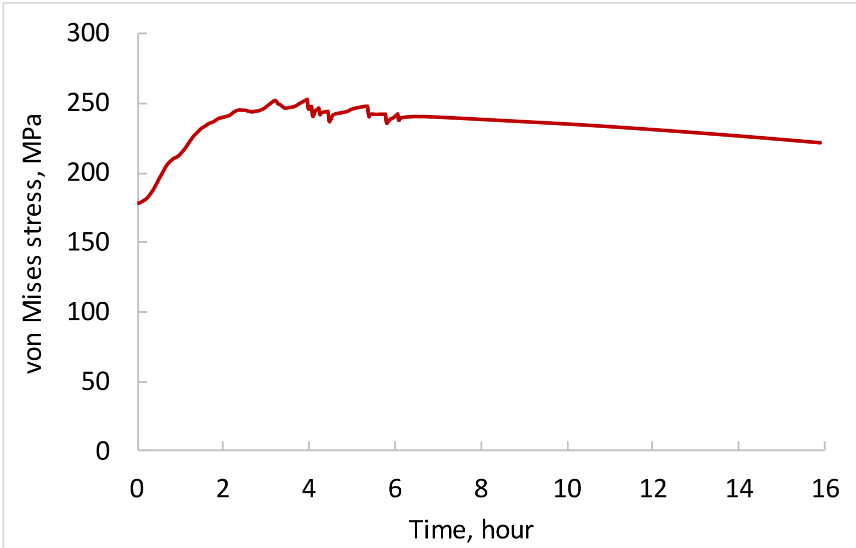

Figure 5-20 Von Mises Stresses at Node 6

- The day analyzed was selected to be representative of an average day with intermittent clouds. This day may, or may not, represent a worst-case condition for floor stresses

- At the start of the calculation, the stresses in the floor are taken to be equal to the stresses on the first day of commercial service. However, the calculation was developed based on plant operating data from (say) Day 905 of commercial service. During this 905 day period, the stresses are expected to evolve due to stress relaxation in the weld regions, plastic deformations associated with creep, plastic deformations generated by high friction forces coincident with changes in the inventory temperature, lateral movement of the tank due to non-isotropic thermal expansion and contraction, and vertical movement of the tank due to foundation settlement. The stress evolution over this 905 day period are unknown, and as such, the initial stress state for the calculation are also unknown. This necessarily introduces some level of uncertainty in the values shown in Figure 5-20.

The evolution of the floor stresses over months or years is difficult to determine, in large part due to the large computational requirements. Nonetheless, it is clear that even modest temperature differentials (25 to 30 °C) in the inventory, either radial or circumferential, can generate stresses that are nominally twice the allowable values discussed in Section 5.15.11.

5.11.3 Optimization Studies for the Inlet Distribution Header

As discussed in the introduction to Section 5.11, inlet distribution systems in commercial projects use either a series of holes in the header or a number of mixing eductors welded to the header. The effectiveness of mixing between the incoming flow and the tank inventory will influence the temperature gradients, and the associated stresses, in the floor.

A parametric study of the diameter (fraction of tank diameter) of the distribution header, and the number and the orientation of eductors, was conducted to help define the elements of an optimum design [20]. Three sets of parametric studies were conducted.

First Parametric Study

Two load cases were considered, as follows:

- Salt entered the distribution header at a temperature which was 175 °C below the initial reservoir temperature. Flow rates ranged between 10 percent and 100 percent of the design value, and the salt level in the tank was the minimum

- Salt entered the distribution header at a temperature which was 60 °C above the initial reservoir temperature. Flow rates ranged between 10 percent and 100 percent of the design value, and the salt level in the tank was the minimum.

The load cases were developed from operating data provided by a commercial project.

The first parametric study showed that cold salt injection developed the largest temperature gradients in the floor.

Second Parametric Study

A second parametric study was based on the following parameters:

- Distribution header with a diameter equal to 55 percent of the tank diameter

- Option 1: Distribution header with 48 orifices distributed along the top of the pipe

- Option 2: Distribution header with 2 eductors; one pointed inwards, and the other pointed outwards. Both eductors had a 15 degree pitch relative to the horizontal, and both eductors were offset by 10 degrees from the radial orientation

- Cold salt injection, with a flow rate equal to the design value.

[20] Vast Energy, 'Reducing Thermal Loads in Tanks through Sparger Design', Presentation at SolarPACES 2024, 10 October 2024

With Option 1, the peak range in the floor temperature was 34 °C; with Option 2, the peak value was 17 °C. As such, the eductor arrangement in Option 2 is more effective at homogenizing the inventory temperature than the orifice arrangement in Option 1.

Third Parametric Study

A third parametric study was conducted, based on the following parameters:

- Distribution header with a diameter equal to 17 percent of the tank diameter
- Eductors with a pitch of 15 degrees, in combination with radial offsets of 10, 15, and 20 degrees
- Eductors with a pitch of 10 and 20 degrees, in combination with a radial offset of 15 degrees.

The arrangement with an eductor pitch of 15 degrees and a radial offset of 15 degrees showed the smallest range in floor temperature (17 °C). However, all of the combinations of pitch and radial offset showed ranges in the floor temperature that were no higher than 21 °C.

It should be noted that the parametric study examined only one tank diameter and a limited number of eductor arrangements. For a specific project, the optimum design for the distribution header will be a function of the tank dimensions, the allowable pressure drop between the downcomer and the tank inventory, and the selected process requirements (i.e., allowable difference in temperature between the salt in the downcomer and the salt in the tank).

5.12 Operator Actions

During receiver startup, the temperature of the salt leaving the receiver starts at the cold salt temperature (295 °C), and then increases to the normal design temperature (565 °C). Early in the startup process, salt is directed to the cold tank to prevent a noticeable decay in the inventory temperature of the hot tank. When the salt temperature in the downcomer reaches a defined crossover temperature, the flow is directed to the hot tank.

The crossover temperature is a function of the inventory temperature in the hot tank. A typical crossover temperature is 20 to 50 °C below the inventory temperature. Note that this phase of the startup process results in a small decay in the inventory temperature. However, the energy available in the salt at temperatures between the crossover temperature and the design temperature is still useful for electric energy production.

The decay in the inventory temperature is a function of the crossover temperature and the inventory level in the hot tank. The crossover temperature can be programmed in the DCS, and the control system will automatically open and close the tank diversion valves as necessary. However, as with most setpoints in the DCS, the operator is free to revise the setpoint. If the crossover setpoint is set to a low value, then additional thermal energy will be stored in the hot tank for electric energy production. During the project warranty and guarantee period, this can be an important consideration for the EPC contractor. However, the lower the setpoint, the greater the risk to the tank in terms of non-uniform temperature distributions, particularly in the floor, and the greater the potential for exceeding the limits from the vendor on the allowable rate of temperature change. Experience from more than one commercial project has shown that protecting the low cycle fatigue life of the tank often takes secondary importance to meeting the contractual requirements on energy production.

5.13 Cumulative Effects

As discussed above, plastic deformations in the floor could result from welding the floor plates, preheating the tank, and filling the tank with salt. The deformations may well take the form of buckles, or ridges, spanning a significant fraction of the diameter of the tank.

Once in commercial service, the tank will undergo a series of changes in level and changes in temperature. Some of these changes will place the floor into compression. If some of these loads cause the floor to yield, then the displacements are likely to appear as increases in the height of the ridges. The deformations can be compounded by local transient thermal stresses in the floor associated with receiver startups and receiver trips.

In tanks constructed from Type 347H, stress relaxation cracking will begin at the start of commercial service. The mechanism will progress at the highest rate at those locations with the largest residual stresses and the highest strains. The regions include the weld zones and the tops of the buckles.
At some point, 1) the progression of internal cracks and micro-voids generated by stress relaxation cracking, 2) in combination with cyclic compression / tension loads generated by friction, 3) in combination with a reduction in fatigue life at locations subject to plastic strains, 4) produces a crack at the top of the ridge. The crack is the source of the leak in the tank. This failure mechanism has been observed in a number of commercial projects.

It can be noted that ultrasonic examination of the welds in the floor and in the wall of a commercial tank has shown evidence of voids. The examinations were conducted after the tank had been in service for about 2 years. The formation of voids in 2 years is consistent with expected progression of stress relaxation cracking. If stress relaxation cracking is present, then strain localization at the grain boundaries can accelerate the damage due to low cycle fatigue.

5.14 Solutions

The question then arises: What solutions can be effected to prevent damage to the tank? Two approaches can be considered:

- A change in the tank design Codes
- Methods to reduce compressive loads on the floor.

5.14.1 Changes in the Tank Design Codes

Current Approach

To date, commercial tanks have been designed to the following combination of Standards and Codes:

- API Standard 650, Welded Steel Tanks for Oil Storage. However, the maximum design temperature in the Standard is 260 °C
- To overcome this limit, allowable material stresses are typically taken from Section II Part D Subpart 1A of the ASME Code for design temperatures above 260 °C
- Certain portions of the tank can operate at stresses greater than those listed in Section II. To ensure that the tank has a suitable fatigue life, the design by analysis requirements specified in Section VIII Division 2 are often adopted.

Stress Categories

The tank is subjected to a range of stress categories, including the following:

- Primary membrane stress, P_m, associated with static fluid pressures, operating pressures, and dead loads
- Local membrane stress, P_L, is a membrane stress typically generated by a discontinuity in the geometry
- Bending stress, P_b, produced, for example, by pressure applied to the central portion of a flat head
- Secondary stress, Q, produced by constrained thermal expansion or the bending stress at a structural discontinuity
- Peak stress, F, which does not cause any noticeable distortion but can be a source of a fatigue crack or a brittle fracture. An example is the thermal stress in the wall of a vessel caused by a rapid change in temperature.

Allowable Stress Values in Section VIII Division 2

In Section VIII Division 2, the allowable values for various combinations of stress categories is illustrated in Figure 5-21 and include the following:

- Primary membrane stress $P_m = S$, where S is the value listed in Section II Part D Subpart 1. For Type 347H stainless steel at a temperature of 565 °C, a representative value for S is 117 MPa
- Local membrane stress $P_L = 1.5 * S$, or 234 MPa
- Local membrane stress P_L + Bending stress $P_b = 1.5 * S$, or 234 MPa
- Local membrane stress P_L + Bending stress P_b + Secondary stress $Q = S_{PS}$, where S_{PS} is the larger of 1) 3 * S from Section II, Part D, Table 5A, and 2) 2 * S_y (yield stress) from Section II, Part D, Table Y-1. For Type 347H stainless steel at a temperature of 565 °C, a representative value for S_{PS} is 352 MPa
- Local membrane stress P_L + Bending stress P_b + Secondary stress Q + Peak stress $F = S_a$, where S_a is alternating stress. The limit for the stress is obtained from a fatigue curve for the specified number of operating cycles, with corrections applied to the curve for mean stresses other than zero.

The values for the stresses are generally determined by finite element analyses.

Stress Category	Primary			Secondary Membrane plus Bending	Peak
	General Membrane	Local Membrane	Bending		
Description (For examples, see Table 5.2)	Average primary stress across solid section. Excludes discontinuities and concentrations. Produced only by mechanical loads.	Average stress across any solid section. Considers discontinuities but not concentrations. Produced only by mechanical loads.	Component of primary stress proportional to distance from centroid of solid section. Excludes discontinuities and concentrations. Produced only by mechanical loads.	Self-equilibrating stress necessary to satisfy continuity of structure. Occurs at structural discontinuities. Can be caused by mechanical load or by differential thermal expansion. Excludes local stress concentrations.	1. Increment added to primary or secondary stress by a concentration (notch). 2. Certain thermal stresses which may cause fatigue but not distortion of vessel shape.
Symbol	P_m	P_L	P_b	Q	F

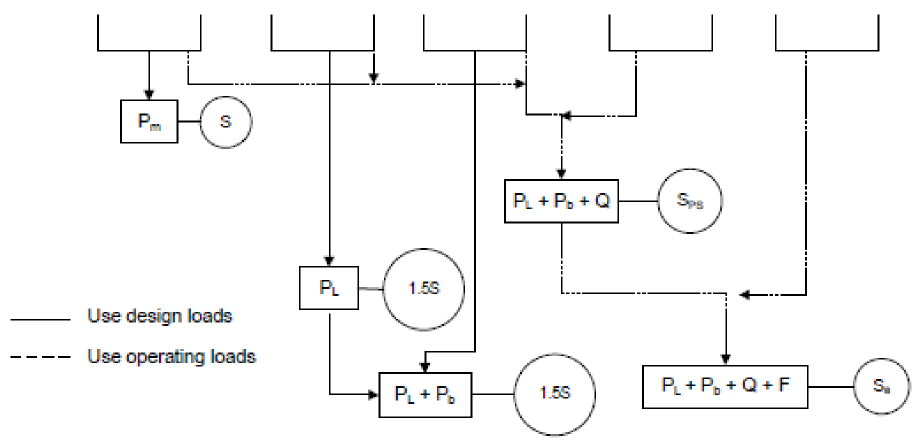

Figure 5-21 Combinations of Stresses and Allowable Values in Section VIII

<u>Limitations of Section VIII Division 2</u>

In the stress categories outlined in Figure 5-21, all of the allowable values are based on time-independent properties of the material. In particular, the effects of creep are not considered in the design.

In this design approach, the equipment is assumed to operate below the creep range by providing design margins against the following failure modes:

- Failure by plastic Instability or necking
- General structural collapse under a single application of limit load

- Time-independent buckling
- Incremental collapse or ratcheting under cyclic loading
- Fatigue under cyclic loading
- Fast fracture.

Nonetheless, preliminary calculations of the stresses in one commercial tank show values which are high enough (> 300 MPa) to 1) reduce the fatigue life to values less than the 30-year life of the project, and 2) initiate creep at the temperatures characteristic of a hot salt tank. Granted, none of the commercial tanks built to date have failed due to creep, but this may be due to a condition in which other failure mechanisms have reduced the life of the tank to values which are too short to allow significant quantities of creep to develop. In any event, all of the hot salt tanks built to date have failed in one way or another. As such, one could ask if the requirements in the Standards and Code sections noted above is the correct combination to use in the design and the analysis of the tank.

Alternate Design Codes

The requirements of Section III, Rules for Construction of Nuclear Facility Components, apply to materials in service at high temperatures.

Section III Division 1 Subsection NB provides rules for the design and the evaluation of pressure vessels, including the effects of fatigue. Nonetheless, the Subsection largely follows the design approach described for Section VIII Division 2. In addition, the effects of creep are largely avoided by limiting the maximum design temperature to 427 °C.

In contrast, Section III Division 1 Subsection NH provides rules for the design and the evaluation of pressure vessels, including the effects of both fatigue and creep. The Subsection applies to design temperatures up to 850 °C.

Operation at elevated temperature introduces time-dependent failure modes. The following six time-dependent failure modes are considered in the high-temperature design:

- Creep rupture under sustained primary loading
- Excessive creep deformation under sustained primary loading
- Cyclic creep ratcheting due to steady primary and cyclic secondary loading

- Creep-fatigue due to cyclic primary, secondary, and peak stresses
- Creep crack growth and nonductile fracture
- Creep buckling.

The process for equipment evaluation in Section NH is illustrated in Figure 5-22. The evaluation process, compared to Section VIII Division 2, includes an additional set of stress values and factors: S_o, S_m, S_t, S_{mt}, K, and K_t. The derivations of the values and factors are described below.

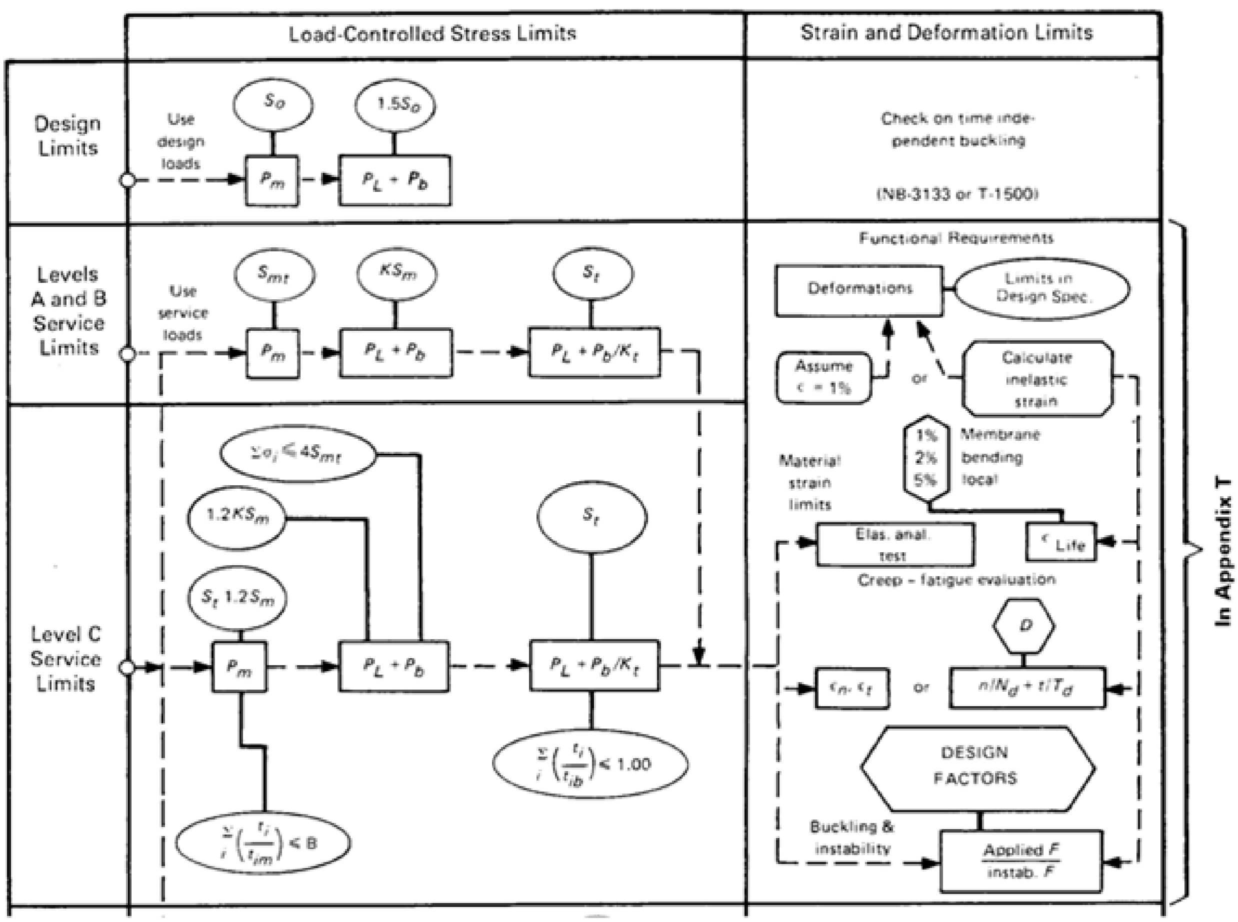

Figure 5-22 Equipment Evaluation Flow Diagram from Section III Subsection NH

S_o for Use in the Design Limits Calculation

S_o is the greater of the following two values:

- The maximum allowable stress value S in Section II Part D Table 1A. For Type 347H stainless steel at a temperature of 565 °C, the value is 110 MPa

- The S_m stress intensity at 300,000 hours in listed in Subsection HBB of the upcoming version of Section III Division 5, High Temperature Reactors. The text has yet to be published; however, publicly available inputs to the Section are available from Oak Ridge National Laboratory, Pacific Northwest Laboratory, Argonne National Laboratory, and NUMARK Associates. The value for S_m is listed as 53 MPa in the ORNL report [21].

As such, the value for S_o is 110 MPa.

Time-Dependent Stress Value, S_t

In the design rules of Subsection NH, the material has assumed to reach a temperature where creep can produce deformations of the structure. S_t is a time-dependent allowable stress, and is defined as the lesser of the following parameters:

- 100 percent of the stress required to produce a permanent creep strain of 1 percent in a defined period. The allowable stress is determined through the use of a Larson Miller curve, which plots the stress as a function of the metal temperature and the logarithm of the operating period. An example for Type 316 stainless steel is shown in Figure 5-23.

  The estimated stress to produce a 1 percent strain in 100,000 hours is 105 MPa

- 80 percent of the minimum stress to initiate tertiary creep. The creep characteristics are often divided into three phases: primary; secondary; and tertiary. The primary phase is generally short, and shows a relatively rapid change in dimension with time. The secondary phase is typically much longer. As the material deforms, its cross sectional area will reduce. However, the material also strain hardens. The increase in the strength generally offsets the reduction in area, and the true stress value remains nominally constant. At some point in the process, the effects of strain hardening cease and the material enters the tertiary phase. Gross deformations appear, which is generally followed soon after by rupture. Using a separate Larson Miller plot, the allowable stress to initiate tertiary creep is 84 MPa for a time span of 100,000 hours

[21] Ren, Weiju, et. al. (Oak Ridge National Laboratory, Oak Ridge, Tennessee), 'Technical Input for the Nuclear Regulatory Commission Review of the 2017 Edition of the ASME Boiler and Pressure Vessel Code, Section III, Division 5, High Temperature Reactors', Technical Letter Report ORNL/SPR-2020/1653, August 2020

- 67 percent of the minimum stress to cause rupture. Using a separate Larson Miller plots, the allowable stress is 106 MPa for a time span of 100,000 hours.

As such, the value for S_t is 84 MPa.

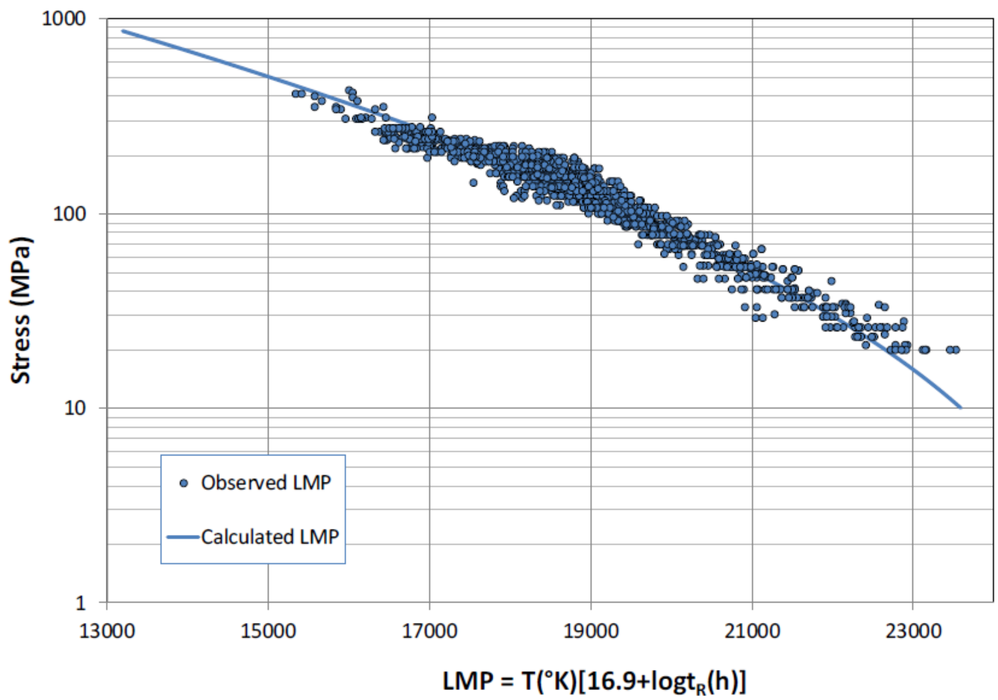

Figure 5-23 Larson Miller Diagram for the Stress to Develop 1 Percent Strain

<u>Time-Independent Stress Value, S_m</u>

S_m is the lesser of the following two values:

- 2/3 of the yield stress. For Type 347H stainless steel at a temperature of 565 °C, the value is 2/3 * 155 MPa = 103 MPa

- 1/3 of the tensile strength. For Type 347H stainless steel at a temperature of 565 °C, the value is 1/3 * 396 MPa = 132 MPa.

As such, the value for S_m is 103 MPa.

Lastly, S_{mt} is defined as the lesser of S_m (103 MPa) and S_t (84 MPa). As such, the value for S_{mt} is 84 MPa.

K has a value of 1.5 for shells and solid sections, and K_t is defined as (K + 1) / 2 = 1.25.

From the Design Limits portion of the flow chart in **Error! Reference source not found.**, the allowable p rimary membrane stress, P_m, is equal to S_o = 110 MPa. The allowable sum of the local membrane stress, P_L, and the bending load, P_b, is equal to 1.5 * S_o = 165 MPa.

For the Level A and B Service Limits, the allowable primary membrane stress, P_m, is equal to S_{mt} = 84 MPa. The allowable sum of the local membrane stress, P_L, and the bending load, P_b, is equal to 1.5 * S_m = 154 MPa. The allowable sum of the local membrane stress, P_L, and the bending load, P_b, modified by the K_t factor is equal to S_t = 84 MPa.

Comparison of Section VIII Division 2 with Section III Subsection NH

Effects of Creep

The effects of creep are associated with operation at high temperatures, and the rate of creep is influenced by the stress. One of the contributions to the total stress can be a thermal stress produced by temperature gradients in the equipment.

In Section VIII Division 2, thermal stresses are treated as secondary stresses. As shown in Figure 5-21, secondary stresses are not components in the design limit calculations involving the primary membrane stress, the local membrane stress, and the bending loads. As such, any creep generated by thermal stresses is not considered in the design calculations.

In contrast, in Section III Subsection NH, the flow diagram in Figure 5-22 requires an analysis of the following:

- Deformations, based on either 1) a maximum allowable strain of 1 percent, or 2) the results from an inelastic analysis
- A creep-fatigue evaluation based on summations of the damages associated with the number of fatigue cycles and creep durations
- Buckling and instability criteria.

Allowable Stresses

In Section VIII Division 2, the highest numerical value for the allowable stress is S_{PS}, with a value of 352 MPa. In contrast, in Section III Subsection NH, the highest numerical value for the allowable stress is 1.5 * S_o (165 MPa). This value is about one-half of the design value from Section VIII Division 2.

To date, no commercial tanks have been designed and built to the requirements of Section III Subsection NH, and direct comparisons to commercial tanks are, to some degree, conjectural. Nonetheless, differences are likely to be present in the following areas:

- Design limit and fatigue calculations from a representative commercial project show peak stresses on the order of 220 MPa at the connection between the floor and the wall. The calculations are based on a coefficient of friction of 0.2 between the floor and the foundation. Evidence from other studies indicate that the coefficient is more likely to be in the range of 0.5 to 1.0. If the tank stress calculations were repeated with a higher coefficient of friction, it's not clear that the design could satisfy the requirements of Section III Subsection NH

- As discussed in Section 5.7, steady state radial temperature gradients in the floor on the order of 5 °C can produce thermal stresses in the floor approaching the allowable value listed in Section II Part D Table 1A. In the design approach listed in Section VIII Division 2, these stresses are treated as secondary stresses, and do not influence the design limit calculations. In Section III Subsection NH, the thermal stresses in the floor will influence the creep and the fatigue assessments. This, in turn, may have an influence on the required design for the floor, which, in turn, would influence the buckling characteristics of the floor

- Based on the operating experience from a number of commercial tanks built to the requirements of API Standard 650, the vendor will often specify an allowable rate of temperature change. A representative value is 1 °C/min. However, operating data from the Crescent Dunes project has shown rates of change at least an order of magnitude higher. The fatigue damage associated with these rates of change has yet to be calculated. But, in future projects, the operating procedures must be specified in such a manner that the 30-year fatigue life of the tank can be satisfied.

Observations

Commercial tanks built to date have been designed using API Standard 650, Section II, and Section VIII Division 2. Essentially all of these tanks have developed leaks or other failures. Nonetheless, no studies have been conducted which demonstrate that this combination of design standards and codes, in combination of historical operating data on the tanks during transient conditions, has resulted in the tank failures. Similarly:

- Section III Subsection NH offers a more conservative set of design stresses and rules than Section VIII Division 2. However, no studies have been conducted which demonstrate that a tank, designed to the rules of Section III, would survive the life of the project

- The stresses in some portions of the tank, such as the wall and the roof, are generally predictable. As a result, it should be possible to estimate the creep and the fatigue life of these sections with an accuracy sufficient for a commercial project. In contrast, the stresses in the floor are not well understood, and the accuracies of the creep and fatigue calculations are generally unknown. As such, it may be possible to design the wall and the roof to the Codes typically used in previous commercial projects (i.e., API 650 and Section VIII Division 2), and adopt the more conservate design rules in Section III Division 5 for the floor.

Whichever combination of design rules is selected for the tank, the effect on the capital cost of the tank is likely to be modest. For example, in API Standard 650, the floor is essentially treated as a liquid boundary, and the thickness of the floor can be thin (i.e. 8 mm). However, following the rules of Section III Division 5, the allowable stresses associated with a creep and fatigue life of 30 years are relatively modest (~85 MPa), in which case the thickness of the floor may need to be double that of an API-style tank. Doubling the thickness of the floor increases the mass of steel in the tank by about 15 percent, which means, to a zeroth-order, that the capital cost of the tank also increases by 15 percent. A cost increase of this order will have essentially no effect on the financial status of the project.

To some extent, the industry is faced with the following conundrum:

- Can a set of analyses be conducted that convinces the financial community that a tank designed to the requirements of Section III Division 5, or a comparable international Code, will have an availability of 99.99 percent?

- In an ideal case, a flat bottom tank experiences uniform friction forces around the circumference of the tank. However, industry experience indicates that this may not be the case, as lateral movement of a tank in a commercial project has been observed. If it is not possible to determine the actual distribution of friction forces on the floor, then it may not be possible to determine the actual stresses in the floor. If so, an alternate tank concept, one that avoids a flat floor on a flat foundation, may be required to reach an availability of 99.99 percent. However, there will be no industry experience with an alternate tank design, and this will necessarily incur some form of technical and financial risk to the Owner

- The best, and perhaps the only, method to prove which design codes are the correct codes, and which tank concept is the correct tank concept, is to design, fabricate, and test a full-size tank at a commercial project over a period of several years. However, it's not clear who would be prepared to fund such a development program.

5.14.2 Methods to Reduce Loads on the Floor

Multiple Tanks

The peak loads in the floor are, to some degree, a function of the tank diameter. Substituting two 50-percent capacity tanks, or three 33-percent capacity tanks, for one 100-percent capacity tank could reduce the loads in the floor to values below a yet-to-be-defined damaging threshold. The relationship between floor stresses due to friction and tank diameter are discussed in Section 5.10.4.

In addition, multiple tanks provide a degree of redundancy, and eliminate the single point of failure problem with one 100-percent capacity tank.

Nonetheless, the failure mechanisms in commercial tanks are not yet fully understood. Adopting smaller tanks may be a step toward a reliable design approach, but the maximum allowable tank dimensions have yet to be defined and demonstrated.

Radial Gradients

A few methods for controlling the radial temperature gradient in the floor include the following:

<u>Insulation Design</u> The radial temperature gradients can be reduced by changing the insulation design at the perimeter of the tank. This may consist of greater insulation thicknesses at the base of the tank, and the addition of insulation on the refractory ring wall beneath the wall. Nonetheless, a radial temperature gradient will still develop, and if the inventory reaches, or approaches, a stagnation condition, then damaging stresses in the floor will result.

<u>Perimeter Heat Addition</u> The radial gradient can also be reduced by some form of heat addition at the tank perimeter. The heat addition might take the form of radiant electric heaters, installed beneath the wall insulation. The principal liability would be a slow response time due to limited radiation heat fluxes from radiant heaters to the tank wall. Alternately, electric heaters could be embedded in the refractory ring wall. As above, the principal liability would be a slow response time due to the combination of a modest thermal conductivity, and a high thermal inertia, of refractory materials.

<u>Multiple Distribution Headers</u> An alternate approach to controlling the radial gradients is a dedicated distribution ring at the perimeter of the tank. Salt flow to the distribution ring would be supplied by recirculation from one of the hot salt pumps. The goal would be to move salt from the bulk inventory to the tank perimeter, and thereby provide forced convection heat transfer to compensate for the higher heat losses at the perimeter. The ability to move heat by forced convection is generally large relative to conduction heat transfer. As such, it should be a straightforward exercise to reduce the magnitude of the radial gradient.

On a related point, the hot salt tank at the 10 MWe Solar Two demonstration project did not use a distribution ring header near the floor. Instead, a series of spray nozzles, supported from the inside of the roof, introduced salt into the tank. The (flawed) goal of the nozzles was to prevent the mixing of salt from the receiver, at a temperature of 565 °C, with the bulk inventory in the tank, which would normally be at a temperature less than 565 °C. The intent was to intentionally stratify the inventory, and only send salt, at a temperature of 565 °C, to the steam generator. This approach, of course, reduced mixing within the inventory, which promoted undesirable vertical radial temperature gradients in the floor. However, adding salt to the top of the inventory, rather than introducing salt near the floor by a distribution header, effectively isolated the floor from any transient conditions in the downcomer. To what extent this reduced the local transient stresses in the floor is unknown. However, the hot tank operated safely, without leaks, during the 3-year test and evaluation period.

In principle, a commercial project could also replace the conventional distribution header near the floor with a series of spray nozzles, or some other flow distribution arrangement, located inside the roof. Thermal stratification will inevitably occur. However, the methods discussed above, and below, should be effective in limiting both the vertical and the horizontal stratification to acceptable levels.

<u>Tank Scale Mixing Device</u> An alternate method to control the radial and the circumferential temperature gradients is to provide some form of a mixing device that spans the full dimensions of the tank. This might consist of a vertical shaft located at the center of the tank. Two to four vertical perforated plates would be attached to the shaft. The horizontal dimension of the plate would be somewhat less than the radius of the tank, and the height of the plate would be perhaps one half of the maximum liquid level. Rotating the shaft at a low speed, say 1 rpm, would keep the inventory mixed.

A second approach might be a perforated plate, with a diameter slightly less than the diameter of the tank. The plate would vertically traverse the depth of the inventory once every few minutes. Forcing a portion of the inventory to pass from the top of the plate to the bottom, and vice versa, would promote convection mixing at the perimeter of the tank.

It can be noted that the two approaches to whole-tank mixing are only conceptual, and additional design work is required to demonstrate that the concepts will work as intended. Nonetheless, the calculation of the floor stresses produced by radial temperature gradients (Section 5.7) and by circumferential temperature gradients (Section 5.11.2) indicate that intra-tank temperature differentials should be held to values no higher than perhaps 5 °C. It is unlikely that the static mixing generated by either one or two inlet distribution headers will satisfy a 5 °C limit, particularly at low flow rates or following a trip of the receiver. As a result, some form of active mixing device may be mandatory to protect the tank.

<u>Friction Forces with a Tank Scale Mixing Device</u> It can be noted that friction forces can develop in the floor, even with if the inventory temperatures are always isotropic. The effect occurs during startup of the receiver, as discussed in *Friction Forces*. As such, the use of a tank scale mixing device can help to control, but not fully eliminate, transient thermal stresses in the floor.

<u>Cold Tank Diversion Valve Failure and Tank Scale Mixing Device</u> On a related topic, the temperature distribution in the hot salt tank is determined by 1) conditions where the equipment (valves, instruments) operates as intended, and 2) conditions where the equipment does not operate as intended. One example of the latter is the following scenario:

- At the start an operating day, the hot tank is at the minimum level
- The receiver, after reaching normal operating conditions, trips. The receiver pumps are tripped. The circuit inlet control valves move to the 100 percent open position, and cold salt is supplied to the receiver from the pressurized inlet vessel
- The heliostat field, except for a limited number of heliostats providing a preheat flux, is defocused. The defocusing period requires about 60 seconds. During this period, the air pressure in the inlet vessel, and the salt flow rate to the receiver, follow an exponential decay
- The diversion valve in the downcomer, which directs flow to the cold salt tank, then malfunctions (fails to open). The temperature of the salt entering the hot tank decays from an initial value of 565 °C to the cold salt temperature of 295 °C at the projected rate of 360 °C/min.

The flow through the receiver is then stopped, and the receiver is drained. The temperature of the inventory in the hot tank, assuming perfect mixing, is shown in Figure 5-24.

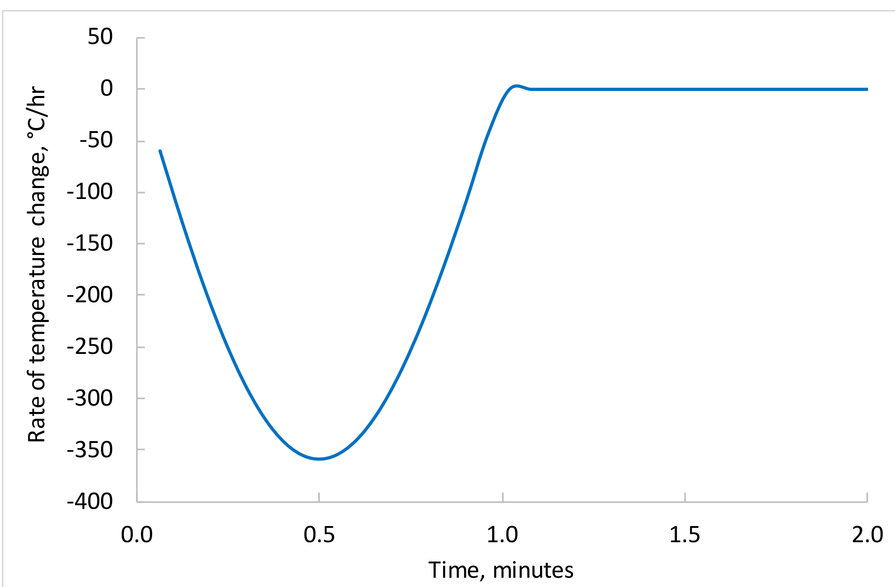

Figure 5-24 Hot Tank Temperature Following a Failure of the Cold Tank Diversion Valve

The peak cooling rate of -350 °C/hr is approximately 6 times the typical maximum rate allowed by the tank supplier. The stresses associated with this scenario have not been calculated, but local stresses above the yield value, and some loss in the fatigue life, would not be unexpected.

The failure of the cold tank diversion valve represents a single point failure, and would not be considered an improbable condition. As such, the design basis for the project should include this scenario, together with other potential single point failures, in an analysis of the fatigue life. If the analysis shows that damage to the tank can only be prevented (or meaningfully reduced) by some form of active mixing, then a mechanical mixer must be a feature of the tank design.

Friction Forces

During overnight hold periods, the temperature of the salt inventory in the tank decays. The tank thermally contracts, which places the floor in tension. Following the startup of the receiver, the temperature of the salt inventory increases. The tank starts to thermally expand, which 1) reduces the tensile stresses in the floor, and then 2) places the floor into compression. As discussed in Section 5.10.3, an increase in the inventory temperature of about 30 °C is sufficient to change the friction in the floor from the maximum tensile stress to the maximum compressive stress. The magnitude of the tensile or the compressive stress is directly proportional to the height of the salt in the tank.

During the plant design, finite element calculations of the stress in the floor should be developed for various combinations of temperature change, both positive and negative, and salt height. Allowable combinations are defined, such that the floor stresses satisfy the creep and the fatigue requirements. The allowable combinations are programmed into the distributed control system in the form of permissives. The permissives provide two useful functions:

- The operator is not allowed to make ad hoc decisions regarding inventory temperature and level that could have a detrimental effect on the creep and the fatigue life of the floor

- Over the course of a day, the inventory temperatures increase to values as high as possible, consistent with the allowable stresses in the floor. This, in turn, maximizes the daily electric output of the Rankine cycle, without compromising the long-term availability of the storage system.

As discussed in Section 5.10.3, a static coefficient of friction of 0.3 between the floor and the foundation may be high enough to produce yield stresses near the center of the tank. The most common lubricant for commercial tanks is sand. One reference for data on friction coefficients between steel and sand is a paper Usegusi [22]. However, in general, there are little data on the coefficients for sand at high temperatures. If experiments show that the coefficients are greater than about 0.4, then sand may not be a suitable solid lubricant.

An alternative high temperature lubricant may be boron nitride. During construction, the boron nitride would be applied to the top of the foundation material (presumably refractory bricks) as a water/boron nitride suspension. However, there are no data on how long the boron nitride layer might survive. If the layer becomes eroded, it may be possible to renew the lubricant by injecting a water/boron nitride suspicion through an array of pipes installed at the top of the foundation. A series of experiments, at the full design temperature of the tank, would need to be conducted to demonstrate the feasibility of this approach.

An alternate solid lubricant is graphite. However, the galvanic potential between carbon and stainless steel is large. Pitting corrosion of the stainless steel is likely, which makes graphite a poor candidate.

Tanks Without Flat Floors

Flat bottom tanks, with self-supporting dome roofs, have been universally adopted in the solar industry due to their low cost. However, this design is not the only option for the industry.

<u>Elevated Tanks</u>

Elevated water storage tanks, in capacities up to 11,300 m^3 (3,000,000 gallons), are commercially available from a number of suppliers. To replicate the storage volume at Crescent Dunes (17,500 m^3) two tanks, similar to that shown in Figure 5-25, would be required. For a solar project, the tanks would be elevated by only a small amount, perhaps 1 m, above grade.

The tanks are supported either on single column, as shown above, or on a series of legs, attached to the side of the tank. With this arrangement, there are no friction loads on the floor, and many of the structural problems with flat bottom tanks can be avoided.

Naturally, this type of tank has a number of characteristics which will increase the cost relative to a flat bottom tank, as follows:

[22] Uesugi, Morimichi, et. al., (Department of Architectural Engineering, Chiba University, Japan), 'Friction Between Sand and Steel under Repeated Loading', Soils and Foundation Volume 29, No. 3, 127-137, September 1989, Japanese Society of Soils Mechanics and Foundation Engineering

Figure 5-25 11,300 m^3 (3,000,000 gallon) Elevated Water Storage Tank

- The vertical loads are taken either at a central location or by a series of columns located around the circumference of the tank. The concentrated loads, relative to a flat bottom tank, will incur a significant increase in the cost of the foundation

- The bottom of the curved tank is exposed to hydrostatic loads which are higher than those seen in a flat bottom tank. This will lead to an increase in the thickness, and the cost, of the bottom of the tank.

Nonetheless, the cost of the hot salt tank in a solar project is on the order of 2 to 3 percent of the cost of the project. If switching from a flat bottom tank to an elevated tank doubled the cost of the tank, then the net change to the project is perhaps a 2 to 3 percent increase in the capital cost. However, if the availability of the project improves by, say, even 5 percent due to the avoidance of a tank failure, then the increase in the cost of the tank is fully justified.

<u>Horizontal Tanks</u>

The lowest risk approach is, perhaps, a field of horizontal cylindrical tanks. The tanks are supported on saddles, which avoids any problems with friction. Further, the geometry is favorable in terms of accommodating both high rates of temperature change and non-uniform temperature distributions in the inventory.

Horizontal tanks are available from a number of commercial suppliers. The maximum practical diameter and length are on the order of 3.5 m (11 ft.) and 40 m (130 ft.), respectively, based on shipping considerations. To replicate the storage volume at Crescent Dunes (17,500 m^3), some 44 tanks would be required.

On a related point, it may be possible to reduce the number of tanks to 24 using an N + 1 arrangement. Specifically, one of the tanks would always be a cold tank, one of the tanks would always be a hot tank, and the balance of 22 tanks would operate either as a cold tank or a hot tank, depending on the state of charge in the storage system. Naturally, switching from cold tank status to hot tank status would result in rapid changes in the metal temperature. Finite element calculations of the transient stresses in the tank would first need to be conducted to verify the practicality of this approach.

Returning to the original estimate of 44 tanks, the mass of steel in 44 horizontal tanks is about 2.8 times the mass of steel in a single, flat bottom tank, and a cost comparison of the two options would reflect this difference. The surface area of 44 horizontal tanks is slightly more than 6 times the surface area of a single, flat bottom tank. It would be prohibitively expensive to insulate 44 horizontal vessels, particularly if the cost of the heat loss through the insulation was considered in the analysis. However, it may be possible to locate the 44 vessels in a common enclosure, and then insulate the outside of the enclosure.

To a first order, replacing a single, flat bottom hot tank with 44 horizontal tanks is likely to triple the cost of the hot tank. However, as noted above, the cost of the hot tank is 2 to 3 percent of the cost of the project. If the cost of the tank triples, then the cost of the project increases by something approaching 6 percent. However, if the flat bottom tanks are judged to be unsuitable for service as a hot tank, then the maximum penalty incurred by switching to a low risk design is on the order of 6 percent.

5.15 Lifetime Assessment

The material in a tank is subjected to cyclic stresses, environmental effects (i.e., corrosion), and continuous stresses. The life of the material, N_f, is a function of the accumulated damage due to fatigue, corrosion, and creep, and can be represented as follows:

$$\frac{1}{N_f} = \frac{1}{N_f^{Fatigue}} + \frac{1}{N_f^{Oxidation}} + \frac{1}{N_f^{Creep}}$$

A range of considerations in evaluating the fatigue, the corrosion, and the creep lives of the tank are outlined in the sections below.

5.15.1 Fatigue Assessment

The number of stress (or strain) cycles that a material can tolerate before fracture is a function of the material, the temperature, and the range of the stress (or strain). Fatigue data are typically generated for smooth bar samples, with a nominal cyclic strain rate of 0.001 in/in-sec.

Representative S-N (Stress-Number of cycles to failure) curves for Type 316 stainless steel are shown in Figure 5-26.

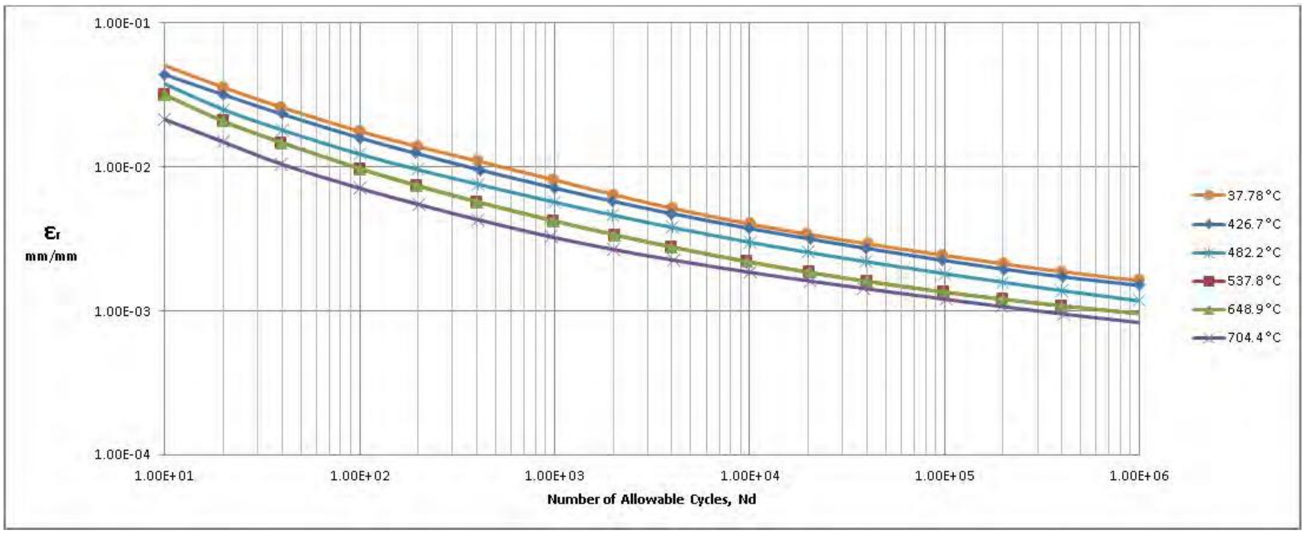

Figure 5-26 S-N Curves for Type 316 Stainless Steel

Nonetheless, and as might be expected, the material in a salt tank, particularly after welding, has markedly different fatigue characteristics than a smooth bar sample. The factors which influence the fatigue life include weld surface fatigue strength reduction factors, weld misalignment fatigue strength reduction factors, and fatigue life knockdown factors.

Weld Surface Fatigue Strength Reduction Factors

When a metal is welded, changes occur in the material properties, the grain structure, and state of stress. As might be expected, the fatigue properties in the weld region are generally inferior to the fatigue properties of the parent material. The fatigue properties of a weld, in turn, are influenced by the type of the weld, the surface condition, and the non-destructive examination methods. The effects are incorporated in the fatigue analysis by a fatigue strength reduction factor. The factor is a stress intensification value which accounts for the effect of a local structural discontinuity (stress concentration) on the fatigue strength. The factor is the ratio of the fatigue strength of a component without a discontinuity or weld joint to the fatigue strength of that same component with a discontinuity or weld joint. The factor is a multiplier on the alternating stress value used in the S-N curves; it is not a reduction factor on the fatigue life.

Fatigue strength reduction factors for a range of weld surface conditions are presented in Table 5-2. The weld quality levels are defined in Table 5-3.

Table 5-2 Weld Surface Fatigue Strength Reduction Factors - Table 1 of 2

Weld Condition	Surface Condition	Quality Levels (see Table 5.12)						
		1	2	3	4	5	6	7
Full penetration	Machined	1.0	1.5	1.5	2.0	2.5	3.0	4.0
	As-welded	1.2	1.6	1.7	2.0	2.5	3.0	4.0
Partial Penetration	Final Surface Machined	NA	1.5	1.5	2.0	2.5	3.0	4.0
	Final Surface As-welded	NA	1.6	1.7	2.0	2.5	3.0	4.0
	Root	NA	NA	NA	NA	NA	NA	4.0
Fillet	Toe machined	NA	NA	1.5	NA	2.5	3.0	4.0
	Toe as-welded	NA	NA	1.7	NA	2.5	3.0	4.0
	Root	NA	NA	NA	NA	NA	NA	4.0

In commercial tanks, the floor plates are typically welded using backing strips. The backing strips aid in the alignment of the welds between plates, which helps to reduce the fatigue strength reduction factors associated with weld misalignments (see Section *Weld Misalignment* below).

<u>Code Guidelines</u>

Section NH-3352(c) in Section III states *When Category B joints with backing strips not later removed are used, the suitability for cyclic operation shall be analyzed using a fatigue strength reduction factor of not less than 2 under conditions where creep effects are insignificant [NH-3211(c)]. For conditions where creep effects are significant, see NH-3353(b).* Category B joints are butt joints, which is the typical weld joint in a floor.

Further, Section NH-3352(e) states *Where partial penetration welds are used, a fatigue strength reduction factor of not less than 4 shall be used for any related fatigue and analysis under conditions where creep effects are insignificant [NH-3211(c)]. For conditions where creep effects are significant, see NH-3353(b).* Anecdotal evidence from the postmortem examinations of floors in commercial projects show evidence of misaligned welds with incomplete penetration.

As discussed in the section of this report titled *Comparison of Section VIII Division 2 with Section III Subsection NH*, creep effects in a hot salt tank are not likely to be insignificant. Along these lines, Section NH-3353(b) states *For meeting the analysis requirements of NH-3251 at elevated temperature weld regions, the assumed weld surface should model the most severe strain concentrations expected in the actual weld placed in service. This geometry may be prescribed on a drawing or may be recorded by prior observation. Prior observations of weld surface geometry can be visual; remote visual (e.g., using a borescope device or making a surface replica); or ultrasonic, based on a weld mockup test in which the same weld procedures are used on the same nominal pipe diameter and wall thickness, or based on a radiographic technique that is suitable for inspection of internal surfaces.* (Section NH-33353(b) references *Welded Joints*, and the Section is likely applicable to joints other than piping connections.)

Table 5-3 Weld Surface Fatigue Strength Reduction Factors - Table 2 of 2

Fatigue-Strength-Reduction Factor	Quality Level	Definition
1.0	1	Machined or ground weld that receives a full volumetric examination, and a surface that receives MT/PT examination and a VT examination.
1.2	1	As-welded weld that receives a full volumetric examination, and a surface that receives MT/PT and VT examination
1.5	2	Machined or ground weld that receives a partial volumetric examination, and a surface that receives MT/PT examination and VT examination
1.6	2	As-welded weld that receives a partial volumetric examination, and a surface that receives MT/PT and VT examination
1.5	3	Machined or ground weld surface that receives MT/PT examination and a VT examination (visual), but the weld receives no volumetric examination inspection
1.7	3	As-welded or ground weld surface that receives MT/PT examination and a VT examination (visual), but the weld receives no volumetric examination inspection
2.0	4	Weld has received a partial or full volumetric examination, and the surface has received VT examination, but no MT/PT examination
2.5	5	VT examination only of the surface; no volumetric examination nor MT/PT examination.
3.0	6	Volumetric examination only
4.0	7	Weld backsides that are non-definable and/or receive no examination.

Notes:

1. Volumetric examination is RT or UT in accordance with Part 7.
2. MT/PT examination is magnetic particle or liquid penetrant examination in accordance with Part 7
3. VT examination is visual examination in accordance with Part 7.
4. See WRC Bulletin 432 for further information.

With floor plate thicknesses in the range of 6 to 8 mm, two weld passes would be typical. In terms of weld examination, the most problematic location would be the bottom of the root pass; i.e., the weld surface which is in contact with the top of the weld backing plate. Two problems can occur:

- Currently, there is no mechanism to visually examine the surface of this weld, looking for signs of the following:
    - Incomplete penetration or fusion
    - Oxidation. The quality of the weld will depend, in part, on the ability of the weld backing strip to capture and retain the cover gas (argon) in the weld zone. Any oxygen present in the weld zone can cause the filler material and the edges of the heat affected zone to oxidize. The result can be a weld with a high porosity and a low strength.

- There is a long total length of the welds to examine in a floor. Common non-destructive examinations typically include dye penetrant and vacuum box tests due to their speed and low cost. These examination methods can result in a low value for the weld quality presented in Table 5-3.

Based on these assessments, a weld surface fatigue strength reduction factor in the range of 2.5 to 4.0 can likely be justified.

Weld Misalignment Fatigue Strength Reduction Factors

Steel plates for the tank floor are typically fabricated to nominal dimensions for length, width, thickness, and flatness. Allowable tolerances on the dimensions are defined in ASTM A480, Standard Specification for General Requirements for Flat-Rolled Stainless and Heat-Resisting Steel Plate, Sheet, and Strip. For a floor plate which has a width of 2.5 m, a length of 12.0 m, and a thickness of 8 mm, the allowable tolerances include the following:

- Variation in thickness of -0.00 mm to +1.30 mm

- Panels cut by shearing
    - Variation in width of -0 mm to +20 mm
    - Variation in length of -0 mm to +75 mm

- Panels cut by water jet
    - Variation in width of -0 mm to +3.2 mm
    - Variation in length of -0 mm to +3.2 mm

- Variation in flatness of 14 mm.

When the panels are arranged on the foundation prior to welding, the tolerances will result in the following effects:

- The tops of all of the plates will not all be in the same horizontal plane
- The bottoms of all of the plates will not all be in the same horizontal plane
- The edges of the plates will not all be parallel.

As a consequence, some level of weld misalignment is inevitable.

The effects of weld misalignment on the fatigue life of a structure are discussed in Part 8, Assessment of Weld Misalignment and Shell Distortions, in API 579-1 / ASME FFS-1. The effects are calculated using the following expression:

$$\Delta S_p = \sigma_{ms}\left(1 + R_b^{pc} + R_b^{pa}\right) K_f$$

where ΔS_p is the range of primary plus secondary plus peak equivalent stress, MPa
σ_{ms} is the membrane stress from supplemental loads, MPa
R_b^{pc} is the adjustment factor for centerline misalignment, [ ]
R_b^{pa} is the adjustment factor for angular misalignment, [ ]
K_f is weld fatigue strength reduction factor, [ ].

Supplemental loads include, but are not limited to, the weight of the component, contained fluid, insulation or refractory; loads resulting from the constraint of free thermal expansion, thermal gradients or differences in thermal expansion characteristics; occasional loads due to wind, earthquake, snow, and ice; loads due both to environmental and operating conditions; reaction forces from fluid discharges; loads resulting from support displacements; and loads due to process upset conditions.

Equations for calculating the R_b factors are listed in Table 5-4.

<u>Centerline Misalignment</u>

Centerline misalignment in flat plates with a butt weld is defined in Figure 5-27. 'P' is the applied load, 't' is the plate thickness, and 'e' is the weld offset.

<u>Angular Misalignment</u>

Angular misalignment in flat plates with a butt weld is defined in Figure 5-28. 'P' is the applied load, and Θ_p is the angular misalignment. The dimension 'L' is defined in Figure 5-29.

Table 5-4 Equations for Calculating the R Factors in the Equation for ΔS_p

Type Of Misalignment	Equations For R_{bs}
Flat Plate – Centerline Offset (see Figure 8.2) (1)	$R_{bs}^{pc} = 6\left(\frac{e}{t_{1c}}\right)\left(1+\left(\frac{t_{2c}}{t_{1c}}\right)^{1.5}\right)^{-1}$ Limitations: $0.0 \le e \le t_{1c}$, $t_{2c} \ge t_{1c}$
Flat Plate – Angular Misalignment (see Figure 8.4) (1)	$R_{bs}^{pa} = 3\left(\frac{\delta}{t_c}\right)C_f$ where: $\delta = \frac{L\theta_p}{4}$ $(\theta_p \ in \ radians)$ $C_f = \left(\frac{2}{\beta}\right)\cdot\tanh\left[\frac{\beta}{2}\right]$ $(for \ fixed \ ends)$ $C_f = \left(\frac{2}{\beta}\right)\cdot\tanh\left[\beta\right]$ $(for \ pinned \ ends)$ $\beta = \frac{L}{t_c}\sqrt{\frac{3\sigma_m}{E_y}}$ $(in \ radians)$ Limitations: $\theta_p \ge 0.0$
Note: The equation for R_b and R_{bs} are dimensionless.	

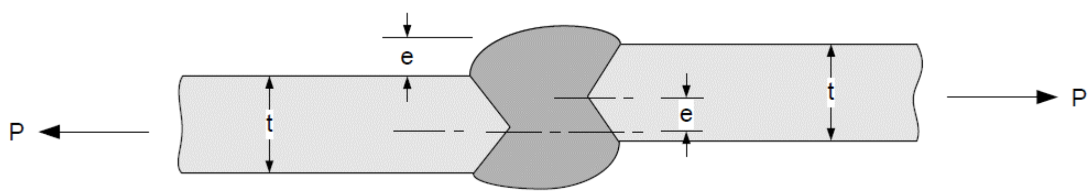

Figure 5-27 Centerline Offset Misalignment of Butt Welds in Flat Plates

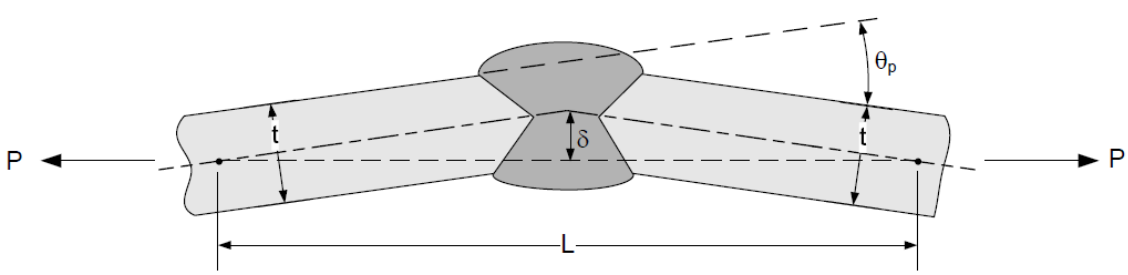

Figure 5-28 Angular Misalignment of Butt Weld Joints in Flat Plates

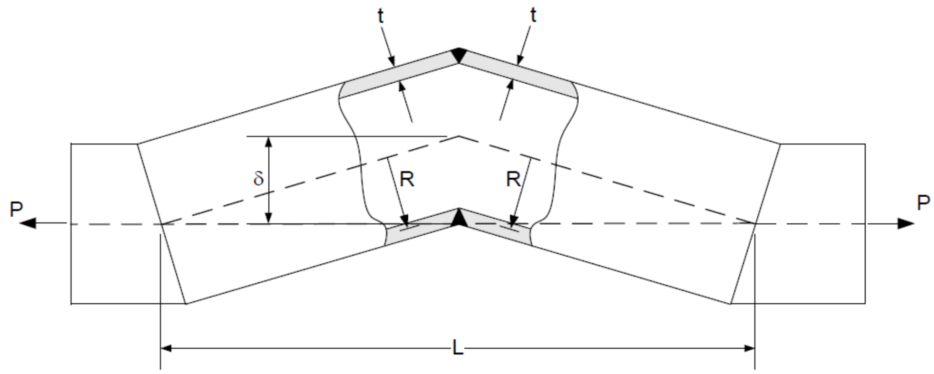

Figure 5-29 Definition of Dimension L in Figure 5-28

The calculated value for R_b^{pc}, the adjustment factor for centerline misalignment, for a range of offsets is shown in Figure 5-30.

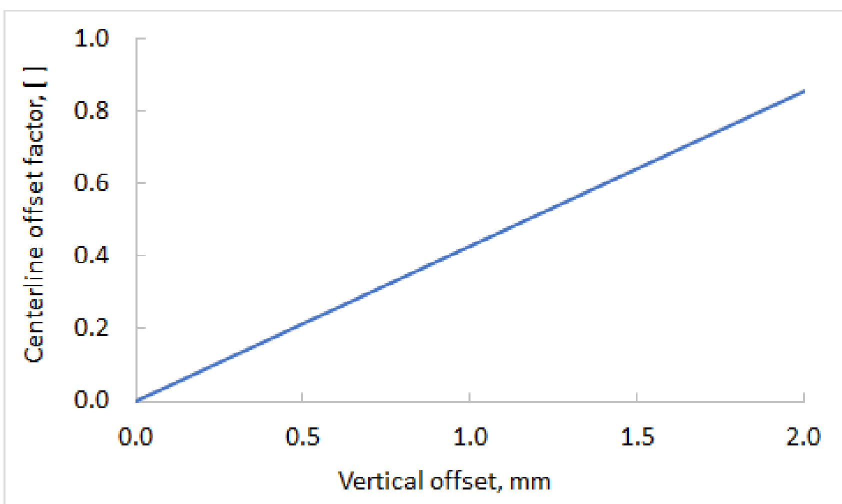

Figure 5-30 Adjustment Factor for Centerline Misalignment

The calculated value for R_b^{pa}, the adjustment factor for angular misalignment, for a range of angles is shown in Figure 5-31. For the purposes of the example, the sum of the supplemental loads is taken to be 200 MPa.

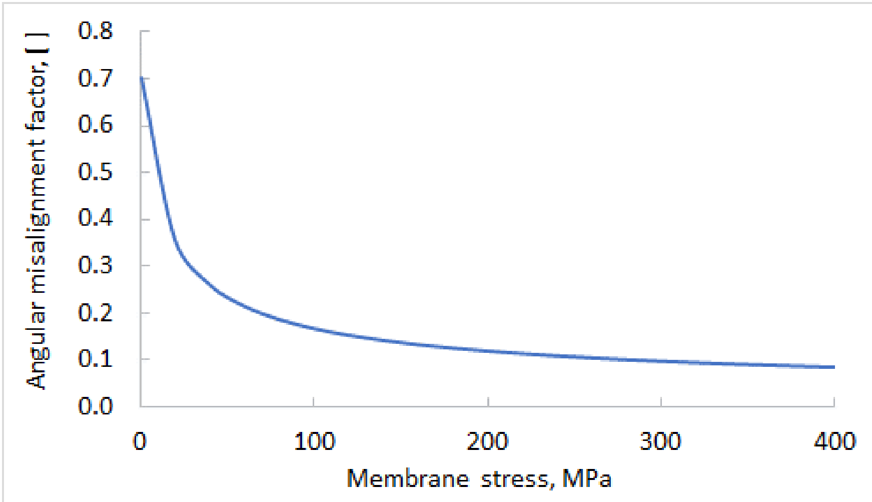

Figure 5-31 Adjustment Factor for Angular Misalignment

<u>Representative Misalignment Factors</u>

The centerline offsets and the angular misalignments in the tank in a commercial project likely span a fairly broad, and perhaps random, set of values. For the purposes of this discussion, the minimum centerline offset between adjacent plates is judged to be not less than 0.5 mm (1/64 in.). This is particularly so if the plate, as delivered, 1) deviates from flat by the maximum allowable value of 14 mm, and 2) the plate must be mechanically pushed flat against the foundation prior to welding. If the centerline offset is 0.5 mm, then the fatigue adjustment factor is on the order of 0.2.

Defining an angular misalignment is somewhat more problematic. With the plates arranged on the foundation, prior to welding, the angular misalignment should be zero. To start the welding process, the plates are tack-welded to one another, but this should not influence the angular misalignment. However, when Plate 1 is welded to Plate 2, the two plates start to form a domed shape. If the height of the dome, after the welding is complete, is 100 mm (see Section 5.5.2), then the out-of-plane angle at the edge of the plate is approximately $\tan^{-1}$(100 mm/1,250 mm) = 4.5 degrees, where 1,250 mm represents one-half of the width of the plate. When the tank is initially filled with salt, hydrostatic loads push the plates flat against the foundation. The bending stresses at the edges of the plates are equal to, or somewhat higher, than the yield stress. As such, most of the 4.5 degree angular misalignment disappears. However, some residual value of the stress will remain, which will retain some level of bending displacement at the edge. For purposes of the discussion, the residual bending misalignment is taken to be 0.25 degrees. If the stresses in the floor are in the range of 100 to 200 MPa, then the value for the angular misalignment factor is approximately 0.15.

With these representative factors, the weld fatigue strength reduction factor selected above in the Section titled *Weld Surface Fatigue* Strength Reduction Factors is further multiplied by a factor of (1 + 0.2 + 0.15) = 1.35. This would result in composite reduction factors in the range of 1.35 * 2.5 = 3.4 to 1.35 * 4.0 = 5.4.

It can be noted that increasing the thickness of the floor reduces the centerline offset misalignment factor (assuming that the vertical offset is maintained at 0.5 mm). However, the angular misalignment factor remains unchanged with a thicker floor.

Fatigue Strength Knockdown Factors

For areas not adjacent to welds, the fatigue life of commercial equipment is likely to be shorter than the fatigue life measured in smooth bar tests. The effect on the fatigue life, in areas not adjacent to welds, can be estimated using fatigue life knockdown factors. Several of these factors are outlined in Table 5-5. Unlike the fatigue strength reduction factors discussed in the sections above, the knockdown factor is a divisor on the smooth bar fatigue life, rather than a multiplier on the alternating stress.

The size effect factor accounts for equipment which has larger dimensions, and therefore has a shorter fatigue life, than the small samples typically used to develop fatigue data. Similarly, the surface finish effect accounts for equipment surfaces which are rougher, and therefore have a shorter fatigue life, than smooth far samples. The data scatter factor accounts for the statistical nature of the smooth bar fatigue curves, and provides a degree of conservatism in the estimated life of the commercial equipment. Environmental effects are discussed below in the Section 5.15.2.

Using the factors in the column labeled ASME results, and an allowance for a surface finish factor of 1.5, results in an overall knockdown factor of 2.5 * 1.5 * 2 = 7.5.

5.15.2 Corrosion Assessment

Stainless steel, when exposed to salt, develops an outer corrosion layer. The layer consists of various nickel and iron oxides. The corrosion layer controls the principal corrosion mechanism for stainless steel, which is the diffusion of chromium from the metal into the salt.

In corrosion studies conducted at Sandia and at other laboratories, the corrosion coupons are typically free of internal and external stresses. However, under cyclic conditions, corrosion layers can develop when the material is at a high temperature and under compressive stress. During the balance of the cycle, the material can cool and the compressive stress can switch to a tensile stress. This can form microcracks in the oxide layer, which expose the parent material to an accelerated corrosion rate due to thinning, or the local removal, of the oxide layer.

Table 5-5 Fatigue Life Knockdown Factors

Item	ASME	PVRC Working Group on S-N Data		PVRC Working Group on Evaluation Methods	
		Best Estimate Of Margin Needed	Conservative Estimate Of Margin Needed	Best Estimate Of Margin Needed	Conservative Estimate Of Margin Needed
Size Effect	2.5	1	1.2	1.0	1.2
Surface Finish	4 (1)	1.5	2	1.0	1.5
Data Scatter	2	2	2.5	2.0	2.5
Environmental Effects	4 (1)	2.5	4	---	---
Loading time history Effects	NC	1	1	1.0	2.5
Multi-Axial Stress Field	---	---	---	1.0	1.3
Sum	20	7.5	24	2.0	14.6

Notes:
1. Surface finish and environmental combined with a margin of 4.
2. From WRC 487, Table 1.

This corrosion mechanism could occur in the floor of a hot tank due to a combination of 1) receiver start and stop cycles, 2) daily reversals in friction direction, and 3) changes in the stresses due to changes in the radial temperature gradient. If the floor is operating at stresses above than the yield stress, then the associated strains could be large enough to damage the outer oxide layer. This could change the shape of the corrosion rate-versus-time curve from parabolic (desired) to linear (not desired).

In general, the magnitude of this potential effect is largely unknown. Only after one or more commercial tanks have been in service for several years, and the inner surfaces examined for signs of non-uniform corrosion layers, can some form of an assessment be made.

5.15.3 Creep Assessment

WRC Bulletin 541

The Welding Research Council publishes Bulletin 541, Evaluation of Material Strength Data for Use in API Standard 530. Standard 530, in turn, is the Calculation of Heater-tube Thickness in Petroleum Refineries. The methods described in Bulletin 541 optimize the Larson-Miller Parameter (LMP) stress-rupture coefficients of the materials listed in API Standard 530.

The time to rupture, L [hours], is estimated by the following equation:

$$log_{10}[L] = \frac{LMP(\sigma)}{T} - C_{LMP}$$

where LMP is the Larson Miller parameter corresponding to the applied stress
σ is the applied stress, MPa
T is the absolute temperature, °K
C_{LMP} is a constant for the material, []

The stresses associated with times to rupture in the range of 1,000 hours to 1,000,000 hours are shown in Figure 5-32. The nominal life of the hot salt tank is 30 years, or 300,000 hours. The associated stress for both Type 316 / 316H and Type 347 H is a nominal value of 134 MPa.

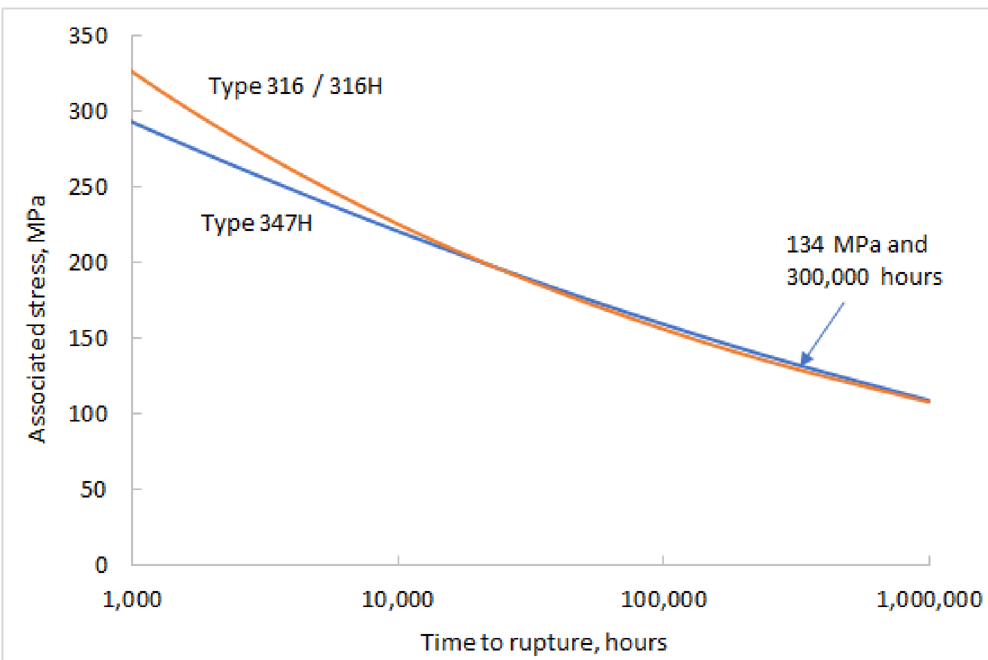

Figure 5-32 Bulletin 541 Time to Rupture and Stress For Type 316/316H and Type 347H

To a first order, any permanent stress in the tank cannot exceed a value of 134 MPa; otherwise, that portion of the tank can fail due to rupture.

Project Omega

The assessment techniques developed under the Materials Properties Council (MPC) Project Omega program provide a method for estimating the remaining life of a component operating in the creep regime. A strain-rate parameter and multi-axial damage parameter (Omega) are used to predict the rate of strain accumulation, creep damage accumulation, and remaining time to failure as a function of stress state and temperature.

The equations are presented in Annex 10B - Material Data for Creep Analysis (Normative) in API 579-1 / ASME FFS-1. Equation coefficients for Type 347H are listed in Table 10B.1M, MPC Project Omega Creep Data (MPa, °C).

The stresses associated with times to rupture in the range of 1,000 hours to 1,000,000 hours are shown in Figure 5-33. With a creep rupture life of 300,000 hours, the associated stress for Type 347 H is a nominal value of 127 MPa.

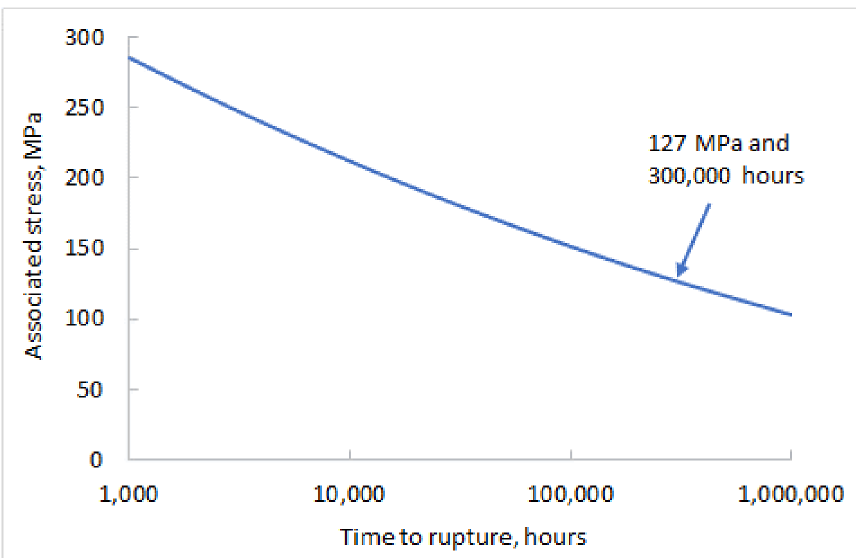

Figure 5-33 Project Omega Time to Rupture and Associated Stress For Type 347H

The permanent stress in the tank cannot exceed a value of 127 MPa if the creep rupture life is to exceed 30 years.

5.15.4 Subset of Creep Assessment in Weld Regions

The coefficients for the Larson Miller equation (LMP(α), C_{LMP}) in WRC Bulletin 541 and in Project Omega are based on materials in the as-received condition; i.e., prior to welding. The value for C_{LMP} is typically taken as a constant for the material.

The value for C_{LMP} is obtained by plotting experimental creep data in log(time [hours]) versus 1/(Absolute Temperature[K]). An example for an austenitic stainless steel is shown in Figure 5-34 [23].

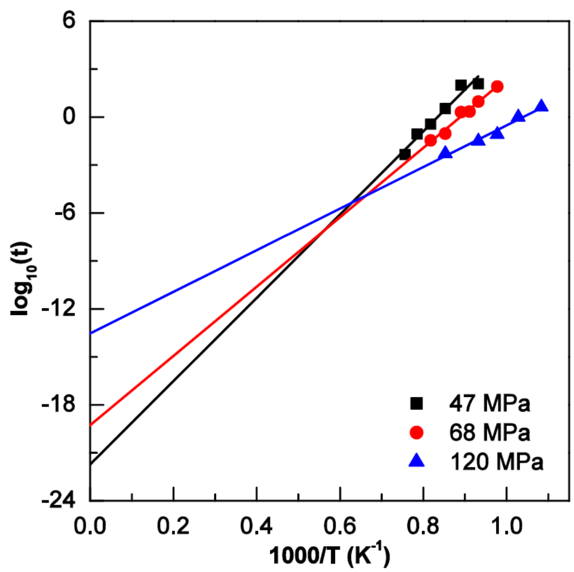

Figure 5-34 Graphical Calculation of Larson Miller Coefficient C_{LMP}

As noted in the Figure, the value for C_{LMP} is not a constant; it is a function of the applied stress.

During welding, residual stresses are developed in the weld region. The stresses are a function of the weld filler material, the heat input to the weld, the number of passes, and the location in the weld zone. The last item incorporates the fusion zone, the partially melted zone, and the heat affected zone.

The creep life will be a function of the sum of the operating stresses and the residual welding stresses. This implies that the Larson Miller coefficients will vary among the fusion zone, the partially melted zone, the heat affected zone, and the zones which are not welded. Further complicating the calculation of the creep life is the expected relaxation of the residual welding stresses over time, as shown in Table 5-1 Stress Relief as a Function of Temperature.

[23] Ghatak, A., and Robi, P. S. (Department of Mechanical Engineering, North Eastern Regional Institute of Science and Technology, Nirjuli, India), Modification of Larson–Miller Parameter Technique for Predicting Creep Life of Materials, Transactions of the Indian Institute of Metals, DOI 10.1007/s12666-015-0803-6, December 2015

To account for the variation in C_{LMP} with stress, the authors in the referenced paper propose the following modified equation to estimate the creep lifetime:

$$log_{10}[L] = \frac{LMP(\sigma)}{T} - C_{LMP1} - C_{LMP2}\sigma$$

where LMP is the Larson Miller parameter corresponding to the applied stress
σ is the applied stress, MPa
T is the absolute temperature, °K
C_{LMP1} and C_{LMP2} are constants for the material, []

Ideally, different values for LMP(σ), C_{LMP1}, and C_{LMP2} would be developed for the fusion zone, the partially melted zone, the heat affected zone, and the zones which are not welded. However, the degree to which the ideal can be approached has yet to be determined. Specifically, the various coefficients are developed experimentally. Further, the accuracies of the coefficients are improved if the experiments are conducted at temperature representative of a commercial project; i.e., 600 °C. However, at these temperatures, creep lifetimes can be the order of tens of years if the stresses are modest (< 150 MPa). As a result, the uncertainties in the estimates of creep lifetime, particularly in the weld zones, are likely to remain high for at least the next generation of commercial projects.

5.15.5 Subset of Creep Assessment in Buckled Regions

In several commercial projects, the tank floors have developed buckles, with the buckles largely spanning the diameter of the tank. For the purposes of discussion, the thickness of the floor is taken to be 7 mm, and the inner radius of the plate at the top of the buckle is assumed to be 50 mm. Bending the floor in this shape generates a tensile strain of 0.065 on the top surface of the buckle, and a compressive strain of - 0.065 on the bottom surface of the buckle.

Using information from Section VIII, Division 2, Annex 3.D, for 300-series stainless steel at a temperature of 565 °C, a strain of 0.065 represents a true stress of approximately 260 MPa, as shown in Figure 5-35. The true stress and the true strain values include the effect of strain hardening.

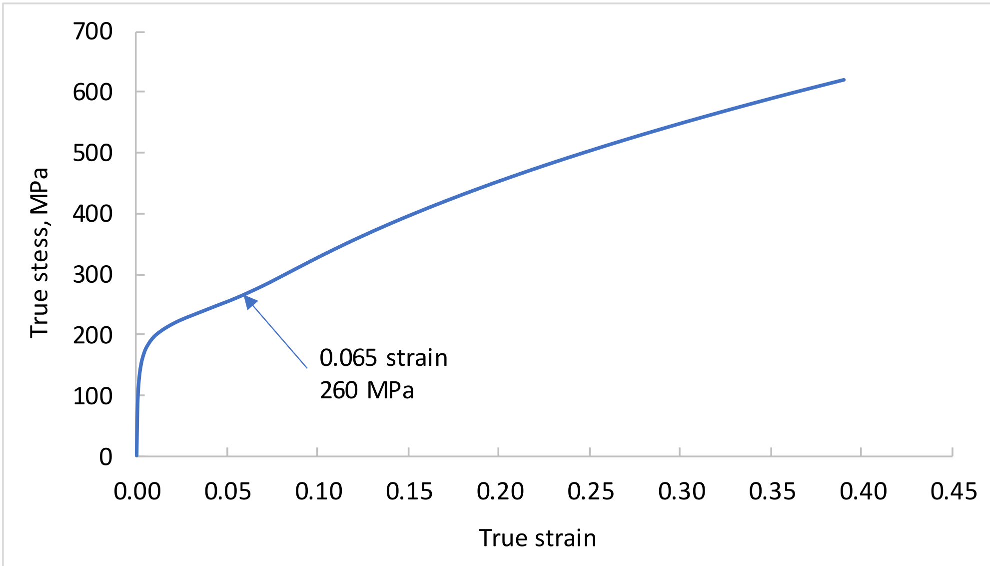

Figure 5-35 True Stress as a Function of True Strain for Type 347H at 565 °C

It should be noted that the equations in Annex 3.D are applicable only for temperatures up to 482 °C. As such, the calculated stress of 260 MPa likely incurs some error. However, for the purposes of the discussion, the estimated stress should be the correct order of magnitude.

The inventory temperatures during commercial operation are well below the temperatures at which significant stress relaxation occurs (800 to 900 °C). As such, the calculated stress of 260 MPa is likely to persist for the life of the tank.

Using information for Larson Miller parameters from API 579-1 / ASME FFS-1, Table 10B.4M, the creep life as a function of stress for Type 347H at 565 °C can be calculated, as shown in Figure 5-36.

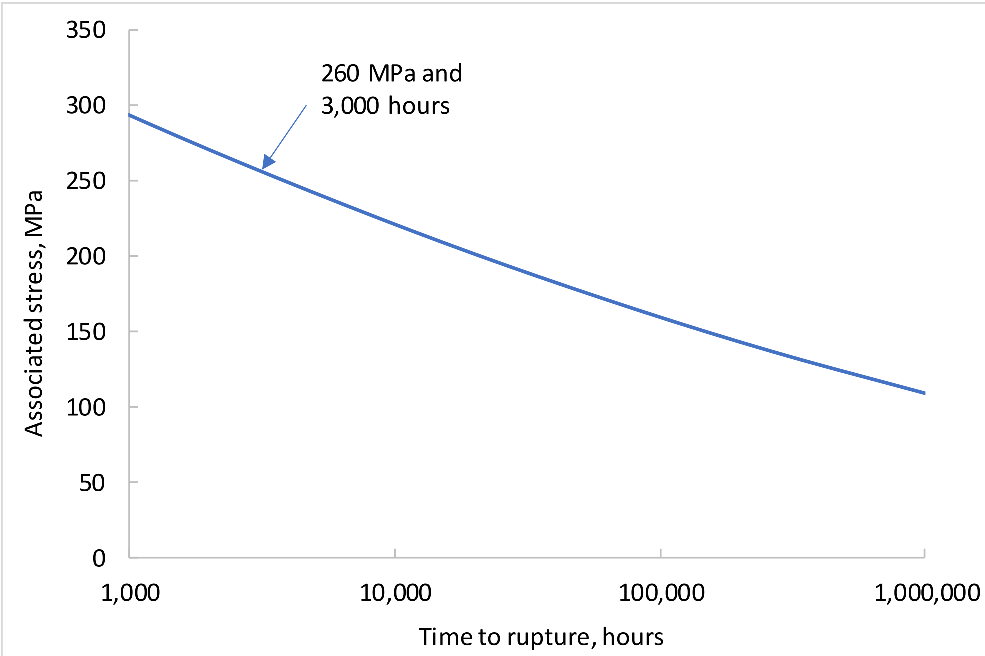

Figure 5-36 Time to Rupture as a Function of Stress for Type 347H at 565 °C

The calculated time to rupture is only several months if the tank is always operating at a temperature of 565 °C. However, in commercial projects, the temperature of the inventory is typically less than 565 °C due to the following effects:

- During overnight hold periods, the inventory level is typically low, and the temperature of the tank can decay by values in the range of 5 to 10 °C

- During receiver startup, salt is introduced into the tank at temperatures in the range of 500 to 565 °C.

If the annual average inventory temperature is 520 °C, rather than 565 °C, then the estimated creep life increases to some 26,000 hours. This period is a nominal 3 years, which is roughly consistent with the crack development times experienced at commercial projects.

Clearly, the above calculations are only a zeroth-order analysis. The shape and the dimensions of the floor buckles in commercial projects, if present, are unique to each project. Further, the stresses in the buckled regions are also influenced by friction forces, thermal stresses generated by radial temperature gradients, and bending loads produced by hydrostatic loads. As such, it is difficult to accurately predict the creep life of a buckled region in the floor. Nonetheless, if the required creep life of the floor is 300,000 hours (30 years), then the stresses in the floor must be limited to about 127 MPa, as noted above in Section 5.15.3. A stress of 127 MPa is produced by a strain of 0.0015, which would be produced by a 'buckle' with a radius of about 2,400 mm. This represents a rather gentle curvature in the floor, which implies that even small permanent deformations of the floor could result in a creep life less than required.

5.15.6 Creep Assessment with Consideration of Residual Welding Stresses

Estimates of creep lifetimes can be developed using the methods outlined in Section 5.15.3; i.e., WRC Bulletin 541 and Project Omega. The coefficients in the equations are typically generated for materials as supplied from the mills; i.e., prior to cutting, fabrication, or welding.

When the floor plates are welded using the standard 347 filler material (E347-16 for SMAW, or ER347 for GTAW), residual welding stresses can reach peak values in the range of 350 to 500 MPa [24]. These values fall between the yield stress and the rupture limit at ambient temperature.

It can be noted that different weld fillers are being investigated as an alternative to 347 to reduce residual stresses in this application. A common choice is ER16-8-2, which is often termed a lean austenitic. The principal benefit to ER16-8-2, compared with 347, is an increase in ductility, which allows a portion of the residual welding stresses to relax. However, qualifying filler materials can involve months to years of laboratory testing to verify the long term mechanical, corrosion, and chemical properties.

With a stress of 500 MPa, the estimated time to rupture for Type 347H stainless steel at a temperature of 25 °C is billions of years.

During preheating, the temperature of the tank is raised to approximately 300 °C. With a stress of 500 MPa, the creep life is reduced, but it is still in the range of thousands of years.

During commissioning, the temperature of the tank first reaches its design value of 565°C. With a stress of 500 MPa, the creep life is predicted to be only 5 hours. Clearly, tanks in commercial service have creep lifetimes longer than 5 hours, which means that a significant level of stress relaxation is occurring between the end of fabrication and the start of commercial service.

5.15.7 Relaxation of Residual Stresses Prior to Tank Commissioning

Tanks in commercial service are exhibiting lifetimes of at least 3 years. The sources of the failures are many and varied. Nonetheless, it is apparent that the creep life must exceed 3 years, as the tank failures to date are showing failure mechanisms other than creep.

---

[24] Osorio, J. (National Renewable Energy Laboratory, Golden, Colorado), Failure Analysis for Molten Salt Thermal Energy Tanks for In-Service CSP Plants, DOE Award Number DE-EE00038475

As a bounding exercise, for Type 347H stainless steel at a temperature of 565 °C, the stress cannot exceed 200 MPa if the material is to reach a creep life of 26,000 hours (3 years). This implies that some form of stress relaxation is occurring, early in the commercial life of the tank, which reduces the peak stress by a nominal 60 percent; i.e., from 500 MPa to 200 MPa.

Residual stresses can be relaxed by thermal mechanisms, mechanical mechanisms, or a combination of the two.

Thermal Mechanisms

An increase in the metal temperature results in a decrease in the yield stress. When the yield stress decreases to the residual stress, the material plastically deforms. This, in turn, relieves a portion of the residual strain and relieves a portion of the associated stress. The degree of stress relaxation is a function of temperature and time, with the former the principal determinant.

The largest degree of relaxation occurs during solution annealing, when the metal is heated to about 1,050 °C. The residual stresses are reduced by some 95 percent; i.e., from 500 MPa to 25 MPa [25]. However, prior to the start of commercial service, tank temperatures are limited to a nominal 300 °C during preheating and initial filling. At 300 °C, the material undergoes only stress relief, and relaxation of the residual stresses is limited to about 30 percent (from 500 MPa to 350 MPa).

At a temperature of 300 °C, and at a stress of 350 MPa, the creep life is measured in billions of hours. As such, any creep damage which occurs during preheating can safely be ignored.

During commissioning, the temperature of the tank is raised from the preheat value of 300 °C to the design value of 565 °C. At a temperature of 565 °C, and at a stress of 350 MPa, the creep life is only 200 hours. Since the tanks in commercial projects are not suffering creep failures at 200 hours, additional relaxation of the residual stresses must be occurring during the heating period from 300 °C to 565 °C.

At temperatures in the range of 550 to 650 °C, the degree of stress relief is on the order of 35 percent. This implies that the peak residual stress is reduced to approximately 230 MPa (i.e., 0.65 * 350 MPa) at the start of commercial service. At a temperature of 565 °C, and at a stress of 230 MPa, the creep life is on the order of 7,000 hours. As above, the tanks are not suffering failures due to creep in the first year of service, and additional relaxation of residual stresses must be occurring before the start of commercial service.

Mechanical Mechanisms

[25] Peckner, D. and Bernstein, I., Handbook of Stainless Steel, Chapter 4, Table 25, ISBN 0-07049147-X, 1977

Cyclic loading is a known mechanism for reducing residual stresses.

Late in the tank fabrication process, the floor is welded to the wall. The wall has a radial and a circumferential stiffness that is several orders of magnitude greater than the radial and tangential stiffness of the floor.

The tank, after fabrication but prior to preheating, undergoes some number of daily temperature cycles due to solar heating and nighttime cooling. The temperature of the wall will be out of phase with the temperature of the floor because 1) the heat transfer rate from the wall to the floor is low, and 2) the thermal inertia of the foundation, relative to thermal inertia of the wall, is essentially infinite. As such, the wall will place the floor into a number of compression and tension cycles, with a total of perhaps 100 to 200 cycles, depending on the project schedule. Some level of stress relief can be expected, but developing an accurate estimate is still likely to involve large uncertainties.

Summary

As noted above, commercial tanks have a creep life in excess of 26,000 hours. To achieve this life, the sum of the operating stresses and the residual stresses must be reduced from 230 MPa at the start of commercial service to values no higher than 200 MPa soon after the start of commercial service.

There is some combination of thermal and mechanical mechanisms, as yet undefined, which are at work to reduce the stress. Deciphering these mechanisms, and quantifying their effects, will be an important element in predicting the creep lifetime of the tank.

5.15.8 Required Relaxation of Residual Stresses to Achieve a 30-Year Creep Life

The tank has a design life of 25 to 30 years, which corresponds to 220,000 to 260,000 hours. Due to a range of uncertainties in the estimates of the operating and the residual stresses, a case could be made for some level of conservatism in the calculation of the creep life. As a point of departure, a design life of 300,000 hours could be adopted. At 565 °C, the corresponding allowable stress is 135 MPa.

For a commercial-size tank (35+ m diameter), the operating stresses, exclusive of residual stresses, are already in the range of 100 to 125 MPa. This implies that the residual stresses must be reduced by 75 to 90 percent to reach a creep life of 300,000 hours. However, as noted above, the degree of stress relief early in commercial service is only about 50 percent. Potential, and in some cases only partial, solutions to the problem of stress relief are outlined below.

Comprehensive Approach to Stress Relief

A post weld heat treatment on the tank, at the solution annealing temperature of 1,050 C, will almost completely remove the residual stresses (approximately 25 MPa remaining).

Practically speaking, solution annealing at a temperature of 1,050 °C, while maintaining the integrity of the tank shell, will be a challenging task. As outlined in the Code, it is preferable to heat the entire vessel in a closed furnace. However, this is not feasible for a large structure such as a tank, and alternative methods must be considered. The tank must either be internally heated, or different parts heated separately before joining, followed by local heat treatment of the remaining joints. In either case, the shell must be protected from damaging thermal gradients throughout the heating and cooling process.

Heat treatment of the wall may be relatively straightforward, as there are specialty contractors for this work. Nonetheless, the strength of the material at the annealing temperature will be quite low, and the wall may need to be temporarily reinforced to prevent plastic deformations.

The more problematic element is the floor. Achieving the required heating rates, the hold times, and the cooling rates may not be feasible due to the presence of the foundation. However, if the floor is elevated during fabrication, the heat treatment process is considerably more practical. Also, with the floor elevated, welding can be conducted from both above and below, which 1) eliminates the need for backing strips, and 2) reduces the heat input to the welds and the associated residual stresses.

It can be noted that in tanks designed to API 650 requirements, the principal function of the floor is to form a liquid boundary; i.e., it is not intended as a structural element. If welding results in changes to the metal chemistry, or the development of residual stresses, these conditions are unlikely to affect the primary function of the floor. As such, post weld heat treating of the floor is not normally performed.

Conceptually, the post weld heat treatment of the wall and the floor might consist of the following steps:

1. The floor, in an elevated position, is welded, and local post weld heat treatments are conducted as the welds are completed. The process would be similar to the post weld heat treatment of pipe welds. (It should be noted that a successful local or global post weld heat treatment is not guaranteed. Stainless steels typically have sufficient uniaxial ductility to accommodate the plastic strains associated with stress relaxation. However, if the material is constrained, as it would be at the edges of adjoining plates, then strains can develop in multiple axes of the heat affected zones. Stainless steels with a high carbon content have a multiaxial failure ductility as low as 1 percent. The creep strain that occurs during the relaxation of the weld residual stresses could be sufficiently large to exceed the multiaxial failure ductility, and cracks could develop in the weld zone.)

2. The bottom course of the wall is assembled and welded.

3. The perimeter of the floor is welded to the bottom of the wall.

4. A post weld heat treatment is conducted on the bottom course. The heat treatment would incorporate the thick fillet weld connecting the floor to the bottom of the wall.

Heat treating the bottom course thermally expands the wall, which places the floor into tension. As long as the wall and the floor remain in the elastic range, then no new residual stresses will be imposed on the floor.

Approach to Partial Stress Relief

If solution annealing is impractical, it may be possible to achieve a sufficient degree of stress relief by heating the tank to an intermediate temperature, and then holding the tank at this temperature for an extended period.

The intermediate temperature should be one which reduces the yield strength as far as possible, but does not result in fundamental changes to the metal chemistry. For Type 347H stainless steel, a representative value might be 625 °C.

The preheating period for an empty tank (ambient to 300 °C) is nominally 30 days. In principle, the preheating temperature could be extended to 625 °C, and the preheating period could be extended to, as an example, 60 days.

An engineering analysis could be conducted to determine the optimum combination of temperature, time, degree of stress relief, and preheating cost.

Methods to Increase the Creep Life

One method for increasing the creep life is to reduce the tank temperature. For the purpose of the discussion, the tank design temperature is assumed to be reduced by 50 °C from the typical commercial value of 565 °C to a new value of 515 °C. With a creep life of 300,000 hours, the allowable stress increases to 200 MPa. If the operating stress, through careful tank design and process control, can be limited to 100 MPa, then the allowable residual stress can be 200 MPa - 100 MPa = 100 MPa. This, in turn, requires a stress relief of (230 MPa - 100 MPa) / 230 MPa = 55 percent. However, at a temperature of 515 °C, a stress relief of 55 percent is not assured, and the approach constitutes only a partial solution.

An alternate approach for increasing the creep life is to reduce both the tank design temperature and the design life. This necessarily requires the fabrication of replacement tanks during the project. For the purposes of the discussion, the design temperature is set to 515 °C and the design life is set to 10 years (100,000 hours). The allowable stress increases to 230 MPa. If the operating stress can be limited to 100 MPa, then the allowable residual stress can be 230 MPa - 100 MPa = 130 MPa. This, in turn, requires a stress relief of (230 MPa - 130 MPa) / 230 MPa = 40 percent. At a temperature of 515 °C, a stress relief of 40 percent cannot be guaranteed, and this approach only constitutes a partial solution.

Summary Observations

The estimates above of allowable residual stresses is only approximate because a full understanding of the operating stresses, and the degree of stress relief, in commercial tanks are not fully understood. Nonetheless, it is clear that sum of the operating stresses and the residual stresses could well exceed the allowable stresses associated with a creep life of 30 years. At some point, the solar industry may decide that some form of stress relief must be conducted if the tank is to achieve a creep life of 30 years.

5.15.9 Code Interpretation of Residual Stresses

The creep life is a function of the material, the temperature, and the stress. The last item includes operating stresses due to temperature gradients (self-restraint) and due to friction. However, the Code is somewhat ambiguous regarding the use of residual stresses in the creep analyses.

A review of Fitness-for-Service API 579-1 / ASME FFS-1 shows the following:

PART 9 - ASSESSMENT OF CRACK-LIKE FLAWS
ANNEX 9D - RESIDUAL STRESSES IN A FITNESS-FOR-SERVICE EVALUATION

9D.4.1 Post Weld Heat Treatment

If the type of PWHT cannot be established, the residual stress distribution for the as-welded condition shall be used in the assessment. If the weld joint is in a component operating in the creep range (i.e. long-term operation), then the residual stress based on the PWHT condition may be used in the assessment.

PART 10 – ASSESSMENT OF COMPONENTS OPERATING IN THE CREEP RANGE

10.4.2.1 The Level 1 assessment for a component subject to a single design or operating condition in the creep range is provided below.
a) STEP 1 – Determine the maximum operating temperature, pressure, and service time the component is subject to. If the component contains a weld joint that is loaded in the stress direction that governs the minimum required wall thickness calculation, then 14ºC (25ºF) shall be added to the maximum operating temperature to determine the assessment temperature. Otherwise, the assessment temperature is the maximum operating temperature.

PART 14 - ASSESSMENT OF FATIGUE DAMAGE

14.8.3 Loading Time History
The loading time history showing the historical and assumed future start-up, normal, upset, and shut-down conditions should be reported. In addition, any additional loads and stresses considered in the assessment, e.g. stresses from supplement loads, thermal gradients and residual stresses.

PART 14 - ASSESSMENT OF FATIGUE DAMAGE

10.5.1.4 A sensitivity analysis should be performed as part of the assessment regardless of the method chosen.
b) Remaining life estimates in the creep range are sensitive to materials data, applied stresses, and corresponding temperature. Therefore, sensitivity studies should be performed to evaluate the interaction of these variables in regards to the remaining life prediction.

Summary Observations

The Fitness-for-Service Code provides some guidance regarding the use of residual welding stresses in the calculation of creep life. However, the texts in Parts 9 and 14 use terms such as 'may' and 'should', and as such, are not mandatory requirements. However, in Part 10, the term 'shall' is used. Nonetheless, adding 14 °C to the design temperature to account for creep damage may, or may not, result in an accurate lifetime assessment.

Operating stresses in the floor, due to temperature gradients and due to friction, are likely in the range of 100 to 125 MPa. For a 30-year tank life, the allowable creep stress is on the order of 130 MPa. This implies that residual stresses associated with welding must be quite low.

The Code is not specific regarding a mandatory requirement to include residual stresses in the assessment of creep. Nonetheless, it is clear that residual stresses must be included if the creep evaluation is to be accurate. As a minimum, the allowable residual stress will point to the degree of stress relief required to reach a 30-year tank life. To this end, a requirement to include residual stresses, even if not mandated by the Code, should be included in the tank procurement specification.

5.15.10 Combined Fatigue and Creep Damage

A common approach to estimating the cumulative effect of successive fatigue cycles is Miner's Rule [26]. The approach is based on the following assumptions:

- The damage accumulated by the material during each cycle is a function only of the stress, σ

[26] Lalanne, Christian, "Fatigue Damage, Mechanical Vibration and Shock Analysis, Third edition - Volume 4", Library of Congress Control Number 2014933740,ISTE Ltd and John Wiley & Sons, 2014

- For n cycles, the damage (or fraction of fatigue life) at the specified stress is

$$d = \frac{n}{N}$$

  where N is the number of cycles to the failure at the stress level σ.

- The damages, d_i, are added linearly, as follows:

$$D = \sum_{i=1}^{k} d_i = \sum_i \frac{n_i}{N_i}$$

- It is assumed that damage accumulates without the influence of one level on another. In this case, failure occurs when:

$$D = \sum_i \frac{n_i}{N_i} = 1$$

A similar approach can be used to estimate the cumulative effect of creep damage, with cycles (n) replaced by time (t).

As might be expected, the accumulation of fatigue damage reduces the ability of the material to accommodate creep damage. Allowable combinations of fatigue damage in conjunction with creep damage, for stainless steel and two ferritic steels, are shown in Figure 5-37.

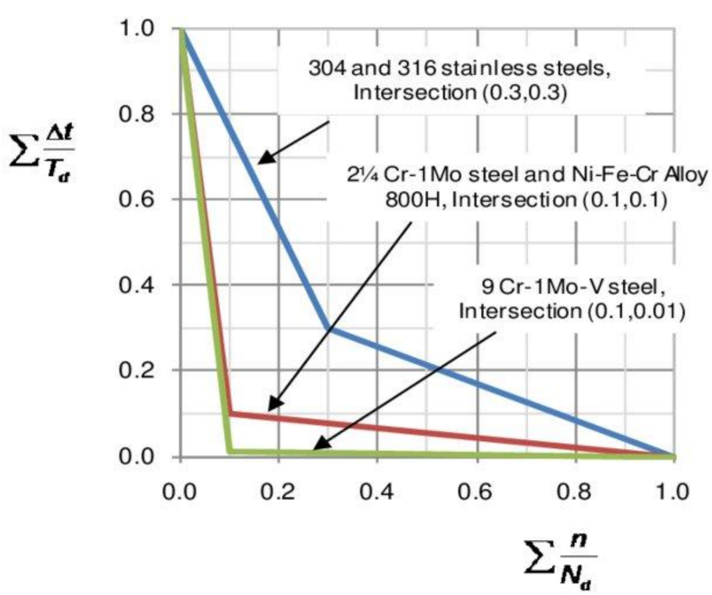

Figure 5-37 Allowable Combinations of Fatigue and Creep Damage

5.15.11 Preliminary Lifetime Assessment

The sections above discuss methods for assessing the fatigue, the corrosion, and the creep lifetimes of the tank. However, quantitative assessments are not presented, as the calculation of stresses (steady state, transient, and cyclic) are beyond the scope of the Design Basis study.

As a surrogate, representative values for the stresses have been developed from a Federal laboratory study evaluating the low cycle fatigue life of hot salt tanks [27]. Inputs to the computational fluid dynamics model are based on operating data from Crescent Dunes on the following parameters, each as a function of time:

- Downcomer flow rate and temperature
- Hot salt flow rate to the steam generator
- Inventory temperature and level.

Calculations of the floor temperatures and the floor stresses were developed for 3 representative days: clear; partly-cloudy; and intermittent clouds. The cycle of days are assumed to repeat, until a period of 30 years is reached.
Estimates of the cumulative fatigue damage, and the cumulative creep damage, were developed using the methods presented in ASME Section III, Division 1, Subsection NH and in API 579-1 / ASME FFS-1.

For floor radii between 0 and 75 percent of the tank radius, the creep and fatigue damage results are shown in Figure 5-38. For floor radii between 93 and 100 percent of the tank radius, the results are shown in Figure 5-39. In both figures, the combined fatigue and creep damage should remain beneath the limits defined by the red and the blue lines.

For floor locations between 0 and 75 percent of the tank radius, the fatigue damage is minor; perhaps 1 percent of the allowable damage. Creep damage is in the range of 90 to 105 percent of the allowable damage, and lifetimes of the floor at these locations are projected to last the duration of the project.

In contrast, for floor locations between 93 and 100 percent of the tank radius, the cumulative fatigue damage is in the range of 2 to 15 percent of the allowable value, while the cumulative creep damage is a

[27] Osorio, J. (National Renewable Energy Laboratory, Golden, Colorado), Failure Analysis for Molten Salt Thermal Energy Tanks for In-Service CSP Plants, DOE Award Number DE-EE00038475

factor of 10 to 20 times the allowable value. A review of the calculated floor stresses from the CFD / FEA model show values that are routinely above the yield value. In general, stresses in this range are inconsistent with a multi-decade creep lifetime.

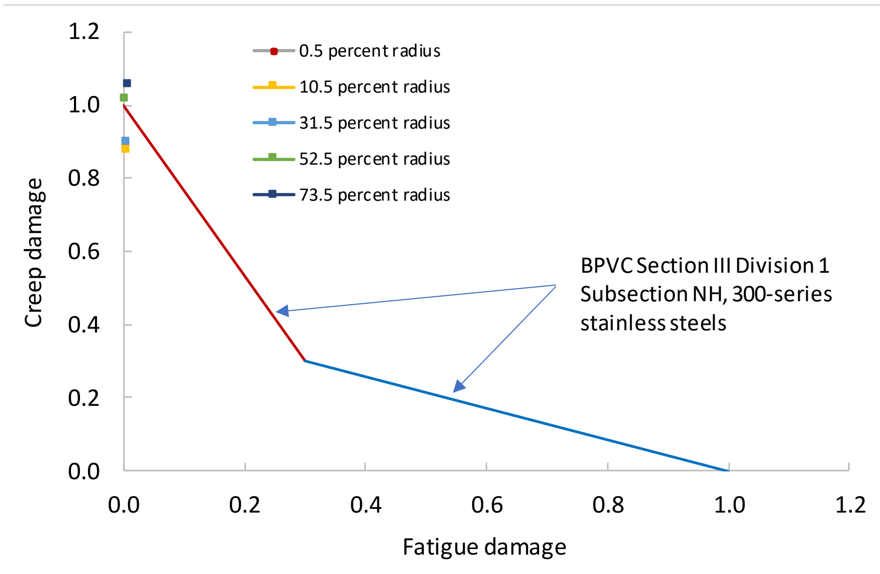

Figure 5-38 Combined Creep and Fatigue Damage for Tank Radii Less than 75 Percent

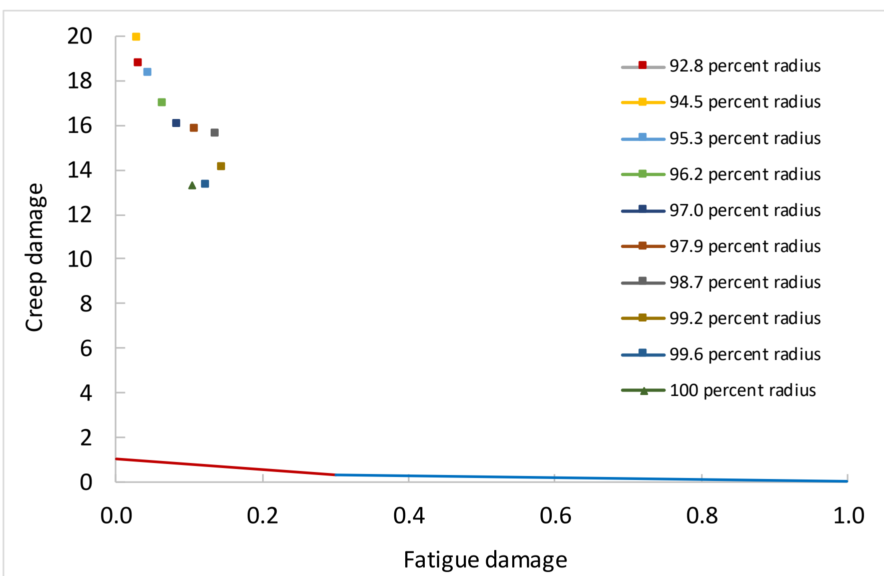

Figure 5-39 Combined Creep and Fatigue Damage for Tank Radii Greater than 93 Percent

The floor stresses are likely the result of a combination of 1) friction loads, and 2) self-restraint due to thermal stresses generated by radial temperature gradients. The relative contributions of the two effects are not yet known. Methods to reduce the stress values may involve some combination of the following:

- Limits on the maximum coefficient of friction between the floor and the foundation; i.e., certain materials in contact with the floor may be excluded from design consideration

- Constraints on tank operating procedures; i.e., if the tank level is W m, if the inventory temperature is X °C, and if the downcomer flow rate is Y kg/sec, then the receiver outlet temperature cannot exceed Z °C.

5.16 Material Selection

5.16.1 Stabilized and Non-stabilized Stainless Steel

Non-stabilized Stainless Steel

The hot salt tank at the 10 MWe Solar Two demonstration project was fabricated from Type 304H stainless steel. The tank operated at temperatures above 538 °C (1,000 °F). As such, the Code required the use of an 'H' grade of stainless steel, with a carbon content of at least 0.04 percent, to provide the required resistance to creep. However, the H grades of stainless steel are susceptible to a failure mechanism known as intergranular stress corrosion cracking if the following four conditions are met simultaneously:

1. Sensitization. The stainless steel becomes sensitized when the carbon in the steel reacts with chromium to form chromium carbide. At temperatures above 500 °C, the time required to form the chromium carbide is measured in hours. The chromium carbide preferentially forms at the grain boundaries, as there is space in the matrix to do so. With the chromium depleted at the grain boundaries, the material is susceptible to corrosion at the grain boundaries.

2. Tensile stresses. Tensile stresses can arise due to process conditions, or due to residual welding stresses.

3. Chlorides. The nitrate salt, depending on the purity, contains chlorides in the range of 0.05 to 0.4 percent.

4. Liquid water. The water acts both as a transport mechanism for the chlorides and as an electrolyte.

If all of these conditions are present, then corrosion-induced cracks can develop at the junctions between grain boundaries, and the cracks can then progress along the grain boundaries due to the tensile stresses. Interestingly, once the cracks start to appear, removing the liquid water does not halt the progression of the cracking.

Project Locations Near the Coast

Coastal locations are subject to salt spray from the ocean. Fabricating a tank from an H-grade of a non-stabilized stainless steel carries the risk of the tank developing intergranular stress corrosion cracking during the fabrication process. To minimize this risk, the Owner may elect to fabricate the tank from a stabilized stainless steel, and then accept the risk of stress corrosion cracking developing at some future date. In all likelihood, the Owner would need to make regular payments to a fund, which would be used to finance the construction of a second tank at some point in the future. The cost of the periodic payments would be reflected in the financial model for the project.

Project Locations in the Desert

For plants in a desert location, the risk of intergranular stress corrosion cracking developing during the fabrication stage of a tank constructed from a non-stabilized stainless steel is small. In addition, once the tank enters normal operation, the potential for intergranular stress corrosion cracking is nil. The first three of the four conditions noted above are present, but the operating temperatures of the tank preclude the presence of liquid water.

Nonetheless, if the tank must be drained for maintenance, and if the tank cools to ambient temperature, then there is the possibility of liquid water forming inside the tank due to moisture condensing from the air. Were intergranular stress corrosion cracking to begin, there would be no mechanism to halt the progression. In the worst case condition, the tank would need to be condemned.

Stabilized Stainless Steel

One method for reducing the potential for intergranular stress corrosion cracking is to use a stabilized stainless steel. A stabilized steel adds niobium (Type 347) or titanium (Type 321) as an alloying element. In Type 347, the niobium bonds with the carbon to form niobium carbide; in Type 321, the titanium bonds with the carbon to form titanium carbide. Both carbides reduce the free carbon in the matrix, which reduces the potential for forming chromium carbide. This, in turn, reduces the potential for intergranular stress corrosion cracking.

The solar industry has essentially adopted Type 347H for the fabrication material for the tanks, piping, pumps, and heat exchangers on the hot side (> 450 °C) of central receiver projects. Type 347H also offers higher strength at elevated temperatures than Types 304H and 316H. The higher strength translates to lower fabrication masses, and potentially reduced costs. Nonetheless, Type 347H is not a complete solution to the problem of intergranular stress corrosion cracking, as follows:

- During welding, the metal temperatures are high enough to dissolve the niobium carbide. This releases free carbon back into the matrix. As the weld cools, equilibrium considerations lead to a combination of niobium carbide, chromium carbide, and free carbon, depending on time-at-temperature and cooling rates. A common result is the preferential formation of chromium carbide at the edges of the heat affected zone. This leaves two thin zones, on either side of the weld, which become susceptible to intergranular stress corrosion cracking. The phenomenon is known as knife line attack.

- A post weld heat treatment can be performed, which raises the metal temperature high enough to dissolve both the chromium carbide and the niobium carbide. The metal is then held for a defined period at a defined temperature, which leads to the preferential formation of niobium carbide. The weld is then cooled rapidly through the temperature which preferentially forms chromium carbide. The high cooling rates can be achieved on piping, but cannot be effected on the thick metal sections in tanks, pumps, and heat exchangers.

- Welds with high residual stresses can be susceptible to a failure mechanism known as stress relaxation cracking. High residual stresses can result from thick metal sections with multiple welding passes, or from thin metal sections with long continuous weld lengths. This topic, discussed below in Section 5.16.2, is inherent characteristic of using niobium as an alloying element.

As such, Type 347H can reduce the potential for, but cannot eliminate the possibility of, intergranular stress corrosion cracking. Further, Type 347H introduces potential failure mechanisms not inherent in Type 304H and Type 316H.

Alternative Material Options

An alternative material option recently identified in research studies is found in the European standard for pressurized vessels EN10028-7. This material is stainless steel 1.4910 (X3CrNiMoBN17-13-3), which has a maximum service temperature of 600 °C.

The closest material to 1.4910 in the ASME Boiler and Pressure Vessel Code is Type 316LN (16Cr–12Ni–2Mo–N), which has a maximum service temperature of 427 °C.

Compared to 316LN, 1.4910 includes a 20 percent higher nickel content and the addition of small amounts of boron, and as such, is referred to as Type 316LNB.

Boron is added to improve the creep properties of the material. Recent studies indicate Type 316LNB has higher allowable 100,000-hour creep rupture stresses than Type 347H at temperatures in the range of 500 to 600 °C [28], and it has similar corrosion properties in nitrate salts [29]. More importantly, there is no niobium in the alloy, which reduces the potential for stress relaxation cracking, as discussed in Section 5.16.2.

For these reasons Type 316LNB is considered a potential material candidate to replace Type 347H; however, alternative failure mechanisms for the new material must be considered. The addition of nitrogen and boron to the alloy must be fully evaluated before considering Type 316LNB as the solution to all metallurgical challenges in the hot tank. Further tests should be conducted on weld samples to determine if the material is susceptible to stress relaxation cracking or other cracking phenomena.

Material Selection for Commercial Projects

The Type 304H stainless steel hot tank at Solar Two operated without failure during its brief 3-year test and evaluation period. However, the tank was never drained, and was never cooled to ambient temperature, for maintenance or repair. Similarly, an internal inspection of the Type 347H stainless steel hot tank at Crescent Dunes showed no signs of cracking, corrosion, or weld failures. However, evidence of stress relaxation cracking has been observed in other commercial projects.

The solar industry, in effect, must choose among potential tank materials, none of which offers a perfect solution:

- Type 304H, and to a lesser extent Type 316H, avoid the potential for stress relaxation cracking due to the absence of niobium. However, the materials are susceptible to intergranular stress corrosion cracking should the tank be exposed to liquid water. As such, if the tank is drained, and then cooled to ambient temperature, then the tank must be exposed to only dry air, without the possibility of moisture condensing from the air. One approach to accomplish this is to introduce only dry air into the interior of the tank. However, moisture could still condense on the outside of the tank. A potential solution is to introduce only dry, and heated, air into the tank such that the metal temperatures never fall below the dew point. To what extent this can be guaranteed by the maintenance company is perhaps an open topic

- Various industries have considered Type 316H as a potential alloy, but the nuclear industry in the past decades have reported hundreds of stress relaxation cracking failures in advanced gas

[28] M. Oum et al., "Therma 4910 for molten salt storage tanks: Improved stress relaxation cracking and high temperature properties", SolarPACES 2022, Albuquerque, NM, USA

[29] A. Bonk et al., "Thermal Energy Storage using Solar Salt at 620°C: How a reactive gas atmosphere mitigates corrosion of structural materials", SolarPACES 2022, Albuquerque, NM, USA

cooled reactors [30]. In general, Type 316H is argued to have high susceptibility to stress relaxation cracking based on various industry failures and lab scale testing

- Type 347H reduces the potential for intergranular stress corrosion cracking, but introduces the potential for stress relaxation cracking. The cracking mechanism is a function of the metal thickness, the number of welding passes, the stress distribution, and the time / temperature history of the tank. If the development rate of the cracking can be predicted with the necessary accuracy, then it might be possible to fabricate a tank in Year 0 of the project, and then fabricate a replacement tank to be placed into service in, for example, Year 10 of the project. However, if the development rate of the cracking cannot be predicted with the required certainty, then the project may be obligated to build two tanks in Year 0 in preparation for an expected failure at an undefined time.

5.16.2 Stress Relaxation Cracking in Type 347H

As noted above, adding niobium to stainless steel results in the beneficial formation of niobium carbide. If the parent metal was never welded, then the material properties would be compelling for use in a solar project. However, welding, and the subsequent chemical reactions, introduce a range of undesirable characteristics.

Source of Cracking

The 3 main contributing factors are 1) susceptible microstructure, 2) residual stresses, and 3) elevated temperature in creep dominated regimes [31].

<u>Susceptible Microstructure</u>

The metallurgical mechanism contributing to cracking is believed to be the non-homogeneous precipitation of niobium carbonitrides (Nb (C,N)) in the grain interiors and at the grain boundaries. The material, in the as-received condition, has typically received a stabilizing heat treatment to homogenize the precipitates in the solid solution alloy. However, welding the material 1) dissolves many of the precipitates, 2) coarsens the grain structure, and 3) imposes a set of residual stresses. In the grain interiors, precipitation of the niobium carbonitrides occurs during elevated temperature service, or during post weld heat treatment. The precipitation mechanism, which is promoted by residual stresses, results in a fine grain structure with a high strength. In contrast, precipitation of the niobium

[30] Pickle, T. (Colorado School of Mines, Golden, Colorado, USA), et al, Evaluation of Alternative Base Materials for Mitigation of Stress Relaxation Cracking in Thermal Energy Storage Tanks, SolarPACES 2024, 30th International Conference on Concentrating Solar Power, Thermal, and Chemical Energy Systems

[31] E. C. B. Dillingh, A; Aulbers, A.P., "Stress Relaxation Cracking-Augmented Recommended Practice," TNO2016

carbonitrides at the grain boundaries results in a coarse grain structure due to a low coherency with the γ-austenite grain boundaries. The coarse structure at the grain boundaries has a lower strength than the fine grain structure within the grain boundaries. As a consequence, a zone develops between the grain interiors and the grain boundaries, and this zone is depleted of niobium carbonitrides. The depleted region is termed a precipitate free zone. A scanning electron microscope image of a precipitate free zone, which is on the order of a few microns wide, is shown in Figure 5-40 [32].

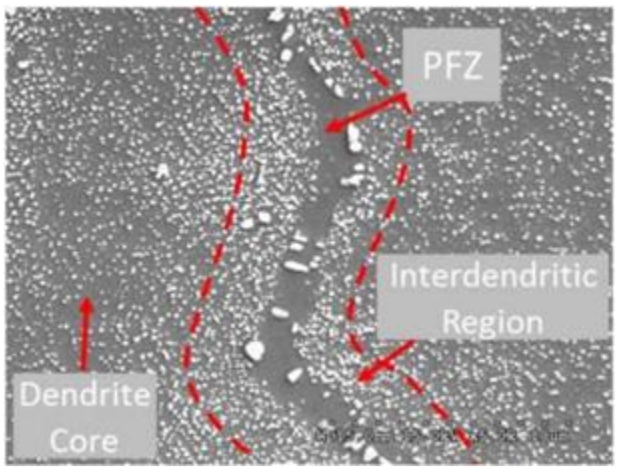

Figure 5-40 Image of a Precipitate Free Zone in the Weld Metal Near a Grain Boundary

It should be noted that the precipitation process occurs on the time scale of years.

<u>Residual Stresses</u>

During welding, the metal in the arc zone undergoes an increase in volume due to 1) the coefficient of thermal expansion, and 2) the change in phase from solid to liquid. After the weld is completed, the zone cools and shrinks. This places the top portion of the weld zone in tension, which is matched by compressive forces in the areas under and adjacent to the weld zone.

The magnitude of the residual welding stresses is a function of the following:

- Section thickness. For section thicknesses greater than about 3 mm, multiple welding passes are generally required. Adding a welding pass to an existing pass generally results in an increase in the residual stresses

- Weld length. Residual stresses are generally additive with weld length.

[32] J. A. Siefert, J. P. Shingledecker, J. N. DuPont, and S. A. David, "Weldability and Weld Performance of Candidate Nickel based Superalloys for Advanced Ultra Supercritical Fossil Power Plants Part II: Weldability and Cross-weld Creep Performance," *Science and Technology of Welding and Joining,* vol. 21, pp. 397-428, 2016

For thick metal sections (i.e., 50 mm), residual stresses can be as high as 500 to 600 MPa. For long weld lengths (> 1 m) in thin plates, residual stresses can reach values up to 600 to 700 MPa. The residual stress values noted here correspond to the material at ambient temperature.

Creep Characteristics

In commercial central receiver projects, the 300-series of austenitic stainless steels are selected for service on the hot side of the plant (565 °C) due, in part, to the creep resistance of the material.

During normal operation, material stresses are limited to ASME allowable values, which are generally in the range of 25 to 30 percent of the yield strength.

Due to the combination of a high resistance to creep and low operating stresses, the material exhibits limited creep produced by dislocations at the grain boundaries. As a result, the potential for the material to relieve residual stresses, welding or otherwise, is limited.

Stress Relaxation Cracking

The residual welding stresses, which, depending on the geometry, can fall in the range between the yield stress and tensile strength, do not relax due to creep. Concurrently, over a period of years, the material develops the precipitate free zones noted above. The zones have a low strength relative to the surrounding grain structure. The combination of high residual stresses and low strength causes the material to preferentially creep at the grain boundaries. Due to the high strains in these limited regions of low strength, the material starts to develop micro voids, which can then develop into cracks.

Since the highest residual stresses are typically below the surface of the weld, the cracks generally begin below the surface of the material and then progress out towards this surface. This leads to two undesirable characteristics:

- Subsurface cracks are difficult to locate
- Once the crack reaches the surface, and the crack is easy to locate; however, the crack has already likely progressed through the full thickness of the material.

Mitigation Measures

A range of mitigation measures are available to reduce the potential for stress relaxation cracking, including 1) conducting a post weld heat treatment, 2) selecting a weld filler material other than E347 (Type 347H), and 3) selecting a non-stabilized stainless steel for the tank.

Post Weld Heat Treatment

Post weld heat treatment offers two benefits for components prior to elevated temperature service: 1) reduction in residual stress, and 2) stabilization of the microstructure [33,34]. Some literature suggests a single heat treatment of 875 °C for a few hours is sufficient for reducing the susceptibility to stress relaxation cracking. However, a heat treatment near the solution temperature (> 1,050 °C) is needed for a complete stress relief and is recommended to retain the ductility in a highly restrained weld.

A multi-step process for the post weld heat treatment could be the best option for preventing stress relaxation cracks in thick weldments, but the procedure must be carefully engineered to prevent relaxation cracking during heat treatment. Parameters such as the heating rates, hold times, temperatures, and quenching rates are all important parameters that influence the final stress state and the final microstructure. A three-step process consists of 1) an initial stress relief, 2) a solution heat treatment to dissolve the microstructure and effect a full stress relief, and 3) a stabilization heat treatment to form the desired precipitates.

1. The initial stress relief is recommended to reduce some of the initial stresses prior to ramping up to the solution temperature

2. The solution temperature helps to dissolve intergranular carbonitrides and reduces δ-ferrite by promoting the formation of γ-austenite in a predominantly two phase field (γ-Nb(C,N)). The reduction of the intergranular carbonitrides helps to minimize the precipitate free zones and allows for coarsening of intragranular Nb(C,N).
3. The final step of stabilization, initially developed by Morishige [35], is a step to further stabilize the microstructure by reducing the remaining free carbon through the nucleation and growth of Nb (C,N) using any of the remaining Nb. This helps to prevent the formation of chromium carbides ($M_{23}C_6$) during cooling.

Figure 5-41 shows an overlay of the three-step post weld heat treatment times and temperatures relative to precipitation C-curves for the formation of coarse niobium carbide, fine niobium carbide, and chromium carbide [36]. The three-step post weld heat treatment method has been used successfully in industry for decades.

[33] J. R.D. Thomas, "HAZ Cracking in Thick Section of Austenitic Stainless Steels-Part 2," *Welding Journal,* 1984
[34] R. D. Thomas, Jr. and R. W. Messler, "Welding Type 347 Stainless Steel- An Interpretive Report," WRC Bulletin1997
[35] N. Morishige, M. Kuribashi, H. Okabayashi, and T. Naiki, "On the Prevention of Service Failure in Type 347 Stainless Steel," presented at the Third International Symposium of the Japan Welding Society, 1978
[36] V. O. B. Messer, T Phillips, "Optimized heat treatment of 347 for high temperature application," *Corrosion,* 2004.

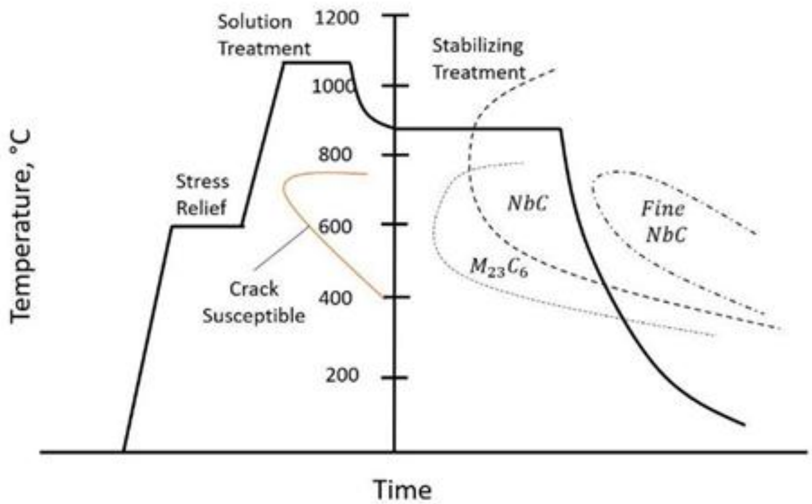

Figure 5-41 Three-Step Post Weld Heat Treatment Time and Temperature Schedule

Weld Filler Material

The principal candidate weld filler materials for a tank fabricated from Type 347H are the following:

- ER347H [37], which is essentially the tank material. It is an austenitic material, with ferrite numbers in the range of 2 to 9, with a typical value of 4.
- E16.8.2 [38], which is an austenitic material with a ferrite number of 1 to 6.

For both of these consumables, bismuth-bearing constituents are held to very low levels (< 0.002 percent Bi) as required by API 582, Welding Guidelines for the Chemical, Oil, and Gas Industries.

E16.8.2 was developed as a more ductile alternative to 347H consumables to avoid failures in the heat affected zones of thick (> 12 mm) 347H base materials. The main benefit of E16.8.2 is reduced δ-ferrite, which is prone to transforming to a brittle σ phase.

[37] Metronode Welding Consumables for High Temperature Alloys, Data Sheet C-11, 347H Stainless Steels, Metronode Products LTD, Surrey, KT16 9LL, March 2016

[38] Metronode Welding Consumables for High Temperature Alloys, Data Sheet C-12, 16.8.2 for High Temperature 3XXH Stainless Steels, Metronode Products LTD, Surrey, KT16 9LL, May 2019

The σ phase is a tetragonal crystal structure, with a precipitation temperature between 600 °C and 1,000 °C [39]. The structure is composed of various intermetallic compounds, including FeCr, FeMo, and $(FeNi)_x(CrMo)_y$. The σ phase can increase the hardness, and decrease both the toughness and the elongation, of steels.

The σ phase issues from the phase transformation of δ → σ (δ-ferrite to σ phase). When the Cr content is below 20 weight percent, the precipitation of the σ phase is not readily observable in austenitic stainless steels; however, the σ phase can be formed quickly when the Cr content is between 25 and 30 weight percent.

The addition of strong ferrite stabilizers other than Cr, such as Si and Mo, can also lead to the formation of the σ phase.

The δ-ferrite is a body centered cubic structure, in which Cr, Si, and Mo can efficiently diffuse. Further, the δ-ferrite regions, compared to the γ-austenitic regions, are rich in Cr. As such, the δ → σ phase transformation preferentially occurs in the δ-ferrite regions. Precipitation can also occur directly in the δ-ferrite particles.

As such, reducing the δ-ferrite in the weld region offers the benefit of increased ductility, which improves the tolerance of strain localizations and mismatches in strengthening mechanisms.

Non-Stabilized Stainless Steels

The potential for stress corrosion cracking in a 300-series stainless steel is directly associated with the addition of niobium to the alloy. If niobium is not present, then the reprecipitation of niobium carbonitrides described above does not occur. This, in turn, results in a matrix which has 1) a more isotropic distribution of strength and ductility, and 2) a lower propensity for the development of internal cracks.

Nonetheless, the alternate candidate stainless steels, including Type 304H, Type 316H, and Type 304LNB, each of which have their own set of advantages and disadvantages. The topic is discussed in some detail in Section 5.16.1.

5.16.3 Stress Relaxation Cracking in Type 316LNB with Lean Austenitic Weld Filler

Type 316LNB is a low carbon version of Type 316, with additions of nitrogen and boron to provide resistance to creep similar to the properties of Type 316H. A recent study compared the resistance to

---

[39] Hsieh, Chih-Chun, and Wu, Weite, (Department of Materials Science and Engineering, National Chung Hsing University, Taiwan), 'Overview of Intermetallic Sigma (σ) Phase Precipitation in Stainless Steels', International Scholarly Research Network, Volume 2012, Article ID 732471, January 2012

stress relaxation cracking of Types 316LNB with Type 347H [40]. The weld filler material for Type 316LNB was a lean austenitic (ER16.8.2, 16 Cr - 8 Ni - 2 Mo), which has demonstrated improved toughness and thermomechanical properties compared to matching filler materials for Type 347H (347H-16).

Testing at 600, 700, and 800 °C show no cracking for the 22-hour test for Type 316 LNB with the ER16.8.2 filler material, while stress relaxation cracking is observed for alloy 347H with the matching filler material.

Future efforts will expand the test matrix, including longer times at 600 °C to simulate the conditions in a commercial tank. The planned work will also investigate the microstructural conditions needed for fracture, such as secondary phases in the partially melted weld zone.

In general, initial test results show that Type 316LNB is less prone to the development of stress relaxation cracking than Type 347H. However, additional testing is required to help predict the long term (30+ year) strength and ductility characteristics of the welded material in commercial service.

[40] Pickle, T. (Colorado School of Mines, Golden, Colorado, USA), et al, Evaluation of Alternative Base Materials for Mitigation of Stress Relaxation Cracking in Thermal Energy Storage Tanks, SolarPACES 2024, 30th International Conference on Concentrating Solar Power, Thermal, and Chemical Energy Systems

6. Nitrate Salt Steam Generators

6.1 Commercial Configuration

The Rankine cycles in essentially all solar projects use a single reheat design. Correspondingly, the steam generators in essentially all solar projects use separate heat exchangers for superheating, reheating, evaporation, and preheating. Separate heat exchangers are required due to 1) differences in the characteristics of latent heat transfer (evaporator) and sensible heat transfer (superheater, reheater, and preheater), and 2) different operating pressures (superheater and reheater).

A common approach to the fabrication of the heat exchangers is a U-tube bundle in a straight shell, with 2 passes on the shell side. The fluid on the shell side is typically salt. This is done for two reasons:

1. The high pressure fluid is the water/steam, and accommodating the high pressure fluid in tubes is easier to accomplish than accommodating the high pressure fluid in the shell

2. The salt in the heat exchanger can reasonably be expected to freeze at least once in the life of the project. If the salt is on the tube side, and freezes in the tubes, then the solid salt can form essentially immovable plugs. Thawing the tubes anywhere along the length of the frozen plug runs the risk of yielding the tube due to the nominal 4 percent increase in salt volume on thawing. If the freeze/thaw cycle is repeated, then there is the possibility of rupturing the tube. (This was the failure mechanism for the tube bundle in the kettle evaporator at the Solar Two demonstration project.) In contrast, if the salt is on the shell side, the thawing process begins by ensuring that the salt in the lines to and from the heat exchanger is liquid. Activating the electric heat tracing on the shell and the channel first melts the salt on the inner surface of the shell and the channel. Since the heat input from the heat tracing is typically a modest value, the initial mass of salt which melts is also a modest number. The volume change on thawing still occurs, but the liquid salt has an exit path through the salt lines. As such, the potential for plastically yielding the shell is low.

Most commercial heat exchangers use a flat tubesheet. During fabrication, the tubes are inserted into the tubesheet, the ends of the tubes are strength welded to the face of the tubesheet, and the tubes are then rolled into the tubesheet. The rolling operation occurs after the welding operation. This prevents any air which might be trapped in the gap between the tube and the tubesheet from heating and expanding into the weld region, which could produce a porous weld.

In some commercial projects, the evaporators use forced circulation, while other projects use natural circulation. The selection is largely the responsibility of the equipment supplier.

6.2 Heat Exchanger Location

Similar to the discussion in Section 3.2, Equipment Location for Oil-to-Salt Heat Exchangers in Parabolic Trough Projects, there is a range of options for the location of the steam generator heat exchangers.

In some commercial projects, the heat exchangers are located on an elevated platform between the storage tanks. The height of the platform is slightly above the mid-point height of the tanks. As such, the heat exchangers can drain to the tank with the lower liquid level.

In other projects, the steam generator is located at grade, and the heat exchangers drain to a tank located below grade. Drain pumps, located on the drain tank, pump salt from the drain tank back to the main storage tanks.

In general, locating the heat exchangers at grade is less expensive than locating the equipment on an elevated platform. However, locating a drain tank below grade is not an inexpensive option. Further, the drain tank must be heat traced on a continuous basis, and this represents a continuous auxiliary energy demand.

6.3 Salt-Side Pressure Relief Valves

In the steam generators at most commercial projects, the salt is on the shell side of the heat exchangers and the water/steam is on the tube side. This is done for two reasons:

- Fluid pressures on the water/steam side are approximately 20 times the pressures on the salt side. The relatively small diameters of the tubes are structurally more efficient than the relatively large diameters of the shells at accommodating the high pressures of the water/steam

- At some point, the salt in the heat exchangers is likely to freeze. If the salt is on the shell-side, then the thawing process can consist of the following steps: activate the heat tracing on the lines to and from the heat exchanger; ensure that the salt in the lines is liquid; and then activate the heat tracing on the shell. The salt will begin to melt in a thin film on the inside of the shell, and the change in the volume during melting is offset by a small flow of salt from the heat exchanger. In this manner, plastic deformations of the shell can be avoided.

6.3.1 Steam Generator Tube Ruptures

At some point in the life of the project, a rupture in a steam generator tube is expected. This will introduce steam into the shell side of the superheater or the reheater, and introduce a mixture of water and steam into the shell side of the evaporator or the preheater. Since the design pressure on the water/steam side is higher than the design pressure on the salt side, a tube rupture will produce a transient rise in pressure on the salt side.

The rupture will also force a mixture of salt, steam, and possibly water through the preheater and into the distribution header at the bottom of the cold salt tank. The two- or three-part flow will leave the header, traverse the inventory in the cold tank, evaporate the remaining water, and introduce a mass of steam into the tank ullage space.

The rupture may also force a mixture of steam and salt backwards through the following hot salt equipment (depending on the use and the location of check valves):

- The hot salt pump. The steam and salt mixture would traverse the pump column downward, traverse the salt inventory upward, and introduce a mass of steam into the tank ullage space
- The minimum recirculation valve for the pump. The steam and salt mixture would enter the recirculation distribution header at the bottom of the hot tank, traverse the inventory upward, and introduce a mass of steam into the tank ullage space.

In addition, the rupture may also force a mixture of steam and salt backwards through the following cold salt equipment (depending on the use and the location of check valves):

- The attemperation pump. The steam and salt mixture would traverse the pump column downward, traverse the salt inventory upward, and introduce a mass of steam into the tank ullage space
- The minimum recirculation valve for the pump. The steam and salt mixture would enter the recirculation distribution header at the bottom of the hot tank, traverse the inventory upward, and introduce a mass of steam into the tank ullage space.

6.3.2 Relief Valve Options

Two options are available for the location of the relief valves:

Roofs of the salt tanks

Each of the salt storage tanks have a) atmospheric vents, and b) pressure/vacuum relief valves. The capacities of the vents and the relief valves would be large enough to accommodate the steam/air flow rates associated with a tube rupture in the steam generator and maintain the ullage pressure within the design limits for the tanks (i.e., + 50 / - 2.5 mbar).

The pressure/vacuum relief valves have only one or two moving parts, and their reliability is excellent. However, the valves require both heat tracing and insulation, and the reliability of the heat tracing and the insulation is not guaranteed. This is particularly so on top of the tanks, where access for maintenance is inconvenient, and therefore infrequent. At the Solar Two demonstration project, the heat trace on the pressure / vacuum relief valve for the hot tank did not fully reach the set point temperature, and a small amount of salt vapor froze in the valve. When the tank filled during one morning startup, the ullage pressure increased to the point where the tank bottom bowed down, and the tank lifted from the foundation. Fortunately, the relief valve opened before the tank ruptured. Apparently, this occurrence is not unique among commercial solar projects. At one plant, the wall-to-roof connection split due to a sticking pressure / vacuum relief valve, and at other plants, more than one instance of the tank lifting from the foundation has occurred.

In the interests of protecting the reliability and the availability of the tanks, the demands on the pressure / vacuum relief valves should be held to the minimum. This can be accomplished by providing separate pressure relief valves in the inter-heat exchanger piping to reduce the transient pressures imposed on the storage tanks.

Roofs of the salt tanks and inter-heat exchanger salt piping

In commercial projects, it is common to provide pressure relief valves on both the storage tanks and in the inter-heat exchanger piping within the steam generator. The relief valves in the steam generator discharge to a safe location, and this location is separate from the ullage space in the main storage tanks.

On a related point, the steam generator system will have some number of control and isolation valves. The valve arrangement will vary from project to project. If it is possible to isolate a heat exchanger by closing the valves, either by placing the valves in manual or during maintenance, then the ASME Code will not a permit a relief design that relies on the valves located on the storage tanks. Instead, local relief valves will be required on the inter-heat exchanger piping, with the number of relief valves dependent on the geometry of the piping and the location of the salt isolation and control valves.

6.4 Cold Reheat Steam Electric Heater

Prior to turbine synchronization, live steam is sent to the condenser through the turbine bypass system. The system consists of a high pressure throttle valve, a steam attemperator, a low pressure throttle valve, and a second steam attemperator.

Early in the startup process, the temperature of the salt entering, and leaving, the superheater is approximately 290 °C. This results in a saturation pressure in both the evaporator and the superheater of about 74 bar.

With the bypass system in service, the steam from the superheater must be reduced in pressure to a value which can be accepted by the reheater. As such, the high pressure throttle valve reduces the pressure to the nominal design pressure of the reheater, which is about 32 bar. The corresponding cold reheat steam temperatures are in the range of 235 to 240 °C.

To provide an adequate margin against salt freezing at the cold end of the reheater, an electric steam heater is located downstream of the high pressure throttle valve and upstream of the cold end of the reheater. The capacity of the electric heater depends on the details of the startup sequence (i.e., steam flow rate and pressure versus time), but is typically on the order of several MWe.

6.5 Cyclic Operation

In a solar project, the steam generator, almost by definition, undergoes a daily startup and shut down cycle.

During overnight hold, cold salt is circulated through the steam generator. The salt is supplied by the cold salt attemperation pump, and the salt leaving the steam generator is returned to the cold salt tank. The heat input from the cold salt compensates for the heat losses from the heat exchangers and associated piping. The heat input also heats the makeup water added to the steam drum to compensate for steam and condensate losses in the Rankine cycle.

To start the steam generator, the hot salt pump is started, and hot salt is blended with cold salt from the attemperation pump at a point upstream of the superheater / reheater. Early in the startup process, the steam flows produced by the superheater and the reheater are not at temperatures high enough to admit to the turbine. The live steam and the hot reheat steam flows are attemperated and throttled, and the flow is then directed to the condenser through a turbine bypass system.

When the live and the reheat steam temperatures reach values which can be accepted by the turbine, a portion of the steam flow in the bypass system is sent to the turbine. The turbine is synchronized, and loaded to a value that will prevent a trip on reverse power. The steam flow in the bypass system is eventually stopped, with all of the steam flow now directed to the turbine.

The relative proportions of hot salt and cold salt at the mixing point upstream of the superheater / reheater are adjusted until the flow of cold salt reaches zero. The output of the turbine is adjusted by changing the speed of the hot salt pump.

To shut down the steam generator, the above process is essentially reversed.

The blending process of adding hot salt to cold salt is a consequence of the vendor limits on allowable rates of temperature change and thermal shock. Typical limits include a maximum rate of temperature change of 10 °C/min, and a maximum thermal shock (Fluid temperature - Metal temperature) of 60 °C. The limits are developed by the vendor to ensure that the heat exchangers have a low cycle fatigue life corresponding to at least 30 years of daily startup and shutdown cycles.

The vendor also specifies a minimum allowable flow rate on both the shell- and tube-sides. A typical value is 16 percent, which corresponds to a turndown ratio of 6:1. At low flow rates, the pressure drops on both the tube- and the shell-sides approach very low values. Local effects due to friction and buoyancy can then influence the flow distribution, which can produce stratified flow, channel flow, or both. If the flow distribution is not uniform, then the temperature distribution within the heat exchanger is also not uniform. Non-uniform temperature distributions can produce internal stresses which are non-uniform, unpredictable, and oscillating. These stresses may add to, or subtract from, the normal process stresses, which can lead to meaningful reductions in the low cycle fatigue life of the equipment.

6.6 Project Experience

6.6.1 Overnight Hold

The steady state heat losses through the insulation on the heat exchangers, and through the insulation on the steam generator piping, is a fraction of 1 percent of the design duty of the steam generator. However, the water and the steam leakage rates in the Rankine cycle can reach problematic levels if 1) the maintenance staff is not conscientiously repairing the steam and condensate leaks as they develop, and 2) tubes leaks in any of the heat exchangers result in steam being carried into the cold salt tank.

A condition can arise in which the energy in the flow of cold salt from the attemperation pump is not sufficient to compensate for the thermal demand of the steam generator; i.e., the temperature of the salt returning to the cold tank falls below the minimum operating temperature of 275 °C. The first line of defense is to add thermal energy to the drum by operating the electric water heaters that preheat the heat exchangers prior to filling with salt. The second line of defense is to add auxiliary steam to the drum from the auxiliary steam generator. The third line of defense is to blend a very small quantity of hot salt with the cold salt upstream of the superheater / reheater mixing station.

The first two approaches are straightforward to implement and to control, but both increase the auxiliary energy demand in the plant. The third uses energy collected by the receiver, but any energy withdrawn from the hot tank for temperature maintenance reduces the daily electric energy production. Further, the quantity of hot salt required is a small fraction of the flow capacity of the hot salt pump. This can lead to oscillations in the flow of salt from the hot pump, which, in turn, can lead to oscillations in the mixed salt temperature upstream of the superheater / reheater. Oscillations in the mixed salt temperature have been shown to lead to low cycle fatigue damage of the heat exchangers, particularly if the rates of temperature change exceed the vendor limit of 10 °C/min.

The solution to this problem is to generously size the electric water heaters in the steam generator, studiously repair any steam and condensate leaks in the Rankine cycle, and provide a means for artificially increasing the pressure drop on the salt side of the steam generator if the hot salt pump must be operated at a low flow rate.

6.6.2 Low Cycle Fatigue

A commercial project experienced multiple failures of the tube-to-tubesheet connections in the superheater in the first years of commercial service. A possible explanation for the common failure patterns is as follows:

1. During startup and shutdown, the rates of change in the temperature of the mixed salt entering the heat exchanger routinely exceeded the vendor limits. The rates of change were both positive and negative, producing, in effect, oscillations in the inlet temperature. The oscillations generated differential thermal expansions across the diameter of, and through the thickness of, the tubesheet.

2. The differential thermal expansion was exacerbated by the low steam flow rates, and the very low pressure drops, during startup and shutdown. Specifically, the steam flow tended to channel, favoring some tubes over others. This resulted in lower temperatures in some regions of the tubesheet, and higher temperatures in other regions.

3. The non-uniform thermal expansion caused flexing in the tubesheet, which over several thousand cycles, caused a relaxation in the friction forces in the rolled tube-to-tubesheet connections.

4. If the rolled connection is lost, then the tube-to-tubesheet welds must carry the loads associated with differential expansion between adjacent tubes, and the differential expansion between the tubes and the tubesheet. If the stresses are high enough, the welds can crack due to low cycle fatigue.

There is additional evidence that rapid changes in the temperature of high pressure heat exchangers can lead to failures of the tube-to-tubesheet connections. Specifically, the Solar One central receiver project used a superheated steam receiver, operating at nominal conditions of 100 bar and 540 °C. The thermal storage system consisted of a single tank thermocline, filled with a mixture of rock, sand, and mineral oil (Caloria HT-43). Energy was transferred from the receiver steam into the rock/sand mixture by circulating Caloria through an economizer, a steam condenser, and a steam desuperheater. Energy was transferred from the rock/sand mixture by circulating Caloria through an economizer, an evaporator, and a superheater.

To isolate the demineralized feedwater in the Rankine cycle from the Caloria in the storage system, the storage system charging and discharging heat exchangers used a double tubesheet design. Tube-to-tubesheet connections were by means of rolled joints; seal welds were not used. Leaks would be confirmed by the presence of either steam or Caloria in the intra-tubesheet space.

Within 400 hours, the tube-to-tubesheet joints started to leak [41]. Repairs were attempted by applying seal welds to the ends of the tubes and re-rolling the tubes into the tubesheets. However, the repairs were unsuccessful, and the storage system was essentially abandoned in place.

A post-failure finite element model of the heat exchanger, using a rate of temperature change of 9.6 °C/min, showed that the tube stresses at the rolled connections approached the yield value. If a material is operating at or near the yield stress under daily cycling conditions, the low cycle fatigue life is expected to be very short.

6.6.3 Water Chemistry

High levels of O_2 can lead to accelerated corrosion rate, especially if the purity of the condensate and the feedwater purity is degraded by contamination (salts) passing through the demineralization system or from condenser cooling water in leakage. A deaerator can be used to control O_2 levels to the required values. Generally, for all-ferrous systems (those without copper tubing in heat exchangers) the desired levels are in the range of 5 ppb up to a maximum of 100 ppb.

Additionally, the pH of the feedwater is typically adjusted to a value of 9.4 or higher to reduce the solubility of protective oxides formed, and with adequate O_2 present, to support the formation of a stable layer of hematite on the water-side surfaces of the system. This is usually done by adding alkaline agents to the feedwater such as ammonium hydroxide, or ammonium hydroxide in combination with a neutralizing amine, such as ethanolamine.

At the Solar Two project, an examination of the water side of the preheater, after about 1 year of service, showed significant quantities of a loosely adherent deposit. An analysis showed the deposits to be magnetite. This is an undesirable condition, for the following reasons:

- Magnetite is a metal oxide, and due to its low thermal conductivity, deposits can reduce the heat transfer rates in the preheater and in the evaporator. Further, if the deposits form preferentially in some tubes and not others, this can lead to non-uniform flow distributions, non-uniform temperature distribution, and non-uniform stress distributions in the heat exchanger.

- Magnetite deposits are an indication of corrosion upstream of the evaporator. Depending on the water treatment approach selected for the project, the corrosion process generally accelerates if the pH is too low (< 9) and / or the dissolved oxygen levels are too low (< 5 ppb). This combination of pH and dissolved oxygen can occur in the feedwater if 1) the dosing of the alkaline agents is insufficient, and / or 2) the deaerator venting is too effective. Under two-phase

[41] S. E. Faas, et. al., (Sandia National Laboratories, Albuquerque, New Mexico), 10 MWe Solar Thermal Central Receiver Pilot Plant: Thermal Storage Subsystem Evaluation - Final Report, Sandia Report SAND86-8212, June 1986

conditions in the evaporator, low oxygen will always occur, and low pH may occur depending on local two-phase conditions and the alkaline agents applied.

- In the evaporator, oxide deposits can come out of suspension at the locations in the tubes where evaporation begins. If the evaporator uses austenitic tubes, then a passivation layer is expected to form on the tubes. However, defects or local variations in the passivation layer can lead to sensitization and pitting corrosion. Specifically, the chemical conditions under the deposits (sodium, chloride, sulfate, ammonia, and the resulting pH) can be different than the surrounding area. If so, a situation can develop in which the protective oxide passivation dissolves and active corrosion can initiate. In the case of pitting corrosion, this can become autocatalytic. Specifically, the dissolution of iron within the pit generates positive iron ions, which draw in and concentrate mobile, acidic ions, such as chlorides, within the pit.

- If the evaporator is a forced recirculation design, then oxide particles in the feedwater can damage the bearing, erode the impellers, and damage the shaft seals in the steam drum recirculation pumps.

Possible Sources of the Deposits

<u>Hematite</u>

Hematite (Fe_2O_3), in a hydrated form, is formed on carbon steel in an oxidizing environment, as follows:

$$Fe + 2\ H_2O \rightarrow Fe(OH)_2 + H_2$$

$$4\ Fe(OH)_2 + O_2 \rightarrow 2\ Fe_2O_3H_2O + 2\ H_2O$$

In general, hematite is a desirable form of iron oxide. It forms an adherent corrosion layer and isolates the parent metal from continued corrosion. It also exhibits a very low solubility in water compared to magnetite.

<u>Magnetite</u>

Magnetite (Fe_3O_4) is generally formed in a relatively reducing environment, through two different reactions:

$$3\ Fe(OH)_2 \rightarrow Fe_3O_4 + 2\ H_2O + O_2 \text{ (at temperatures above 50 °C)}$$

$$3\ Fe + 4\ H_2O \rightarrow Fe_3O_4 + 4\ H_2 \text{ (at temperatures above 150 °C)}$$

In general, magnetite is a less desirable form of iron oxide in flowing feedwater conditions (>100 °C), as 1) it forms a more soluble passivation layer than hematite in water, and 2) it is subject to damage mechanisms such as flow accelerated corrosion, particularly in turbulent locations operating at temperatures between 100 and 250 °C. Removal of the magnetite layer via flow accelerated corrosion exposes new material to the corrosion process. It also results in corrosion products moving through the system, where deposition may occur and lead to further damage mechanisms (e.g. accumulation of deposits in evaporator).

Water Chemistry Control

Although perhaps stating the obvious, the water treatment staff needs to maintain strict control over the water chemistry. The problem is more acute in plants which cycle each day, particularly if the vacuum is broken in the condenser each evening and the condensate in the hot well is exposed to oxygen. Further, the inline instruments for measuring pH and dissolved oxygen need to be maintained in good working order and to receive periodic calibrations.

In general, control of pH in high purity systems is best accomplished through conductivity control, as opposed to strictly relying on direct pH measurement. In addition, older dissolved oxygen measurement technology relying on electrochemical potential measurements are less robust than optical methods employing luminescence technology. Application of 'smart' chemistry monitoring approaches, which incorporate instrumentation validation techniques, can further reduce the expertise required by the operating staff to maintain proper chemistry control.

If the experience from the Solar Two project, and from a range of commercial projects, are any indication, the water treatment system must be fully staffed, and water treatment specialists must be brought in on a periodic basis to review the effectiveness of the treatment system. Failure to satisfy each of these requirements will result in a significant negative effect on the plant availability.

6.6.4 Startup and Shutdown

A common steam generator arrangement in commercial projects consists of the following:

- Two 50-percent capacity steam generator trains
- Three 50-percent capacity hot salt pumps, discharging to a common header
- A common minimum flow recirculation valve for the three hot salt pumps
- Two 100-percent capacity cold salt attemperation pumps, discharging to a common header

- A common minimum flow recirculation valve for the two attemperation pumps
- Salt control valves, at the cold ends of the superheater and the reheater, for distributing the relative flows between the two heat exchangers
- A startup feedwater heater, located downstream of the last high pressure feedwater heater and upstream of the steam generator preheater.

The salt pump and discharge valve arrangement is shown in Figure 6-1, and the intra-heat exchanger salt valve arrangement is shown in Figure 6-2.

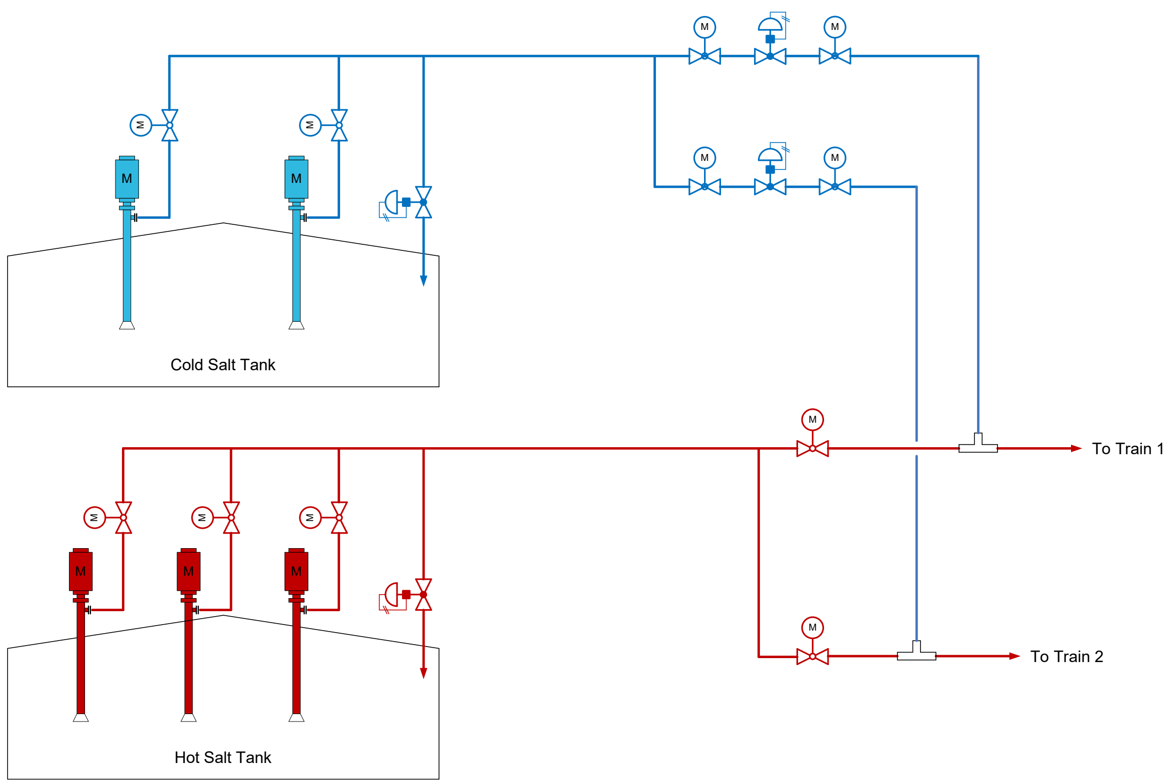

Figure 6-1 Salt Pump Arrangement in a Representative Commercial Project

This arrangement reduces the number of control valves to a minimum, and likely offers the lowest cost piping arrangement. However, the arrangement carries a range of liabilities, as discussed in the following subsections.

Liability 1 - Sequential Startup

By placing the hot salt pumps on a common header, and placing the attemperation pumps on a common header, there is no method to start a second steam generator train if one train is already in service. To start the second train, the metal temperatures in the first train would need to be reduced to essentially the cold salt temperature to avoid thermally shocking the second train. In effect, starting the second train must be postponed until the first train goes through it's normal daily shutdown.

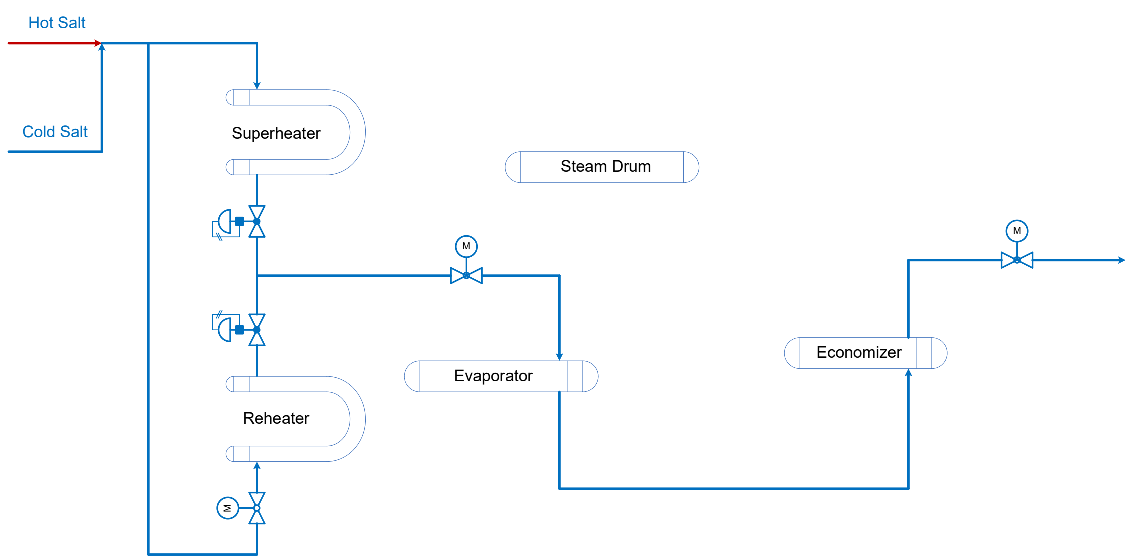

Figure 6-2 Intra-Heat Exchanger Salt Valve Arrangement in a Representative Commercial Project

Liability 2 - Hot Salt Flow Control

The salt control valves downstream of the superheater and the reheater must have Cv values which are high enough to accommodate the design point flow rates with a reasonable pressure drop (< 1 bar). During startup, hot salt is blended with cold salt at the mixing station upstream of the superheater / reheater. The rate at which hot salt is added to cold salt must satisfy the vendor limit regarding the allowable rate of temperature change, which is nominally 10 °C/min. Using representative flow - head curves for the attemperation pump, the acceleration rate at which hot salt can be added to the cold salt is 0.0023 m^3/hr-hr (6 gal/min-min). A flow rate of 0.0023 m^3/hr is approximately 0.15 percent of the design flow rate from the hot salt pump. Further, early in the startup process, the salt flow rate to the steam generator is perhaps 15 percent of the design flow rate. As such, the pressure drop through the steam generator is on the order of $0.15^2 = 2$ percent of the design pressure drop. To control the flow from the hot salt pump with this level of accuracy, in combination with a low discharge pressure, a backpressure must be imposed on the steam generator train. The backpressure is typically provided by the control valves downstream of the superheater and the reheater. However, these valves have reasonably large discharge coefficients, and to provide a meaningful backpressure on the system, the valves are forced to operate in the range of 2 to 4 percent open. Due to the low system pressures, the hot salt pump is already operating at the minimum speed. As such, all of the flow control adjustments during startup must be made by the control valves. As might be expected, the ability to adjust the flow in increments of 0.15 percent per minute is generally poor. The result is oscillations in the flow from the hot salt pump, which results in oscillations in the mixed salt temperature upstream of the superheater and the reheater. The oscillations can result in rates of temperature change which are a factor of 2 to 4 larger than the allowable rates.

Liability 3 - Salt Pump Recirculation Flow Control

The hot salt pumps and the attemperation pumps share a common pressure point at the mixing station upstream of the superheater / reheater. As such, the following parameters all influence one another:

- The discharge pressure of the hot salt pump
- Operating either one or two hot salt pumps
- The position of the minimum flow recirculation valve for the hot salt pump(s)
- The discharge pressure of the attemperation pump
- The position of the minimum flow recirculation valve for the attemperation pump

During the startup of the steam generator, the following characteristics apply:

- The pressure drop in the system is low
- The discharge pressures of the hot salt pump and the attemperation pump are both low
- The flow rate from the hot salt pump to the mixing station is low, which requires the minimum flow recirculation valve to control the (Mixing station flow) + (Recirculation flow)
- Depending on the speed range of the attemperation pump, the minimum flow recirculation valve for the attemperation pump can also be open to control the (Mixing station flow) + (Recirculation flow)

Under these conditions, the system flow stability can be marginal to poor. For example, to increase the flow of hot salt to the mixing station, the minimum flow recirculation valve for the hot pump can be closed slightly. Since the pressure drop in the steam generator flow path is different than the pressure drop in the hot salt pump recirculation line, a change in the recirculation valve position results in a change in the discharge pressure of the hot salt pump. This, in turn changes the effective discharge pressure of the attemperation pump, which changes the flow rate from the pump. In response, the minimum flow recirculation valve for the attemperation pump can change position to provide the required (Flow to the mixing station) + (Recirculation flow). The changes in the discharge conditions for the attemperation pump are then carried over to the hot salt pump, which normally results in a change in the recirculation valve position for the hot salt pump to provide the desired net hot salt flow to the mixing station. The system can then oscillate between two quasi-stable operating points, which results in oscillations in the mixed salt temperate at the mixing station.

Liability 4 - Minimum Steam Side Flow Rates

A typical vendor limit on the minimum allowable flow rate is 16 percent of the design flow rate.

If the design flow rate of the cold salt attemperation pump is 15 percent of the design steam generator flow rate, then operating the attemperation pump at 100 percent speed during overnight hold, and early in the startup process, satisfies the minimum flow requirement on the salt side of each of the heat exchangers.

Some projects use a recirculation pump between the steam drum and the cold end of the evaporator, and a separate recirculation pump between the steam drum and the cold end of the preheater. The flow capacities of each pump are greater than 15 percent of the design water flow rates, and operating the pumps early in the startup process ensures that the minimum water flow rates are always maintained in the evaporator and the preheater.

In contrast, steam flow is initiated in the superheater and in the reheater only when the blending of hot salt with cold salt begins. The steam flow rates begin at 0 percent, and increase with an increase in the flow rate of hot salt. As such, during each startup, the steam flow rates in both heat exchangers are necessarily below the minimum allowable flow rates. Due to the very low pressure drops at these flow rates, the flow distribution among the approximately 900 tubes is expected to be poor. Non-uniform flow distributions lead to non-uniform temperature distribution, which, in turn, lead to unpredictable, and potentially damaging, stress distributions.

Liability 5 - Startup Feedwater Heater

Prior to turbine synchronization, the turbine extraction feedwater heaters are not in service. As such, the temperature of the feedwater leaving the last high pressure feedwater heater is nominally equal to the saturation temperature in the deaerator. This temperature is well below the freezing point of the salt. As such, the temperature of the feedwater supplied to the preheater must be increased to a value which is high enough to prevent salt solidification at the cold end of the preheater.

The same conditions apply once the turbine is synchronized, but with the turbine operating under part-load conditions.

A common approach to preheating the feedwater is to use a startup feedwater heater. The energy source for the startup heater is live steam, which has been throttled and attemperated.

This approach is very effective at preheating the feedwater, but it does incur a range of penalties, as follows:

- Using live steam for feedwater preheating is thermodynamically inefficient. Under part load turbine operating, the penalty in the Rankine cycle efficiency can range from 0.5 to 1.0 percentage points.

- The startup heater can undergo rapid changes in inlet steam flow. Although the steam flow is attemperated, the rates of change in the heater metal temperature can exceed typical commercial values; i.e., 10 °C/min. To what extent this influences the low cycle fatigue life of the heat exchanger is not yet known.

- The startup heater is used daily, and its operation is mandatory to start the steam generator. Further, one 100-percent heater is a typical design approach. As such, if the startup heater is not available, the plant incurs a forced outage.

- Starting the steam generator, synchronizing the turbine, and loading the turbine is an involved process. If the turbine trips due to a spurious control signal, the turbine can be quickly restarted once the trip is cleared. For this to occur, the steam generator must remain in operation; i.e., steam is dumped to the condenser through the bypass system. However, when the turbine trips, the extractions to the feedwater heaters are stopped, and the temperature of the feedwater leaving the last high pressure feedwater heater quickly decays. In response, the startup heater must be brought quickly into service. This produces a thermal shock on the tube side, in combination with a thermal shock on the shell side when live steam is introduced into the heater. To some degree, the low cycle fatigue life of the startup heater under thermal shock conditions is something of a commercial unknown.

6.7 Changes to the Equipment and the System Design

To avoid the problems experienced at a range of commercial projects, different approaches can be adopted regarding process design, fabrication techniques, and material selection.

6.7.1 Process Design

The goals of a revised process design are as follows:

- Allow the equipment to operate continuously at the 1-percent load case without affecting the low cycle fatigue life of the equipment. The 1-percent load case is an arbitrary requirement; i.e., it is no more applicable than the 2- or the 5-percent case. But if the process design, at 1 percent load, can protect the equipment against stress distributions that could reduce the low cycle fatigue life, then the process design can comprehensively protect the equipment over the full range of part- and full-load conditions

- Establishing uniform flow distributions, on both the shell- and the tube-sides of the heat exchangers throughout the full range of startup and shutdown conditions. Uniform flow distributions avoid the potential for non-uniform temperature distributions and the associated potential for damaging stress distributions.

System Availability Requirements

Most commercial projects use two 50-percent capacity steam generator trains due, in large part, to the relatively low availability of the equipment. However, many of the availability problems can be traced to leaks in the heat exchangers. Potential sources of the leaks include the following:

- Relaxation of the tube-to-tubesheet connections in the superheater, likely due to exceeding the vendor limits on rates of temperature change and allowable fatigue cycles [42]

- Pitting corrosion of the stainless steel tubes in the evaporator. The corrosion is associated with solid deposits, which are generated from flow accelerated corrosion of the carbon steel equipment in the condensate system. The accelerated corrosion can be traced to inadequate control over the feedwater chemistry.

An example of a simplified, order-of-magnitude reliability and availability analysis for a steam generator system is discussed in the following sections.

<u>Reliability Block Diagram</u>

In at least two representative commercial projects, the steam generation system consists of the following subsystems:

[42] Aalborg CSP, TEMA SGS/HX U-Tube Type Inspected and Repaired / Replaced by Aalborg Service Department, 2019

- Three 50-percent capacity hot salt pumps. The 3 pumps share a common minimum flow recirculation valve

- Two 100-percent capacity cold salt attemperation pumps. The 2 pumps share a common minimum flow recirculation valve

- Two 50-percent steam generator trains. Each train consists of a superheater, a reheater, an evaporator, and a preheater. The salt flow at the hot end of each train splits into parallel flows between the superheater and the reheater. The salt flow from the cold end of the superheater combines with the salt flow from the hot end of the reheater, and the combined flow passes, in series, through the evaporator and the preheater.

Hot Salt Pump Subsystem The reliability of the pump subsystem is based on the following:

- Each pump group includes the pump, the discharge isolation valve, the discharge control valve, either the limit switches or the positioners on the valves, and the heat tracing on the valves. All of the items in the group operate in series. The reliability of the group is given by:

$$R_{Group} = \prod_{1}^{i} R_i$$

  where R_i is the reliability of component i. The mean time between failure of the pump group is given by:

$$MTBF_{Group} = \frac{1}{\sum_1^i \frac{1}{MTBF_i}}$$

  where $MTBF_i$ is the mean time between failure of component i.

- 2 of the 3 pump groups must be in service to provide the design flow rate. The reliability for a 2-out-of-3 arrangement is:

$$R_{2\ of\ 3} = R_{Group}^3 + 3 * R_{Group}^2 * (1 - R_{Group})$$

- The 3 pump groups operate in series with the minimum flow recirculation valve.

Attemperation Pump Subsystem The reliability of the pump subsystem is based on the following:

- Each pump group includes the pump, the discharge isolation valve, the discharge control valve, either the limit switches or the positioners on the valves, and the heat tracing on the valves. All of the items in the group operate in series.

- The two pumps operate in parallel, and 1 of the 2 pumps must be in service to provide the design flow rate. The reliability of two components operating in parallel is given by:

$$R_{Subsystem} = R_1 * (1 - R_2) + R_2 * (1 - R_1) + R_1 * R_2$$

where R_1 is the reliability of pump group 1, and R_2 is the reliability of pump group 2. The mean time between failures of the subsystem is given by:

$$MTBF_{Subsystem} = \frac{1}{\frac{1}{MTBF_1} * \frac{MTTR_1}{MTBF_2} + \frac{1}{MTBF_2} * \frac{MTTR_2}{MTBF_1}}$$

- The in-service pump operates in series with the minimum flow recirculation valve.

Heat Exchanger Subsystem The reliability of the heat exchanger subsystem is based on the following:

- Train 1 operates in parallel with Train 2. However, both trains must be in service to provide the design steam flow rate

- In each train, the superheater operates hydraulically in parallel with the reheater. However, both the superheater and the reheater must be in operation for the train to be in operation.

Steam Generator System For the steam generator to operate, each of the 3 subsystems above must be in service. Further, the systems operate in series.

<u>Reliability and Mean Time Between Failure Data</u>

Reliability and failure rate data for the components in the hot salt pump and the attemperation pump subsystems are outlined in Table 6-1. For the purposes of the calculations, a reference period, T, of 4,000 hours has been assumed. This represents 1 calendar year of operation in a plant with an annual capacity factor of 45 percent.

It can be noted that there are little or no public data available on the reliability and the availability of salt steam generators in commercial service. The mean times between failures for each of the components in the table are largely based on a non-scientific survey of the experience from a range of parabolic trough and central receiver projects, using a mix of qualitative and quantitative information. In addition, the mean time between failure estimates listed for the superheaters and the evaporators represent a plant in which the heat exchanger reliabilities did not reach expected values. Problems with these heat exchangers have resulted in forced outage periods on the order of 10 to 14 days each. Clearly, the qualitative nature of some of the reliability information, in combination with the small sample size, means that the uncertainty in the calculated availability values is likely to be high. Nonetheless, the general trends shown in the calculations have been observed in commercial practice.

Table 6-1 Inputs to the Reliability Calculations for the Steam Generator - Current Experience

	Mean time between failures,						
System Component	Years	Hours	Failure rate, 1/hr	Reliability, [ ]	Failures per yr., each	Failure repair time, hr	Failures x Repair time, hr
Salt pump	10	40,000	$2.50 * 10^{-5}$	0.905	0.1	48	5
Discharge isolation valve	1	4,000	$2.50 * 10^{-4}$	0.368	1	12	12
Discharge control valve	1	4,000	$2.50 * 10^{-4}$	0.368	1	12	12
Discharge flow meter	0.2	800	$1.25 * 10^{-3}$	0.007	5	1	5
Minimum flow recirculation valve	1	4,000	$2.50 * 10^{-4}$	0.368	1	12	12
Superheater / reheater [1]	2	8,000	$1.25 * 10^{-4}$	0.493	0.5	336	168
Evaporator [2]	0.5	2,000	$5.00 * 10^{-4}$	0.243	2	240	480
Preheater	30	120,000	$8.33 * 10^{-6}$	0.905	0.033	336	11
Salt piping	50	200,000	$5.00 * 10^{-6}$	0.980	0.02	48	1
Heat tracing [3]	1	4,000	$2.50 * 10^{-4}$	0.368	1	12	12

Notes:
1. The superheater and the reheater are supplied with salt in a parallel arrangement; however, both heat exchangers must be in service for the steam generator to be in service. The mean time between failures for the superheater / reheater combination is defined by the mean time between failures for superheater, which is the more problematic of the two due to thicker metal sections associated with higher operating pressures.
2. Evaporator outages are due to tube leaks associated with inadequate control over the water chemistry.
3. There are perhaps 100 heat trace circuits in the steam generation system. The reliability values reflect not a failure of an individual circuit, but a system level failure that would prevent the steam generator from operating.

For the purposes of the calculations, a Weibull probability distribution has been assumed. The distribution of the time to failure, f (Time; Scale parameter, Shape parameter), is given by:

$$(\text{Shape} / \text{Scale})\ (\text{Time} / \text{Scale})^{(\text{Shape} - 1)} \exp\left(-(\text{Time} / \text{Scale})^{\text{Shape}}\right)$$

The cumulative probability of failure, F(Time; Scale parameter, Shape parameter) is given by:

$$\exp\left(-(\text{Time} / \text{Scale})^{\text{Shape}}\right)$$

and the Reliability is 1 - (Cumulative probability of failure).

In the reliability estimate for each of the components listed in Table 6-1, the scale parameter and the shape parameter are both set to values of 1. This is done as there is limited availability of information to support a value other than 1. However, the scale parameter for the superheater and the evaporator are both set to a (somewhat arbitrary) value of 0.5. This is to reflect the damage experienced by these heat exchangers in the early years of commercial service. Damage to the superheater is associated with high rates of temperature change, during startup and shutdown, for the period required to develop the tuning parameters for the control system. Damage to the evaporator is due to corrosion associated with inadequate control over the water chemistry.

System Availabilities Based on Current Heat Exchanger Experience

An estimate of the subsystem and the system availabilities for plants with two 50-percent heat exchanger trains is listed in Table 6-2.

Table 6-2 Steam Generator Availability - Current Experience

Subsystem	Mean Time Between Failures, hr.	Availability
Hot salt pumps	111	0.959
Attemperation pumps	593	0.992
Heat exchangers	741	0.737
Overall system	50	0.701

It can be noted that the availability of commercial solar projects in financial models are often quoted to be in the range of 90 to 92 percent. The steam generator necessarily operates in series with the heliostat field, the receiver system, the storage system, the Rankine cycle, and the balance of plant systems (i.e., water treatment and compressed air). A representative set of availabilities (in some cases, availability goals) for these systems is outlined in Table 6-3.

Table 6-3 System and Plant Availabilities - Current Experience

	Availability
Heliostat field	0.985
Receiver system	0.975
Thermal storage system	0.999
Steam generation system	0.701 [1]
Rankine cycle	0.990
Balance of plant	0.995
Total plant	0.662

Note:

1. Current experience, with two 50-percent trains

From the table, the following can be seen:

- For a project to meet its projected financial requirements, the reliability of the heat exchangers must be improved. This will require changes in items such as process control, fabrication methods, and water chemistry monitoring

- From the reliability information listed in Table 6-1, the availability of one 50-percent capacity steam generator train is on the order of 0.848. However, both trains must be in service to provide the design steam flow rate. For trains in parallel service, but in an arrangement in which both trains must operate, the combined availability of the two trains is 0.848 * 0.848 = 0.737. If the availability of one 50-percent train is below commercial requirements, then adding a second 50-percent train, of the same design and the same availability, does not improve the availability of the system.

System Availabilities Based on Projected Heat Exchanger Experience

If the problems with process temperature control and feedwater chemistry can be solved, then the reliability of a single steam generator train should improve to the values shown in Table 6-4. In the component reliability calculations, the Weibull distribution scale parameter and shape parameter are set to values of 1 to reflect the long-term maturity of the design.

Table 6-4 Reliability Analysis for a Single Steam Generator Train - Projected Performance

	Mean time between failures,						
System Component	Years	Hours	Failure rate, 1/hr.	Reliability, [ ]	Failures per yr., each	Failure repair time, hr.	Failures x Repair time, hr.
Hot salt pump	10	40,000	$2.50 * 10^{-5}$	0.905	0.1	48	5
Discharge isolation valve	1	4,000	$2.50 * 10^{-4}$	0.368	1	12	12
Discharge control valve	1	4,000	$2.50 * 10^{-4}$	0.368	1	12	12
Discharge flow meter	0.2	800	$1.25 * 10^{-3}$	0.007	5	1	5
Minimum flow recirculation valve	1	4,000	$2.50 * 10^{-4}$	0.368	1	12	12
Superheater / reheater [1]	10	40,000	$2.50 * 10^{-5}$	0.905	0.1	240	24
Evaporator [1]	10	40,000	$2.50 * 10^{-5}$	0.905	0.1	240	24
Preheater [1]	10	40,000	$2.50 * 10^{-5}$	0.905	0.1	240	24
Salt piping	50	200,000	$5.00 * 10^{-6}$	0.980	0.02	48	1
Heat tracing [2]	1	4,000	$2.50 * 10^{-4}$	0.368	1	12	12

Notes:

1. Forced outages for tube plugging, which are not coordinated with the scheduled plant-wide maintenance outages.
2. There are perhaps 100 heat trace circuits in the steam generation system. The reliability values reflect not a failure of an individual circuit, but a system level failure that would prevent the steam generator from operating.

With these values, the calculated system availability in a mature design is estimated to be 0.89, as noted in Table 6-5.

To reach a system availability of 0.89, the following must occur:

- The heat exchangers, which have the largest influence on the system availability, must operate with a mean time between failures of perhaps 10 years

Table 6-5 Steam Generator Availability - Projected Performance

Subsystem	Mean Time Between Failures, hr.	Availability
Hot salt pumps	111	0.959
Attemperation pumps	593	0.992
Heat exchangers	5,000	0.939
Overall system	64	0.894

- The allowable types of heat exchanger failures must be restricted to leaks in a small number of tubes; i.e., there are no wholesale failures of the tube-to-tubesheet connections or systemic tube corrosion

- The cumulative number of tubes requiring plugging is no more than the allowance provided by the vendor.

To satisfy these requirements, the process temperature control and the feedwater chemistry must always be correct throughout the life of the project.

Potential for a Single Train Design

If the availability of the steam generation system is increased to a value of 0.89, then the availability of the overall plant is increased to a nominal value of 0.85, as follows:

Table 6-6 System and Plant Availabilities - Projected Performance

	Availability
Heliostat field	0.985
Receiver system	0.975
Thermal storage system	0.999
Steam generation system	0.894 [1]
Rankine cycle	0.990
Balance of plant	0.995
Total plant	0.845

Note:

1. Projected performance, with two 50-percent trains

However, a plant availability of 0.85 is still below commercial requirements. To improve the plant availability, two potential approaches for improving the availability of the steam generation system include the following:

- As shown in Table 6-5, the heat exchangers have the largest influence on the system availability. One approach to improving the availability of the heat exchangers is to switch from two 50-percent trains to one 100-percent train. By doing so, this avoids the following effect on reliability of two trains, operating in parallel, required to meet a design condition:

$$\text{System Reliability} = (\text{Reliability}_{\text{Train 1, 50 percent capacity}}) * (\text{Reliability}_{\text{Train 2, 50 percent capacity}})$$

- Replacing the three 50-percent hot salt pumps with two 100-percent hot salt pumps.

With these changes, the availability of the steam generation system improves to a value of 0.95, and the availability of the overall plant increases to a value of 0.90. A value of 0.90 is consistent with the projections often proposed in financial models.

Informal discussions with steam generator vendors indicate that the heat exchangers for a representative 125 MWe plant can be built in the sizes required for one train. As such, the single train design should be preferred over the two 50-percent train approach.

It can be noted the typical commercial approach to the design of the hot salt pumps (i.e., three 50-percent pumps) allows the use of one hot salt pump to supply the two steam generator trains during startup and shutdown. Compared to one 100-percent pump, the use of one 50-percent pump provides a better match between the H-Q characteristics of the pump with the flow and pressure drop characteristics of the heat exchangers during part load conditions. Nonetheless, using one 100-percent for startup and shutdown can result in acceptable pump performance as long as the following occurs:

- A hydraulic analysis of the steam generation system is conducted to confirm that pump is always operating at acceptable combinations of pump speed, flow, and total developed head

- Simultaneously, the Cv characteristics of the split-range salt control valve at the cold end of the preheater are selected such that the operating points of the hot salt pump, operating in parallel with the attemperation pump, provide the required hydraulic stability.

It should be noted that the reliability calculations in Table 6-1 and Table 6-4 include only the major equipment items. A more thorough analysis would include items such pressure instruments, temperature instruments, heat trace circuits, number of tube-to-tubesheet connections, permissives and interlocks in the logic for the distributed control system, and communication errors. As such, the estimates of availability should be viewed as indicative, rather than quantitative. Nonetheless, the general trends regarding the minimum acceptable values for equipment reliabilities should largely be applicable.

Also, reducing the number of trains by a factor of 2 (i.e., one 100-percent train rather than two 50-percent trains) means that the number of equipment items are also reduced by a factor of 2. Reducing the number of equipment items operating in series generally improves the system availability.

Independent Trains

Even if two 50-percent steam generator trains are selected for a commercial project, each train should be independent of the other. Each train would consist of one 100-percent capacity hot salt pump, one 100-percent capacity attemperation pump, the steam generator heat exchangers, and a steam bypass system to the condenser. The salt pump arrangement is illustrated in Figure 6-3, and the intra-heat exchanger salt valve arrangement is shown in Figure 6-4. (Clearly, the analysis described below for two 50-percent independent trains can readily be extended to one 100-percent independent train.)

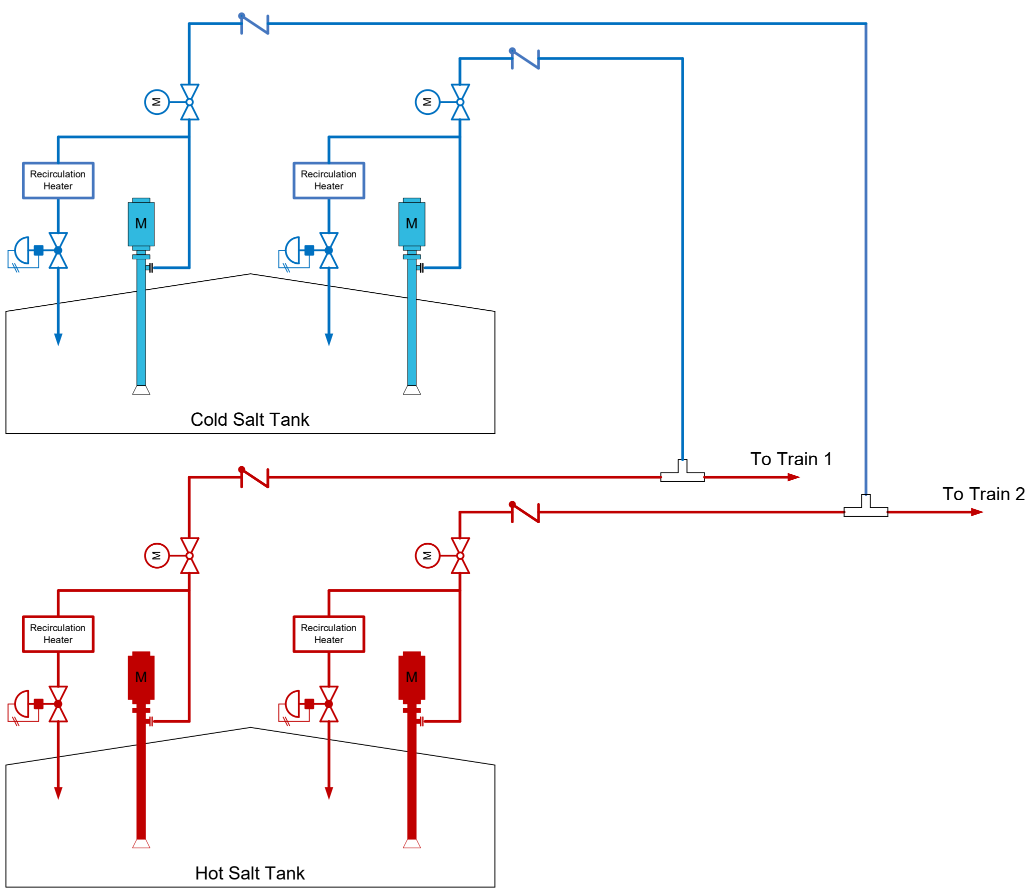

Figure 6-3 Salt Pump Arrangement with Independent Steam Generator Trains

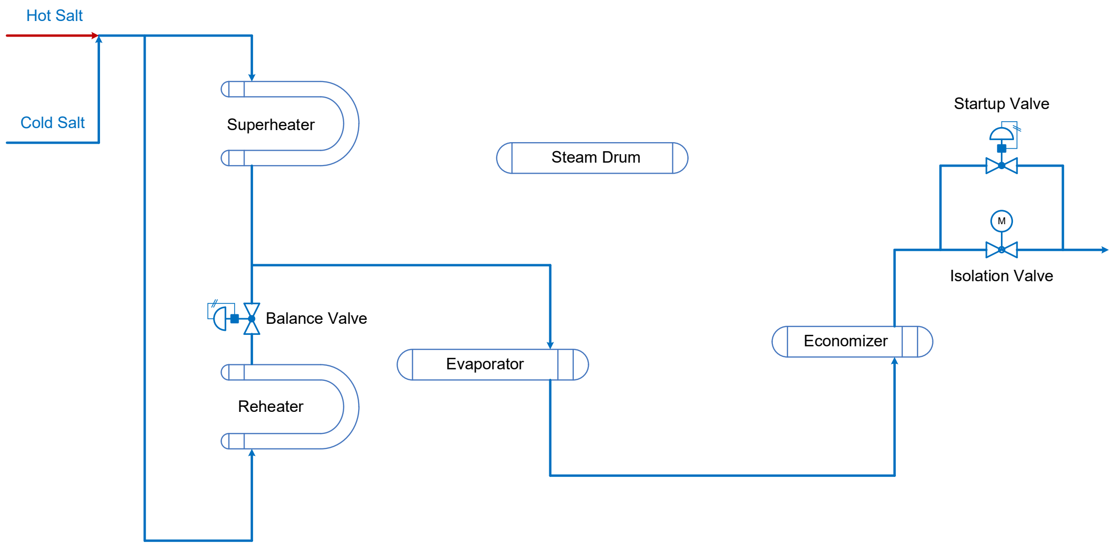

Figure 6-4 Intra-Heat Exchanger Salt Valve Arrangement

Independent trains allow either train to start at any time, regardless of the operating state of the other train. In addition, independent trains avoid a situation in which:

- Multiple pumps share a common discharge header
- Multiple pumps share a common minimum flow recirculation valve
- Multiple hot salt pumps, in parallel with multiple attemperation pumps, share a common mixing station upstream of the superheater / reheater.

The sharing of headers and mixing stations means that the discharge pressure of one pump influences the flow from any one, and perhaps more than one, of the other pumps operating in parallel.

Further, it is recommended that a split-range startup salt valve be added in parallel to the normal isolation valve at the cold end of the preheater. With the isolation valve closed, the startup valve performs two important functions: 1) the valve adds an artificial pressure drop to the system, and 2) the hot salt pump and the cold salt pump now see a common discharge pressure. These function provide the following benefits:

- If the pressure drop in the system is increased, then the pumps are no longer obligated to operate at their minimum speeds. As such, varying the pump speed now becomes a potential means of system control. The value in this approach is that pump speeds can be both accurately measured and accurately controlled.

- If the head - flow characteristics of the pumps are well defined, and if the flow - pressure drop characteristics of the piping, the valves, and the heat exchangers are well defined, then it is possible to both calculate and to accurately control the relative flow rates of hot salt and cold salt. This, in turn, allows the salt temperature at the mixing station upstream of the superheater / reheater to be controlled by changing the relative speeds of the pumps.

- The control approach avoids the need to match the discharge pressures from the two pumps using signals from pressure transmitters, or to set the flow rates from the two pumps using signals from flow meters. The accuracy of salt pressure and flow instruments is generally too low to control an acceleration in the hot salt flow rate on the order of 0.0023 m^3/hr-hr.

- It is possible to select a discharge coefficient for the split range startup valve that allows the minimum flow recirculation valves for both the hot salt pump and the attemperation pump to be set to fixed positions for steam generator flow rates beginning with startup, through turbine synchronization, and then to an intermediate turbine load. As such, all of the system valves remain in fixed positions, and both of the salt pumps see a common discharge pressure, which reduces the potential for oscillations in the mixed salt temperature upstream of the superheater / reheater.

The above approach to steam generator system control during startup was successfully demonstrated at the Solar Two demonstration project [43].

Pump Redundancy

A spare hot salt pump, and a spare attemperation pump, would be stored in the site warehouse. The reliability of salt pumps has been excellent, and providing an installed redundant pump can be counterproductive to the plant availability. Specifically, each pump requires an isolation valve, a startup control valve, a check valve (see below), and a vent valve.

Electric Salt Heaters in Minimum Flow Recirculation Lines

One example is the piping arrangement for the external electric salt heaters for the salt storage tanks. At one commercial project, two 100-percent salt heaters could receive salt from any of the 3 hot salt pumps in the hot tank, or salt from either of the 2 cold salt attemperation pumps in the cold tank. However, a total of 9 salt valves were required to either direct the flow as needed or to drain the equipment. In contrast, an alternate design would locate a separate electric heater in the minimum flow recirculation line for each of the salt pumps. Each heater would be located downstream of the minimum flow recirculation valve, and each heater would be located at an elevation above the salt tanks. The minimum

[43] Kelly, B (Bechtel National Inc., San Francisco, California), 'Lessons Learned, Project History, and Operating Experience of the Solar Two Project', Sandia Report SAND2000-2598, November 2000

flow valve would keep the electric heater flooded during operation, and the piping would be arranged such that the piping and the heater drain automatically when the pump is not in operation. Granted, a typical project might require 2 (or 3) hot salt pumps and 2 attemperation pumps, and as such, would require 4 (or 5) electric salt heaters. Further, the 4 (or 5) heaters could be more expensive than two 100-percent capacity heaters. However, the improvement in plant availability due to the elimination of 9 salt valves will more than offset the marginal cost of the smaller electric heaters. Plus, the use of salt heaters on each of the pumps provides essentially the same redundancy as the two 100-percent heaters in the example commercial project.

Pump Discharge Check Valves

Conventional swing check valves should be provided in the discharge lines on each of the salt pumps. During the early stages of the startup process, the required flow rate of hot salt is very small; something in the range of 2 to 20 m^3/hr. If the flow of hot salt were to be initiated by selecting a pump speed, and then opening an isolation valve in the pump discharge line, the likelihood that a flow as small as 2 m^3/hr could be established is very low. The more likely scenario is that one of the following conditions will occur:

- The discharge pressure of the hot salt pump is slightly too high, in which case the initial flow of hot salt is too high (20 m^3/hr).

- The discharge pressure of the hot salt pump is slightly too low, and cold salt starts to flow backwards towards the hot salt pump.

In either condition, it will not be possible to provide the required control of the mixed salt temperature at the entrance to the steam generator.

The best method for accomplishing this task is to provide a conventional swing check valve at the pump discharge. To initiate a flow, a hot salt pump speed is selected which provides a discharge pressure that is slightly below the cold salt pump discharge pressure. The differential pressure causes the hot salt pump check valve to close. (The pump is protected from overheating by the flow through the minimum flow recirculation line.) The speed of the hot salt pump is then increased in increments of 0.1 percent. The discharge pressure of the hot salt pump eventually rises to a value that is slightly greater than the cold salt pump discharge pressure, the check valve starts to open, and a very small, and stable, flow of hot salt is established.

The shutdown procedure for the steam generator is essentially the mirror image of the startup procedure. As such, the requirement for a check valve on the hot salt pump during startup is mirrored by a requirement for a check valve on the cold salt attemperation pump during shutdown.

6.7.2 Startup and Shutdown Procedures

A proposed heat exchanger and salt valve arrangement is shown in Figure 6-5. The startup valve adds an artificial pressure drop during startup and shutdown. Valve 1 and Valve 2 direct the flow of hot salt early in the startup, and late in the shutdown, process.

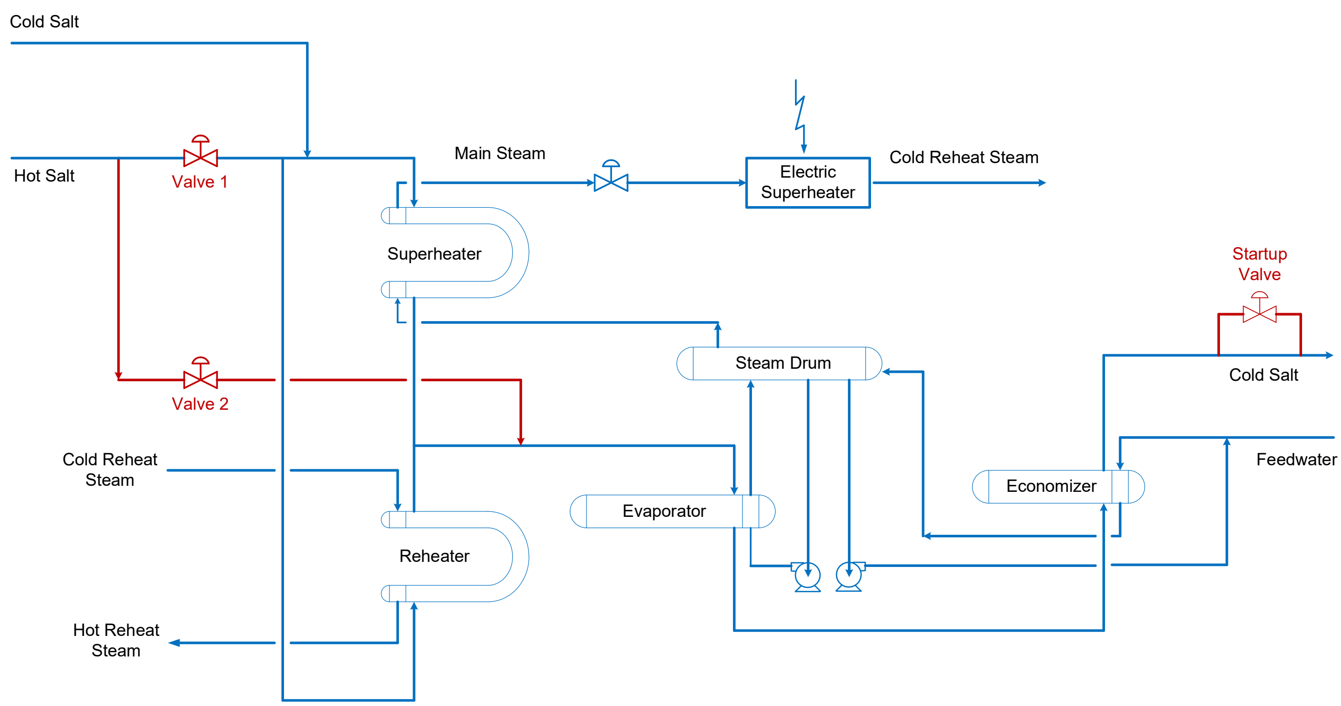

Figure 6-5 Steam Generator Heat Exchanger and Valve Arrangement

Early in the startup process, the temperature of the mixed salt upstream of the superheater / reheater is close to the cold salt temperature. As such, the temperature of the live steam at the hot end of the superheater is also close to the cold salt temperature. To ensure that the temperature of the salt at the cold end of the preheater does not challenge the salt freezing temperature, the saturation pressure in the steam drum is maintained at a nominal value of 100 bar. When live steam from the superheater at 100 bar is throttled to a pressure which can be accepted by the reheater (~ 30 bar), the temperature of the cold reheat steam can drop close to, or slightly below, the freezing temperature of the salt. To prevent salt from freezing at the cold end of the reheater, the temperature of the cold reheat steam is raised by means of an electric steam superheater.

Isothermal Steam Production

As discussed in Section 6.5, the steam flows in the superheater and in the reheater during startup necessarily span the range of 0 percent to the minimum flow rate allowed by the vendor (~ 16 percent). Low flow rates often produce poor flow distributions, which raise the possibility of undesirable temperature and stress distributions. However, if the heat exchanger is operating under isothermal conditions between flow rates of 0 and 16 percent on both the shell-side and the tube-side, then the potential for damaging stress distributions is largely eliminated.

One method for operating the superheater and the reheater under isothermal conditions is to establish a shell-side flow rate of cold salt at a temperature of 295 °C, and simultaneously establish a tube-side flow rate of steam at a temperature of 295 °C. The shell-side conditions are established by operating the cold salt attemperation pump at the design speed. The tube-side conditions are established by 1) selecting a set point pressure of 80 bar for the throttle valves in the steam bypass system to the condenser, and 2) supplying hot salt to a mixing station upstream of the evaporator, and 3) isolating the hot salt flow to the mixing station upstream of the superheater / reheater.

<u>Step 0 - Overnight Hold</u>

During overnight hold, cold salt is supplied to the steam generator, as shown in Figure 6-6. No steam production occurs, and the temperature of the salt passing through the heat exchangers decays only slightly due to the moderate heat losses from the heat exchangers and the system piping.

The recirculation pump from the steam drum to the cold end of the preheater is in service. Steam drum makeup water from the Rankine cycle combines with the recirculation flow at a point just upstream of the preheater. The direct contact heat exchange ensures that the relatively cold makeup water does not cause salt to solidify at the cold end of the preheater.

The startup salt valve at the cold end of the preheater is set to a position which provides the desired additional pressure drop for the salt pumps later in the startup process. A set of hydraulic calculations for a representative commercial project show that the startup valve can be set to a fixed position for Steps 0 through 4 discussed below.

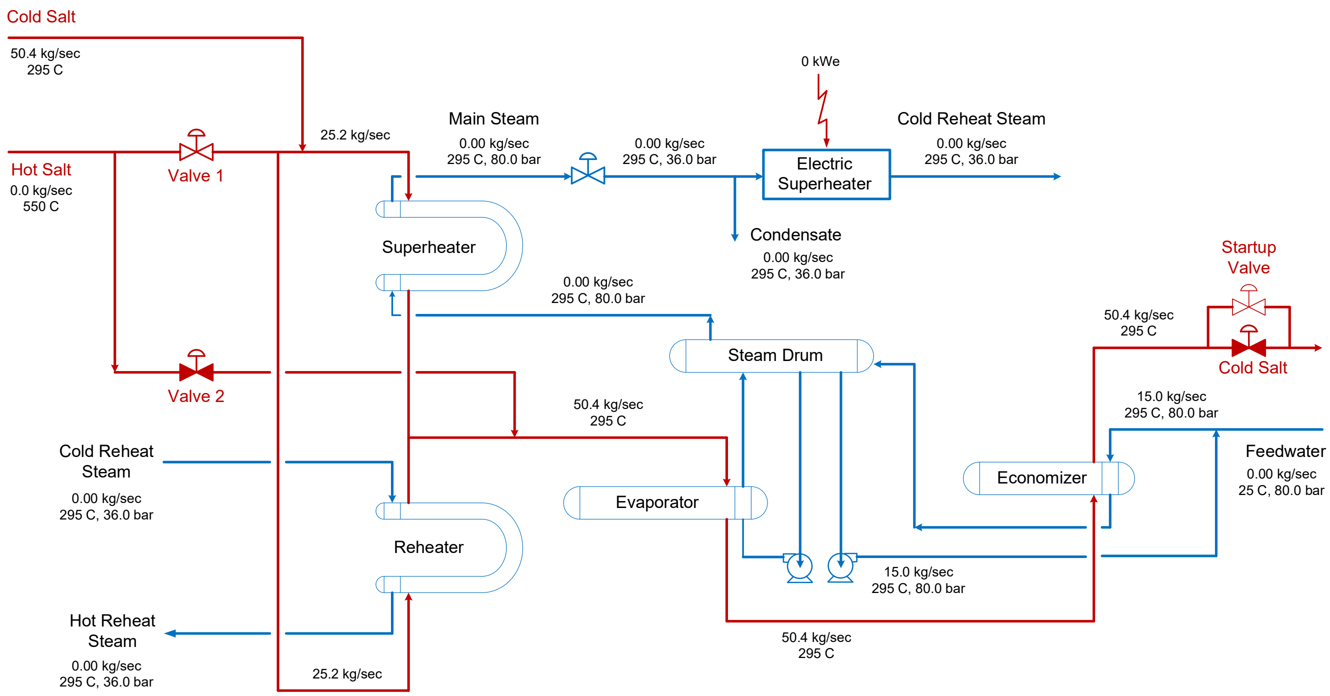

Figure 6-6 Step 0 - Overnight Hold

Step 1 - Isothermal Steam Production

The basic flow arrangement for the first step in this process is shown in Figure 6-7. The salt and steam flow rates are based on a nominal 125 MWe Rankine cycle with two 50-percent steam generator trains.

Cold salt, at a temperature of 295 °C, is supplied to the hot end of the superheater and to the hot end of the reheater. Simultaneously, saturated steam, at a temperature of 295 °C, is supplied to the superheater, and cold reheat steam, at a temperature of 295 °C, is supplied to the reheat. As such, no heat transfer occurs in either heat exchanger, and the temperature of the salt leaving both heat exchangers is 295 °C.

At the salt mixing station upstream of the evaporator, hot salt is added to the flows leaving the superheater and the reheater. This raises the temperature of the salt entering the evaporator to 428 °C, which provides the thermal energy required to 1) generate saturated steam, at a temperature of 295 °C, for delivery to the superheater and the reheater, and 2) establishes steam flow rates equal to 20 percent of the design flow rates in the both superheater and the reheater.

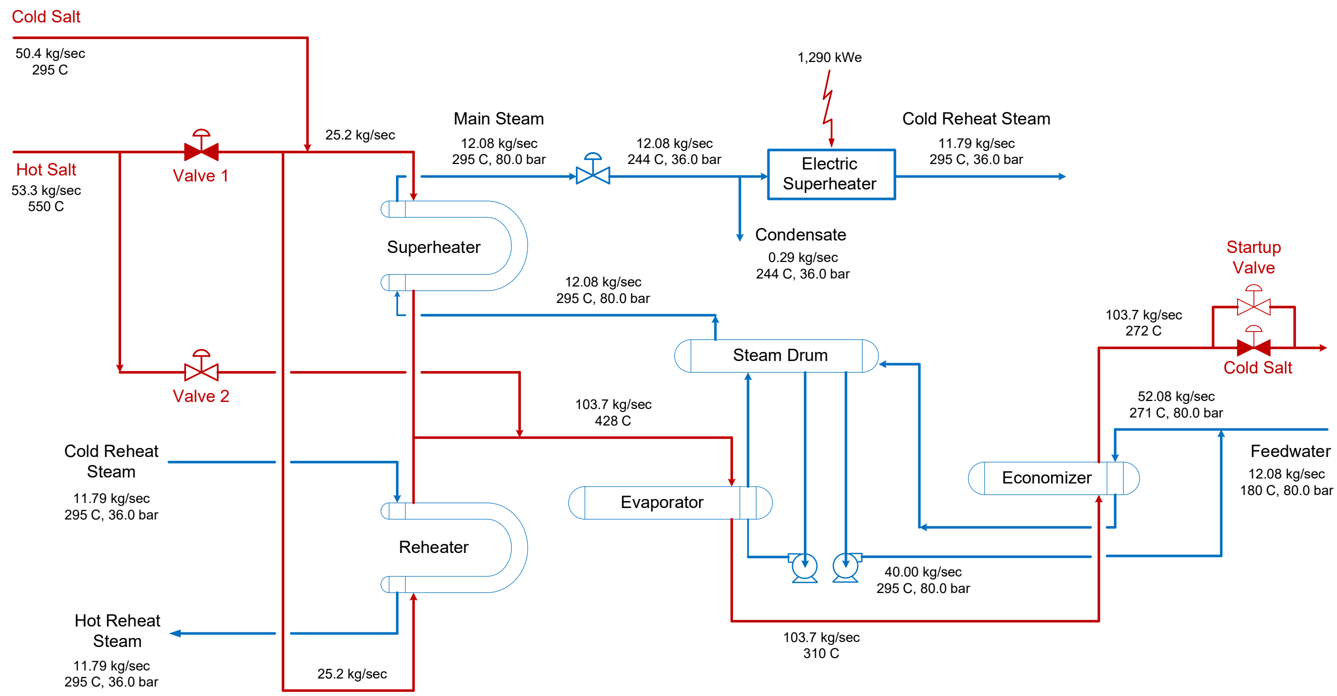

Figure 6-7 Step 1 - Isothermal Steam Production

The saturated steam pressure of 80 bar is established in the drum by the high pressure throttle valve in the steam bypass system to the condenser. A steam flow rate equal to 20 percent of the design flow rate is larger than the minimum required by the vendor (16 percent). However, the steam flow rate decays to 16 percent in the Step 2 below.

Throttling live steam, at a pressure of 80 bar, to the maximum pressure which can be accepted by the reheater (36 bar), results in a decrease of the steam temperature to the saturation temperature corresponding to 36 bar (244 °C). The quality of the steam leaving the high pressure throttle valve is on the order of 97 percent, and 0.3 kg/sec of condensate is removed in a trap prior to the steam entering the cold end of the reheater. To ensure that no heat transfer occurs in the reheater, the temperature of the cold reheat steam is increased to the cold salt temperature (295 °C) by means of a 1.3 MWe electric steam superheater.

The flow rate and temperature of the makeup water from the Rankine cycle are 12.1 kg/sec and 180 °C, respectively. The feedwater temperature assumes that auxiliary steam, at a nominal pressure of 10 bar, is supplied to the deaerator for preheating. The recirculation of saturated water from the drum to the cold end of the preheater raises the mixed feedwater temperature to a value of about 271 °C, which is high enough to prevent salt from freezing at the cold end of the preheater.

As a technical note, all commercial solar projects use an auxiliary steam generator for equipment preheating and to supply steam to the turbine shaft seals to establish a vacuum in the condenser. An auxiliary steam generator is required, as steam generator vendor generally does not permit the use of the main evaporator for small steam flow rates over extended periods of time.

Superheated Steam Production

<u>Step 2 - Switching the Salt Mixing Station</u>

Once flows of 20 percent have been established on the tube-sides of the superheater and the reheater, the hot salt / cold salt mixing station is switched from a point upstream of the evaporator to the normal point upstream of the superheater / reheater, as shown in Figure 6-8.

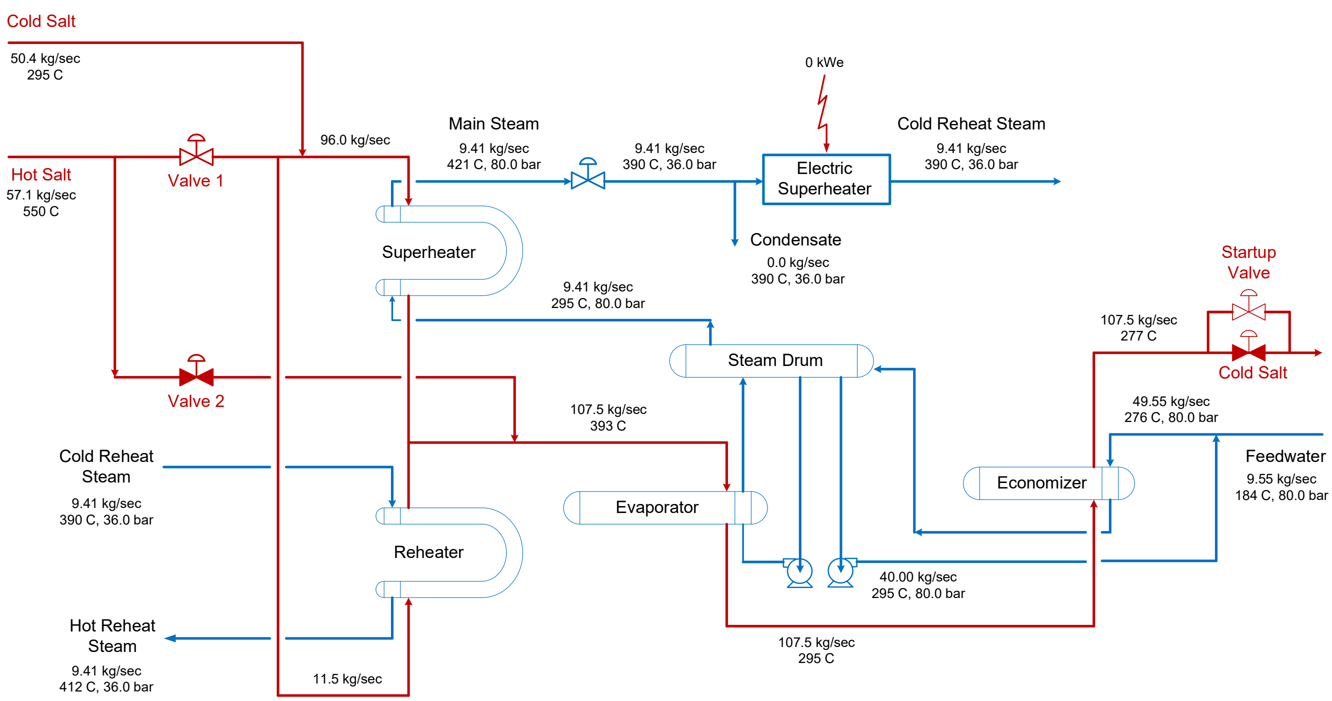

Figure 6-8 Step 2 - Live Steam and Hot Reheat Steam Production

The transition basically involves opening Valve 1 and closing Valve 2 at rates which keep the following sum a constant value: $Cv_{\text{Valve 1}} + Cv_{\text{Valve 2}}$. Under these conditions, no changes occur in either the hot salt or the cold salt flow rates, and the transition should be hydraulically stable. The rates at which Valve 1 and Valve 2 move are:

- Amenable to calculation, based on curves of Cv versus valve position

- Programmed in the DCS such that the mixed salt temperature at the hot end of the evaporator decreases at no more than the vendor limit of 10 °C/min

- Programmed in the DCS such that the mixed salt temperature at the hot end of the superheater / reheater increases at no more than 10 °C/min.

Moving the mixing station to a point upstream of the superheater / reheater raises the temperature of the salt entering both the superheater and the reheater. As such, heat transfer now begins in the superheater and in the reheater, which would normally increase the thermal demand on the steam generator. However, one of the goals of the transition is to maintain the cold salt and the hot salt flow rates fixed in both Step 1 and Step 2. With the flow rates fixed, the feedwater flow rate decreases to a new value of 9.55 kg/sec to offset the increased thermal demands of the superheater and the reheater. A feedwater flow rate of 9.55 kg/sec corresponds to the 16 percent minimum value specified by the vendor.

<u>Step 3 - Turbine Synchronization</u>

At the end of Step 2, the steam generator has nominal live steam and hot reheat steam flow rates of 16 percent, and live steam and hot reheat steam temperatures slightly above 410 °C. This combination of steam flow rate and temperature should be adequate to admit steam to the turbine under the conditions of a warm start, accelerate the turbine to synchronous speed, synchronize the turbine, and load the turbine to a value which is high enough to prevent a trip on reverse power. (If the turbine is undergoing a cold start or a hot start, then steam can be admitted to the turbine starting when the steam temperatures are lower than, or higher than, 410 °C, respectively.)

The steam supplied to the turbine is diverted from the turbine bypass system. Whatever steam is not required by the turbine continues to be bypassed to the condenser.

<u>Step 4 – Low Load Operation</u>

Once the turbine is synchronized, the extraction feedwater heaters are placed in service. However, saturated water from the steam drum continues to be recirculated to the cold end of the preheater to maintain the temperature of the salt at the cold end of the preheater at acceptable values.

To increase the thermal output of the steam generator, and to increase the live steam and the hot reheat steam temperature, the speed of the hot salt pump is increased. The increase in the discharge pressure of the hot pump will result in a decay in the flow rate from the attemperation pump. The rate at which the speed of the hot salt pump is increased is such that the mixed salt temperature at the hot end of the superheater / reheater satisfies the vendor limit of 10 °C/min.

At some point in this transition, the speed of the attemperation pump will need to be reduced. The rate at which the speed of the attemperation pump is reduced is such that the mixed salt temperature at the hot end of the superheater / reheater satisfies the vendor limit of 10 °C/min. Eventually, the flow rate from the attemperation pump stalls. A check valve on the discharge of the attemperation pump prevents a reverse flow through the pump. At this point, the attemperation pump can be stopped, and only salt from the hot pump is supplied to the steam generator.

Once the steam generator trains reaches its design temperature profile (565 °C at the hot end of the superheater / reheater, and 295 °C at the cold end of the preheater), the salt isolation valve at the cold end of the preheater can be opened and the startup valve closed. Opening the isolation valve will reduce the pressure drop in the system, and the speed of the hot salt pump will need to be reduced to maintain a nominally constant flow rate of hot salt. It's unlikely that the valve transition can be accomplished without a change in the hot salt flow rate. However, even if the flow rate does change, the normal temperature profile along the steam generator has already been established, and the potential for thermally shocking the heat exchangers is very low.

Throughout Steps 1 through 4 above, the goals of the process design are as follows:

1. Avoid the use of pressure and flow measurements to set the relative flow rates of hot salt and cold salt. The accuracy of the pressure and flow instruments are inconsistent with the accuracy with which the flow rate of hot salt must be accelerated to satisfy the vendor limits on rates of temperature change.

2. During startup and shutdown, the salt-side pressure drops are very low. To reduce the potential for oscillations in the flow rates from pumps operating in parallel, the 1) the system pressure drop is artificially increased by means of a startup valve, and 2) the following valves are set to fixed positions: the startup valve at the cold end of the preheater; the minimum flow recirculation valve for the hot salt pump; and the minimum flow recirculation valve for the attemperation pump.

3. Process control inputs should be limited to those items which are accurate and reliable. In general, this limits the inputs to temperature measurements.

4. Process control outputs should be limited to those items which can be accurately measured and controlled. To a first order, this includes the speeds of the hot salt and the attemperation pump.

5. Items 2, 3, and 4 are satisfied if the mixed salt temperature to, and the thermal duty of, the steam generator are set by adjusting the relative speeds of the hot salt and the attemperation pumps.

6. During various stages of startup and shutdown, the flows from the hot salt and the attemperation pump will approach a value of zero. To prevent reverse flows through the pumps, conventional

check valves should be provided in the discharge lines. A total of 4 swing check valves were used at the Solar Two demonstration project, and the valves proved to be reliable.

To shut down the steam generator, the turbine is brought to the minimum load, and then tripped to preserve the metal temperatures in preparation for the next startup. The steam generator is shut down in essentially a reverse of the 4 steps above.

Part-Load Steam Generator Models

In Steps 1 through 4, the heat exchangers are operating under part-load conditions. The independent parameters under which the steam generator is operating include the following:

- The hot salt and the cold salt temperatures
- The feedwater flow rate, temperature, and pressure
- The water recirculation flow rates to the cold end of the preheater and to the cold end of the evaporator
- The saturation pressure in the drum, as set by the high pressure throttle valve in the bypass system to the condenser, and the cold reheat steam pressure, as set by the low pressure throttle valve in the bypass system to the condenser
- The evaporator blowdown flow rate
- The saturated steam flow rate to the superheater and the cold reheat steam flow rate to the reheater.

This leaves a number of dependent operating parameters, which must be calculated:

- Hot salt and cold salt flow rates
- Feedwater temperature at the hot end of the preheater
- Live steam and hot reheat steam temperatures
- Salt temperatures at the cold end of the superheater, the cold end of the reheater, the hot end of the evaporator, the cold end of the evaporator, the hot end of the preheater, and the cold end of the preheater.

The calculation involves the following steps:

1. A trial salt temperature profile along the steam generator train is assumed

2. A trial salt flow rate profile is developed, based on matching the duties on the salt side with the duties on the water/steam side

3. From the shell- and tube-side flow rates, heat transfer coefficients are calculated on the shell- and tube-sides. From these, in combination with shell- and tube-side fouling factors, an overall heat transfer coefficient is calculated for each heat exchanger

4. The required log mean temperature differences in each heat exchanger are calculated from the following expression:

$$LMTD = \frac{Q}{U_{Overall} * A}$$

   where LMTD is the log mean temperature difference, °C, calculated in the usual manner
   Q is the heat exchanger duty, W
   $U_{Overall}$ is the overall heat transfer coefficient, W/m^2-°C, calculated in 3 above
   A is the heat transfer area, m^2, calculated at the design point conditions

5. The actual log mean temperature differences in each heat exchanger are calculated from the following temperatures: salt in; salt out; water/steam in; and water/steam out.

6. If the required and the actual log mean temperature differences differ, then a perturbation is made to the salt inlet temperature on a particular heat exchanger. A new salt flow rate is calculated to match the duties on the salt and the water/steam sides, from which new values are calculated for the overall heat transfer coefficient, the required log mean temperature difference, and the actual log mean temperature difference.

7. Full convergences are first developed for the superheater and the reheater. The preheater is then converged, with new calculations developed for the superheater and the reheater at each step in the convergence of the preheater. The evaporator is then converged, with new convergences for the superheater, the reheater, and the preheater at each step in the convergence of the evaporator.

The convergence routines are required to ensure that 1) the minimum allowable shell- and tube-side flow rates are always satisfied, 2) the temperature of the salt at the hot end of the evaporator in Step 1 does not exceed the allowable design value, and 3) the temperature of the salt at the cold end of the preheater is always above the minimum design value.

6.7.3 Static Salt Mixers

During steam generator startup and shutdown, a representative allowable rate of temperature change for the superheater and the reheater is 10 °C/min. At one 125 MWe commercial project, the temperature change rate translates to an allowable rate of change (i.e., acceleration) in the hot salt flow rate of 25 liters/min per minute. As a point of reference, the design flow rate for the hot salt pump is 14,200 liters/min. As such, the allowable rate of change in the hot salt flow rate is 0.17 percent of the design value rate per minute. A comprehensive process design is required to satisfy this limit. The process design must define, as a function of time, the following parameters:

- Hot salt pump: speed, position of the discharge control valve, and position of the minimum flow recirculation valve
- Attemperation pump: speed, position of the discharge control valve, and position of the minimum flow recirculation valve
- Position of the startup control valve at the cold end of the preheater.

Any variation or oscillation in the set point of 25 liters/min per minute will result in a variation or an oscillation in the mixed salt temperature at the hot ends of the superheater and the reheater. One potential method for modulating or damping the variation would be to provide a static mixer at the hot salt / cold salt mixing station upstream of the superheater and the reheater.

There are potentially two conditions under which the static mixer could be operating.

Condition 1: The process design can satisfy the 25 liter/min per minute requirement.

If the relative proportions of cold salt / hot salt are correct, then the purpose of the static mixer would be to limit the degree of radial stratification in the salt temperature in the pipe.

If the flow, when it reaches the superheater / reheater, has a radial stratification, then this could generate a non-predictable temperature, and a non-predictable stress, distribution in the shell near the inlet nozzle. The distribution belt inside the heat exchanger will dissipate much, or all, of this stratification. Nonetheless, there is little design information on what the allowable radial stratifications might at the inlet to the heat exchanger. A possible design approach might be to: 1) develop a CFD model to estimate the degree to which the radial stratification dissipates as a function of distance between the mixing station and the inlet to the superheater / reheater, and 2) develop a CFD / FEA model of the entrance to the heat exchanger to determine if the residual radial stratification imposes unacceptable local thermal stresses.

Three outcomes are possible:

1. The largest radial stratifications are likely to occur early in the startup process, or late in the shutdown process, when the salt flow rates are the lowest. The CFD analyses show that radial stratification levels during low flow conditions do not present a problem with heat exchanger stresses, and the mixer can safely be dropped from consideration.

2. The inverse to the above is that a mixer is required to limit the radial stratification. This is, nonetheless, a useful result, as it quantifies the need for, and the benefits of, a mixer. A note: The mixer would likely be designed for the low flow rates associated with startup and shutdown. As a result, the pressure drop of the mixer during full load conditions could have a measurable effect on the annual auxiliary energy demand.

3. The CFD / FEA analyses might be considered to be overly expensive, too lengthy in terms of the project schedule, or the results might be viewed as inconclusive. The project would then, in effect, be forced into making a guess on the need for a mixer. If so, one possible approach would be to install a mixer as, in essence, a brute force form of insurance. Granted, the penalty would be an increase in the auxiliary energy demand of the salt pumps. However, the benefit would be a reduction in the uncertainties regarding the transient thermal stresses in the superheater and in the reheater.

Condition 2: The process design does not satisfy the 25 liter/min per minute requirement.

The consequences of Condition 2 have been observed in one commercial project, and may well be present in other projects. The flow characteristic is similar to a plug of cold salt, followed by a plug of hot salt, followed by a plug of cold salt, and so on. The flow develops, in effect, a longitudinal temperature stratification.

Under these conditions, there is a basic deficiency in the process control. A static mixer would have no effect on the longitudinal stratification, and there would be no benefit to installing a mixer.

Summary

The process design must, unambiguously, have the control authority to satisfy the 25 liter/min per minute requirement. The process design can be developed using piping isometric diagrams, standard pressure drop formulas for pipes and fittings, H-Q curves for the two salt pumps, and equations listing valve discharge coefficients as functions of the valve positions.

A static mixer would be added only if the CFD / FEA analyses showed that radial thermal stratifications reached values which produced unacceptable thermal stresses at the hot ends of the superheater and the reheater.

6.7.4 Fabrication Techniques

A common joining technique for the tube-to-tubesheet connection is to strength weld the ends of the tubes to the face of the tubesheet, and then plastically deform the tubes into the tubesheets. However, there are alternate joining techniques that use welded connections.

Header / Coil

In conventional heat exchangers, the tubesheet must withstand the pressure differential between the shell- and the tube-side fluids. If the differential pressure is high, then the tubesheet must be thick (150 to 200 mm), as a flat plate is structurally inefficient when subjected to bending loads. However, thick metal sections are generally undesirable in equipment which must thermally cycle each day. The problems with transient stresses are compounded if thick metal sections are joined to thin metal sections.

A more efficient structure for withstanding a large differential pressure is a pipe section, particularly if the high pressure fluid is on the inside of the pipe. A section of pipe can act as a tubesheet, using the following arrangement:

- A series of holes are drilled along the length, and around the circumference, of the pipe
- Short, tapered nozzles are welded to the pipe at each hole
- The ends of the heat exchanger tubes are welded to the ends of the short nozzles.

The fabrication process is illustrated in Figure 6-9.

This fabrication approach offers three important advantages for equipment in cyclic service:

1. For a given differential pressure, the thickness of a pipe wall will be much less than the thickness of a flat tubesheet. Reducing the thickness of metal sections is generally beneficial in terms of controlling transient stresses.
2. All of the tube-to-tubesheet connections are welded. Leaks are much less likely to develop in a welded connection than in a friction connection.
3. The nozzles between the pipe and the tubes are tapered, which provides a transition in metal thickness. A tapered transition, rather than an abrupt transition as occurs between a flat tubesheet and a tube, reduces the transient thermal stresses.

Figure 6-9 Example of Header / Coil Heat Exchanger Fabrication [44]

Internal Bore Welding

In an internal bore welded design, tapered nozzles are machined from the face of a flat tubesheet. The ends of the tubes are then welded to the ends of the nozzle. Due to space limitations, the nozzle-to-tube butt welds are performed by a robotic welder inside the tube. A cross section example of the tubesheet and the welded connection is shown in Figure 6-10.

This fabrication approach offers many of the benefits associated with the header / coil design.

Allowable Rates of Temperature Change

Heat exchanger designs based on strength welding the tubes to the tubesheet, and then expanding the tubes into the tubesheet, have an allowable rate of temperature change of 8 to 10 °C/min, depending on the vendor.

Informal discussions with Aalborg CSP, a supplier of header / coil designs, indicate that allowable rates of temperature change are on the order of 12 to 13 °C/min.

[44] https://energetica-india.net/news/aalborg-csp-header-and-coil-technology-celebrates-its-10-years-leakage-free-anniversary

Figure 6-10 Example of an Internal Bore Welded Tube-to-Tubesheet Connection

The difference between the two allowable rates is not a large value. However, experience with commercial projects has shown that process designs have difficulties complying with a vendor limit of 10 °C/min. Relaxing the limit to 12 °C/min will not solve the problems with current process designs. However, revisions to the process design, as discussed above, in combination with higher allowable limits set by the vendor, should lead to needed improvements in steam generation system availability.

6.7.5 Material Selection in the Evaporator

In a number of commercial projects, the tube material in the evaporator is Type 347H stainless steel. This material certainly provides the strength necessary for operation at both the normal salt inlet temperature of 450 °C, and the tube-side design temperature of 510 °C. Further, the tube material matches the materials in the tubesheet and in the shell, which simplifies the welding processes. Nonetheless, the choice of materials does not have unanimous concurrence [45]. For example, although the steam generator is not designed to ASME Section I requirements, Section I does not permit the use of stainless materials in evaporators due to the potential for stress corrosion cracking. Similarly, European norm EN12952-3, Water Side Boilers, does not permit the use of austenitic materials in boilers or in steam drums.

The stress corrosion mechanism is promoted by chlorides, caustic, or reduced sulfur which may be present in the feedwater. Further, stainless steel is susceptible to pitting corrosion if deposits accumulate

[45] Aalborg CSP, 'NE1 700 MW CSP Project, Material Selection for Evaporator Tubes, CT-SGS', Document 40088C-D156-00006, Revision A, December 2018

on local portions of the surface but do not accumulate on portions adjacent to the deposits. The deposits can result from corrosion of the carbon steel components in the condensate system. The corrosion can result from poor control over the pH and the dissolved oxygen in the feedwater.

An alternate to Type 347H as the tube material is a ferritic alloy with a high chromium content, such as T91 [46]. This material offers acceptable corrosion resistance to salt at the normal operating conditions, and was successfully used in the first of two evaporators at the Solar Two demonstration project. Further, the material does not use nickel as an alloying elements; as such, it is largely immune to stress corrosion cracking mechanisms.

[46] Bradshaw, R. W. and Goods, S. H. (Sandia National Laboratories, Livermore, California), 'Corrosion of Alloys and Metals by Molten Nitrates', Sandia Report SAND2000-8727, August 2021

7. Valves in Salt Service

7.1 Valve Types

Isolation valves in salt service, including gate, ball, angle plug, swing check, and triple offset butterfly, will provide similar isolation characteristics to service in water. Similarly, control valves in salt service, including globe and angle plug, will provide similar control characteristics to service in water. However, not all types of valves are suitable for service in salt if the operating periods are measured in months to years.

Salt is an oxidizing material, and will develop oxide layers on all types of iron and nickel alloys. If the valve uses sliding surfaces, such as a gate valve or a ball valve, then oxide layers will develop on both the sliding and the stationary faces. Further, the oxide layers can mechanically bond to one another if the valve is not moved frequently; i.e., every few days. The corrosion process results in valve binding, even to the extent that the valve operators cannot develop the forces required to overcome the friction and the bonding forces. At the Solar Two demonstration project, the pneumatic actuator on an 8 in. ball valve developed forces high enough to plastically deform the valve stem, yet the valve remained in the open position.

In general, the only types of valves suitable for salt service are the ones where the plug moves perpendicular to the seat. The oxide layers still develop on the sealing surfaces. However, the oxide binding forces are lower if the surfaces move perpendicular to, rather than parallel to, one another. As such, the only suitable valve types are globe, angle plug, and triple offset butterfly. Nonetheless, it can be noted that some of the triple offset butterfly isolation valves at a commercial project developed internal leaks over a period of about 3 years. The source of the leakage was not fully identified, but it may be deformations of the valve bodies that are higher than expected due to the transmission of piping loads that are higher than expected. The solution for the commercial project was to replace the triple offset butterfly valves with valves which have a higher body rigidity; i.e., globe valves.

7.2 Stem Sealing

A common stem sealing material is graphite. The material is soft, which allows it to readily conform to the shape of the stem. Also, in the absence of an oxidizing environment, it is thermally stable. However, in salt service, the salt oxidizes the graphite to CO_2, and the packing eventually disappears.

At the Solar Two project, the recommended stem packing consisted of alternating layers of 1) Teflon washers, and 2) Inconel wire braids impregnated with graphite. Over time (weeks to months), the graphite in the braid oxidized, and the stem packings required periodic replacement of the Inconel braids. In general, this combination of packing materials was judged as marginally adequate. In subsequent commercial projects, other stem packing materials have been used, including various fluoropolymers, mica, and vermiculite. In some cases, the packing performed as intended, and in other cases, the packing developed leaks almost immediately. In general, a robust packing material, with a longevity measured in years, has yet to be identified.

To this end, the only stem seal which has been shown to be effective in preventing a leak is a bellows seal. This, in turn, implies that the preferred valve types are limited to those which can use a bellows seal; i.e., valves with translating stems, such as globe and angle plug valves.

As might be expected, this approach has met with resistance in commercial projects:

- A bellows stem seal is much more expensive than a packing stem seal. Budgetary estimates from a study conducted for DOE indicate that adding a bellows stem seal can triple the cost of a valve

- For isolation service, large globe valves are more expensive than triple offset butterfly valves

- The bellows may, under specific sets if circumstances, rupture. These circumstances include moving the valve with frozen salt in the bellows, or exposing the bellows to high transient pressures generated by a leak in a heat exchanger.

Using bellows seals on valves will increase the capital cost of the project. However, the cost penalty can be reduced by developing process designs that minimize the use of valves. One example is the piping arrangement for storage tank recirculation heaters, discussed in Section 6.7.1. The cost penalty is also likely to be offset by an increase in plant availability. Leakage past the valve stem seals exposes the heat trace cables on the valve body and on the adjacent piping to salt. The cables operate at temperatures which are high enough (> 650 °C) to decompose the salt. Several of the decomposition products are various oxides, which aggressively corrode the outer metal covering on the heat trace cables. Corrosion lifetimes are often measured in weeks. Once the covering corrodes, the internal heating cables are exposed to moisture, and can fail in a matter of days. Failed cables lead to immovable valves and frozen salt piping, which can necessitate forced outages, lasting hours to days. A project economic analysis will often show that the marginal improvement in plant availability and revenue, due to a properly functioning heat trace system, justifies the marginal expense for bellows stem seals.

In a thermal storage system in a commercial parabolic trough project, the salt control valves used bellows stem seals. The valve vendor supplied an engineered insulation enclosure for the valve body and the bellows region. The enclosure included the requisite heat trace cables and control thermocouples. The valve, bellows, and insulated enclosure are operating at expected, with no stem sealing failures due to frozen salt in the bellows.

7.3 Triple Offset Butterfly Valves

In general, and particularly for large valves (> 18 in.), triple offset butterfly valves are less expensive than globe valves. Since the valve provides good sealing characteristics, there is a motivation to use the valves wherever possible. Nonetheless, triple offset valves carry potential liabilities, as follows:

- Conventional stem packings, rather than bellows seals, must be used

- In large sizes, the valve bodies are not as rigid as those for globe valves. There have been instances in which large forces needed to be applied to piping to align the piping with the valve bodies. Once the welding was complete, the alignment forces were removed, which can result in a deformation of the triple offset valve body and a reduction in sealing effectiveness.

7.4 Isolation Valves

In the process design, careful consideration should be given to selection of globe, angle plug, and triple offset valves for isolation service. The detrimental effects on plant availability associated with leakage past valve stems should not be discounted. The selection of a valve with a bellows seal will likely increase the capital cost of the project, yet decrease the levelized energy cost.

7.5 Control Valves

For valve sizes of 20 in. and below, the preferred valve for control service is a globe valve with a bellows seal. For pipe sizes of 24 in. and above, there is a temptation to use a triple offset valve for control service due to cost considerations. However, the Cv versus percent open curves for triple offset valves show strong non-linear behavior, which can lead to difficulties in process control. If a control valve larger than 20 in. is required, the preferred option would be two 50-percent capacity globe valves with bellows seals.

7.6 Alternates to Globe and Triple Offset Butterfly Valves

The discussion above concentrates on the relative benefits and liabilities of globe valves and triple offset butterfly valves. However, alternate valve designs may also be available from commercial suppliers. Early in the project, discussions can be held between the project and potential valve suppliers to determine if alternate valve concepts could offer a suitable combination of structural rigidity, pressure drop, control linearity, hermetic stem sealing, and cost.

7.7 Pressure Relief Valve in Series with a Rupture Disc

Some form of salt pressure relief system is required on the heat exchangers in the steam generator, and on the receiver inlet vessel in a central receiver project. Candidate relief devices include relief valves and rupture discs.

7.7.1 Relief Valves

The relief valves are conventional commercial designs, applicable to a wide range of process conditions.

The valve body, and the piping downstream of the valve, will require heat tracing. Due to the different geometries, separate heat trace zones will be required for the valve body and the discharge piping. The heat tracing must be active at all times.

The principal advantage is the ability of the valve to automatically reseat should the fluid pressure temporarily rise above the set point pressure. The principal liabilities include the following:

- A Code requirement to periodically remove the valve for recalibration
- The potential for seepage through the valve due to 1) corrosion between the valve and the seat, or 2) thermal relaxation of the valve spring.

7.7.2 Rupture Discs

The rupture discs are also conventional commercial designs, applicable to a wide range of process conditions.

The rupture disc, and the piping downstream of the disc, will require heat tracing. Separate heat trace zones may be required for the disc and the discharge piping, depending on the size of the disc and its holder. The heat tracing must be active at all times.

The principal advantages are 1) an immunity from seepage, and 2) no need for periodic removal for recalibration. The principal liabilities include the following:

- The disc, by definition, operates at stresses very close to the yield value. As such, the disc can accumulate a combination of creep and fatigue damage due to the daily plant pressure and temperature cycles. At some point, the disc can develop a crack, either a small one or a large one
- When the disc develops a crack, either due to a pressure above the set point or due to creep plus fatigue damage, the disc will rupture. This will require a forced plant outage to replace the disc.

7.7.3 Passive Pressure Relief Versus Active Pressure Relief

A nuclear project developer is proposing a design in which a nuclear reactor, cooled by sodium, supplies energy to a salt system. The salt system consist of heat transport piping, a thermal storage system, and a steam generation system. Energy is transferred from the reactor loop to the salt system through a sodium-to-salt heat exchanger. One of the goals of the design is to separate nuclear components, and the associated licensing requirements, from the portions of the plant associated with heat transport, thermal storage, and electric power production.

A group of cold salt pumps supply cold salt to the sodium-to-salt heat exchanger. Depending on the final equipment selection, the shutoff head of the pumps may exceed the maximum allowable working pressure of the heat exchanger. To protect the heat exchanger, a pressure relief device, such as a rupture disc or a relief valve, can be used. Ideally the pressure relief device would be passive (i.e., no moving parts) to help satisfy the nuclear regulatory requirements.

In theory, a rupture disc could be viewed as a passive device. However, the piping to and from the rupture disc must be maintained at temperatures above the salt freezing point at all times. The temperatures are maintained by the heat trace system. The heat trace system is an active system, as it relies on 1) thermocouples and logic controllers to monitor the zone temperatures, 2) electric contactors to energize and de-energize the heat trace cables, and 3) transformers and switchgear to supply electric power to the contactors. As such, the regulatory agencies are unlikely to view the rupture disc as a passive device.

7.7.4 Relief Valve in Series with a Rupture Disc

As an alternate to a relief valve or a rupture disc, a relief valve can be located in series with a rupture disc, as shown in Figure 7-1.

A monitoring device registers the pressure in the space downstream of the rupture disc, and indicates whether the disc is intact or not.

Depending on the geometry of the series installation, separate heat trace zones may be required for the disc, the monitoring device, and the relief valve. The heat tracing must be active at all times.

Locating the valve downstream of the disc resolves some of the liabilities noted above, as follows:

- The seat and the plug in the relief valve are isolated from the corrosive effects of salt
- If the rupture disc breaks, then the relief valve continues to operate in the normal manner, and the plant does not incur a forced outage.

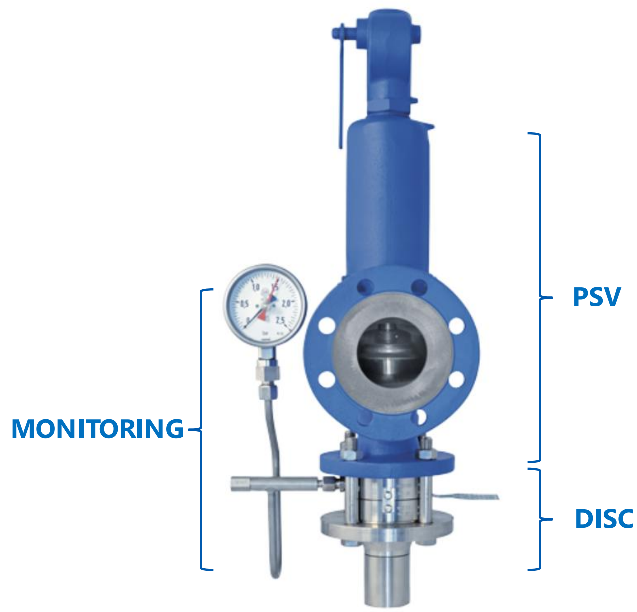

Figure 7-1 Pressure Relief Valve in Series with a Rupture Disc

Nonetheless, the theoretical benefits of the series installation may not be fully realized.

- Given the odd geometry of the detection instrument, this location may require a separate heat trace zone; i.e., heat trace cable, control thermocouples, and thermal insulation. However, the detection instrument, and the associated heat tracing, is not critical to the operation of the plant. As such, this is one location in the plant that 1) might easily be ignored by the maintenance staff, and 2) should it stop working, no one knows that it stopped working.

- If the heat tracing on the detection instrument stops working, or if the insulation on the detection instrument becomes damaged, then the detection instrument can act like a thermal fin. This has to potential to freeze the salt in the stagnant zone between the rupture disc and the relief valve, which would prevent the proper functioning of the relief valve. Salt equipment, with stagnant conditions and small physical dimensions, is almost a guarantee of salt solidification.

Providing a rupture disc in series with a pressure relief valve will eliminate problems with salt weeping through a relief valve. However, the benefits are likely to be temporary. At some point, problems will develop with the rupture disc, the detection instrument, or both, and the theoretical benefits of investing in the rupture disc will be lost.

The design with the highest reliability is likely to be a pressure relief valve. When the valve starts to develop an internal leak, the maintenance staff will have an additional task regarding salt collection from the discharge piping downstream of the valve. However, the additional task will be temporary. The leakage will persist only until the plug and the seat can be resurfaced when the valve is removed for periodic recalibration.

7.7.5 Energy Involved in the Flow Downstream of a Relief Device

The piping downstream of a pressure relief device must be directed to a safe location. Depending on the size of the relief device, the safe location could be a dedicated concrete pit or one of the main storage tanks. In either case, the relief device is discharging to ambient pressure, and all of the pressure head upstream of the device is converted to a velocity head downstream of the device.

At a proposed commercial project, a pressure relief device, located near the discharge of a salt pump, is required to protect a downstream heat exchanger. The relief pressure in this example is 16 bar. With a downstream pressure of 1 bar, the pressure differential of 1,500,000 Pa is converted to kinetic energy with a nominal velocity of 40 m/sec.

Since the relief device is located near the salt pump, the relief device is likely to discharge back to the salt tank. The mass flow rate through the relief device will depend on the H-Q curve of the pump. However, the kinetic energy in the flow returning to the storage tank will be a large value. The kinetic energy is eventually converted to heat in the storage tank, but the amount of energy to be dissipated is such that the conversion device must be robust and not a design afterthought.

8. Piping in Salt Service

In parabolic trough projects using organic heat transfer fluids, both the cold salt and the hot salt piping will be carbon steel, with a typical specification of ASTM A106, Grade B or C.

In parabolic trough plants using inorganic heat transfer fluids, and in central receiver projects, the hot salt piping will be a 300-series stainless steel. The principal candidate materials include Type 304L, 316L, 304H, 316H, and 347H. The 'L' signifies a low carbon alloy, with a maximum carbon content of 0.02 percent. The 'H' signifies a high carbon alloy, with a minimum carbon content of 0.04 percent. Adding carbon to the alloy disrupts the lattice structure, which improves the resistance to creep.

The design temperature in both types of plants is above 538 °C. As such, if the allowable stress values for the piping are to be obtained from Subpart 1 in Section II D of the Code, then the 'H' grades of stainless steel will be required. For example, in Subpart 1, Type 304L is not permitted for equipment designed to Section III or to Section VIII Division 1 at temperatures above 427 °C due to the potential for dimensional changes due to permanent deformations. In contrast, ASME B31.3 lists allowable stresses for the 'L' grades of stainless steel piping for temperatures up to 815 °C.

8.1 Type 304H and Type 316H

At temperatures in the range of 500 to 600 °C, the carbon in Type 304H and Type 316H reacts with chromium to form chromium carbide. The carbide is preferentially formed at the grain boundaries, as there is space in the matrix to do so. This results in a reduction in the corrosion resistance of the alloy at the grain boundaries. If the alloy is exposed to a combination of chlorides (present in the salt), tensile stresses, and liquid water, then cracks can start to develop between the grain boundaries. Once the cracks start to develop, the process cannot be stopped, even if the liquid water is removed. This type of corrosion is known as intergranular stress corrosion cracking.

With the plant in normal service, the metal temperatures never fall far enough for the pipe to be exposed to liquid water. This, in and of itself, is enough to prevent intergranular stress corrosion cracking. However, the pipes can be exposed to liquid water if, during an outage, the equipment cools to ambient conditions, and then 1) it rains, or 2) nighttime temperatures fall below the dew point. Under these conditions, intergranular stress corrosion cracking can develop.

8.2 Type 304L and Type 316L

One method for reducing the potential for intergranular stress corrosion cracking is to use an 'L' grade of stainless steel. With a low carbon content, the potential to form chromium carbide is reduced. This, in turn, limits the depletion of chromium at the grain boundaries, which preserves the resistance to corrosion at the grain boundaries. However, the low carbon content reduces the resistance to creep, which can lead to dimensional changes due to permanent strains.

The allowable stresses for Types 304 L and 316L, at a temperature of 565 °C, are shown in Table 8-1. Also shown for reference are allowable stresses for Types 304H, 316H, and 347H.

Table 8-1 Allowable Stresses (MPa) for 300-Series Stainless Steel Piping at 565 °C

Type	Section II D, Subpart 1	B31.3
304L	Not permitted	43.4
316L	Not permitted	74.5
304H	85.5 [1], 69.6 [2]	84.1
316H	104.1 [1], 77.2 [2]	100.0
347H	111.7 [1], 92.4 [2]	117.9

Notes:

1. Use of these stresses may result in dimensional changes due to permanent strain.
2. Lower allowable stress to reduce the potential for dimensional changes.

The principal penalty to the use of an L-grade material for piping is a lower allowable stress, which translates to thicker wall sections. Since piping is typically priced on $/kg commodity basis, and since the unit prices for Types 304, 316, and 347 all fall within a similar range, selecting an L-grade material increases the cost of the piping by factors in the range of 20 percent to 150 percent.

It can be noted that there is some experience with the use of 304L for hot salt piping. At the Solar Two central receiver project, the design of the downcomer was developed using the properties of an H-grade stainless steel. However, the downcomer was fabricated using 304L, and the mismatch was discovered only after the downcomer had been installed. Rather than replace the downcomer with an H-grade material, the pipe stress analysis was repeated, but with iterations on the supports and the anchors until the stresses reached allowable values. During the (limited) 3-year life of the demonstration project, the downcomer operated as intended.

8.3 Type 347H

To avoid potential problems with intergranular stress corrosion cracking, most commercial projects have adopted Type 347H as the hot salt piping material. The alloy is essentially Type 304H with the addition of niobium. The niobium bonds with the carbon in the matrix to form niobium carbide. This reduces the quantity of free carbon available, which, in turn, reduces the potential for the formation of chromium carbide. If the chromium carbide concentration is reduced, then the potential for intergranular stress corrosion cracking is also reduced.

8.3.1 Knife Line Attack

Nonetheless, the alloy is not without its own set of problems. During welding, the metal temperatures are high enough to dissolve the niobium carbide. This makes available free carbon in the matrix. As the weld cools, the metal temperatures initially favor the reformation of niobium carbide. However, the weld typically cools at a rate that does not allow the equilibrium concentration of niobium carbide to form. Free carbon remains available in the matrix, which then allows chromium carbide to form as the weld continues to cool.

The welding process often results in 5 metal chemistry zones. Zones 1 and 5 are the original parent metal, to the left and to the right of the heat affected zone. Zone 3 is the center of the weld, where the concentration of niobium carbide is relatively high. Zones 2 and 4, which are in the heat affected zone, tend to have low concentrations of niobium carbide, but relatively high concentrations of chromium carbide. Zones 2 and 4 can then be susceptible to intergranular stress corrosion cracking in a phenomenon known as knife line attack. Knife line attack has been observed in Type 347H pipe fittings at the 10 MWe Solar Two demonstration project, and in Type 321H receiver tubes at a parabolic trough test facility in Spain.

8.3.2 Post Weld Heat Treatment of Type 347H

To reduce the potential for knife line attack, the weld can undergo a post weld heat treatment. The heat treatment involves the following steps:

- The residual weld stresses are partially relieved by raising the metal temperature to a nominal value of 650 °C. The goal is to reduce the potential for hot reheat cracking. Hot reheat cracking is a phenomenon in which the interior of the grain becomes strengthened by the precipitation of carbides during welding. Relaxation of residual stresses then occurs in the form of creep deformation at the grain boundaries, which can lead to cracking along the boundaries

- After a hold period for stress relaxation, the welds are solution annealed. The metal temperatures are raised high enough (~1,150 °C) to dissolve both the chromium carbide and the niobium carbide

- The metal temperature are held for a period which is long enough (~1 hour) for the equilibrium concentration of niobium carbide to form. This process reduces, but does not eliminate, all of the free carbon; i.e., there is an equilibrium concentration of niobium carbide, chromium carbide, and free carbon.

- To reduce the potential for chromium carbide formation with the remaining free carbon, the weld zone is cooled rapidly through the temperature range which preferentially forms chromium carbide.

As might be expected, the heat treatment process is time consuming and not without expense. Further, the process is conducted outdoors, and if the time-temperature requirements cannot be accurately met, then it is possible to develop cracks at the weld or to increase, rather than decrease, the concentrations of chromium carbides.

8.4 Project Decisions

The candidate piping materials, in order of probable commercial preference, are as follows:

- Type 347H: The material offers 1) the highest allowable stress among the 300-series stainless steels, which results in the lowest piping mass and installed costs, and 2) the addition of niobium to the alloy reduces the potential for intergranular stress corrosion cracking that can occur in the other H-grade stainless steels. The principal liability is a (relatively low) risk of knife line attack should the piping be exposed to liquid water.

- Type 304L / 316L: Due to the low carbon content, the material is largely immune to intergranular stress corrosion cracking, and due to the absence of niobium, the material is largely immune to knife line attack. The principal liabilities are relatively low allowable stresses, which result in an increase in the pipe mass and the installed cost.

- Type 304H / 316H: The allowable stresses for 304H / 316H are higher than the values for the L-grade materials, but somewhat less than the values for Type 347H. As such, the mass of the piping and the installed cost should fall between these cases. The principal liability is a susceptibility to intergranular stress corrosion cracking should the pipe be exposed to liquid water during a maintenance outage.

Type 347H may be the preferred piping material, for the reasons noted above. Nonetheless, the project must make a decision as to whether, or not, to perform a post weld heat treatment of the piping.

There is no mandatory requirement to perform a heat treatment, as the Code does not require the heat treatment of stainless materials. Further, anecdotal evidence from commercial projects indicates that the reliability and the availability of welds that receive a heat treatment are essentially the same as the reliability and the availability of welds that do not receive a heat treatment. Nonetheless, there may be a benefit to performing a heat treatment, as follows:

- Hot reheat cracking can occur in the heat affected zones of weld when reheated in the temperature range from 500 to 700 °C [47]. At this temperature, residual stresses due to welding relax by creep. The heat affected zone may not be able to accommodate this strain without cracking if the microstructure had been sufficiently altered during welding. Pipe temperatures above 565 °C are not expected during normal plant operation. However, metal temperatures in the range of 600 to 700+ °C can be expected if a heat trace circuit has a lengthy duty cycle of 100 percent due, for example, to a contactor sticking in the closed position. A post weld heat treatment might allow the welds in this zone to avoid hot reheat cracking associated with an infrequent, but not unexpected, failure in the heat trace system.

- During the life of the project, the probability that the hot salt piping will be cooled to ambient temperature, and then opened to the ambient, during a maintenance outage is perhaps one-half to two-thirds. The exposure could result from repairs to a valve, inspection of a heat exchanger, or replacement of a pressure transmitter. During this time, liquid water could come into contact with the inside of the pipe due to rain, water leakage from a steam generator heat exchanger, or from ambient temperatures below the dew point. In addition, salt leakage from valve stem seals or from gaskets on pressure transmitters can expose both the insulation and the exterior of the pipe to salt. If the insulation is removed for replacement, liquid water can come into contact with the outside of the pipe due to rain or ambient temperatures below the dew point. In each case, a post weld treatment of the welds will reduce the potential for knife line attack at the edges of the welds.

In the final analysis, a post weld heat treatment can reduce the risk of hot reheat cracking and intergranular stress corrosion cracking. Nonetheless, in the absence of a post weld heat treatment, the potential for hot reheat cracking and intergranular stress corrosion cracking is generally regarded as low to moderate. The project will need to conduct a cost / benefit analysis to determine if the costs and the risks of post weld heat treatments justify the benefits of the heat treatments.

8.5 Pipe Maintenance

Once the plant enters commercial service, the salt piping, valves, and instruments will have been exposed to salt. When this equipment requires maintenance, the equipment will be cooled to ambient temperature. As such, the equipment can be exposed to liquid water if the metal temperature falls below the dew point, if it rains, or if the equipment is cleaned with water.

Carbon steel, in contact with nitrate compounds and liquid water, can develop stress corrosion cracking, as discussed above in Section 4.2. Stainless steel equipment, in contact with the chlorides in the salt, can develop intergranular stress corrosion cracking, as discussed in Section 5.16.1.

---

[47] Auzoux, Q., et al, (CEA Saclay DEN/DMN/SRMA Yvette, France), "Reheat cracking in austenitic stainless steel", 2001, https://www.osti.gov/etdeweb/servlets/purl/20401493

To reduce the potential for atmospheric condensation, the temperature of the equipment can be maintained above the dew point by means of portable electric or propane-fired air heaters. Temporary tarps or tents can limit the exposure of the equipment to rain. Further, water in any form, including distilled water, must not be used to remove residual salt from the equipment. If the equipment must be cleaned prior to further work, such as welding, then only mechanical methods should be used.

9. Electric Heat Tracing

As discussed in Volumes 1 and 2, the electric heat tracing uses mineral insulated cables, electronic contactors, and pulse width control.

9.1 Design Criteria

Heat tracing is an expensive item, and there is an economic incentive to install as little heating capacity as possible.

The absolute minimum capacity would be one which maintains the equipment at the salt melting temperature (240 °C) at the design minimum ambient temperature and at the design plant operating wind speed. However, any reduction in the output from the heat tracing, or any degradation in the insulation, will result in equipment temperatures below the freezing point of the salt.

Some commercial projects have adopted a piping design criteria based, in part, on maintaining a metal temperature of 275 °C at the minimum design ambient temperature. This criterion is, in effect, an infinite preheat period. As an example, a DN300 (12 in.) line with 125 mm (5 in.) of calcium silicate of insulation requires a heat input of 185 W/m to maintain a temperature of 275 °C at an ambient temperature of 10 °C. However, in a commercial project, the pipe insulation is subject to damage due, for example, to maintenance personnel walking on the pipe. If the insulation is compressed by 25 mm (1 in.), then the local thermal resistance is reduced, and the steady state temperature which can be maintained by the heat trace drops to 232 °C. Similarly, the insulation can develop gaps due to daily thermal expansion and contraction cycles. If the local effective thermal conductivity of the insulation increases by 20 percent, then the steady state temperature which can be maintained by the heat tracing falls to 230 °C. In either situation, if stagnant salt is present in the line, then local freezing can be expected. Further, the heat tracing can no longer raise the pipe metal temperature above the freezing point, and the line will remain plugged until repairs are made to the insulation. When the plant is new, the pipe insulation will provide the required thermal resistance, and the heat trace system will be judged to be adequate. However, as the plant ages, the pipe insulation will degrade, and availability problems with frozen salt lines will start to appear.

A more robust design criterion is a preheat period of, for example, 12 hours. Continuing with this example, preheating the pipe to 275 °C in 12 hours requires a heat input of 354 W/m, or nominally double the heat input if the preheat period is infinite. With a heat input of 354 W/m, the steady state temperature of the pipe increases from 275 °C, as above, to a new value of 516 °C. Further, if the insulation is compressed by 25 mm, then the steady state pipe temperatures can, in principle, be raised as high as 435 °C. Similarly, if the effective thermal conductivity of the insulation increases by 20 percent due to gaps in the insulation, then the pipe temperatures can be raised to a theoretical value of 430 °C. It's unlikely that the duty cycles of the heat trace system would be set so high as to produce pipe temperatures as high as 430 °C, but the available heating capacity would be sufficient to both prevent freezing and to thaw a line should freezing occur. As such, the heat trace system will be adequate both when the plant is new and after the plant has accumulated decades of commercial use.

For a specific project, the preheat time would be selected based on a range of parameters, including the definitions of the plant operating states, the heat trace zone boundaries, the defined transition times between operating states, the importance of a particular zone in terms of plant availability, the installed cost of the heat trace system, and the difficulties in accessing the heat trace zones for maintenance of both the cables and the pipe insulation.

In general, the optimum heat trace preheat period has yet to be identified. A preheat period of 8 hours provides a robust system, but likely results in a system which is more expensive than can be justified. However, the preheat period should not be more than 24 hours, as the margins against insulation degradation are likely insufficient if a commercial project is to reach its availability targets over a time span of decades.

9.2 Control Software Location

Essentially all heat trace suppliers provide a standalone, and often proprietary, programmable logic controller to control the duty cycles of the heat trace cables. The alternate control approach is to use the plant distributed control system for this function. In most commercial projects, the former approach is selected over the latter in terms of convenience, purchase price, and programming price. Nonetheless, the latter is generally preferred over the former, for the following reasons:

- The selection of which heat trace circuits, and the selection of the duty cycles for each circuit, can be readily adjusted based on the plant operating state. This, in turn, reduces the annual demand for auxiliary electric energy, and makes for more stable operating temperatures in each zone

- The control system data historian can be used for the analysis of the heat trace system and the diagnosis of temperature control problems

- Alarms are transmitted directly to the control system operator screens. This avoids the need for an operator to move from an operator station to the heat trace vendor's console to analyze an alarm. This, in turn, makes it more likely that prompt responses will be made to each alarm.

At the Solar Two demonstration project, the original heat trace system installation used a proprietary programmable logic controller supplied by the system vendor. However, modifications to the heat trace components were made over the course of the project, and the control responsibilities were shifted from the vendor equipment to the distributed control system. This arrangement incurred expenses for adding input / output points to the control system. However, the benefits of improved convenience for the operators, improved accuracy in maintaining the zone temperature set points, faster diagnoses of unusual system characteristics (such as valve leakage), and a reduction in auxiliary energy demand more than offset the marginal expense to the control system.

In a commercial project, incorporating the heat trace control into the distributed control system will involve a large number of input and output signals. This, in turn, will increase the cost of the distributed control system. To reduce the change in price, a hybrid control approach may be possible, as follows:

The standard controller provided by the vendor receives inputs from the circuit thermocouples, compares the zone temperatures with the set point temperatures, and sends output signals to the contactors supplying electric power to the heat trace cables

The distributed control system contains the logic for changes to the set point temperatures, and the activation / deactivation of zones based on the plant operating mode

As mentioned in volume 2, all that can be achieved still maintaining vendor PLCs for control of circuits and temperature measurements, and having then a fiber optics communication link to DCS which can be used to send all signals in the PLC. The logics on set-point changes and zones activation/deactivation can reside in the DCS, and also the full historian with everything available in the PLC. The PLC would only have the logics for start/stop when temperature setpoint is reached, hysteresis, and errors management.

9.3 Cable Redundancy

Inquires with heat trace cable suppliers on the topic of cable failure rates indicate that the cables should last the life of the project. However, commercial experience has shown that cable lifetimes are often measured in years, rather than decades. The relatively short lifetimes can be due to the following effects:

- Flexing of the cables produced by the daily thermal expansions and contractions of the piping
- High operating temperatures if the circuit controls mistakenly operate the cables at a duty cycle of 100 percent for extended periods
- High operating temperatures if the zone control thermocouple is located in an incorrect position, or if the thermal insulation around the thermocouple is damaged.

Further, the cable lifetimes can as short as days or weeks if the cables are exposed to salt from a leaking valve stem or from a leaking instrument connection. The cables, when active, can produce surface temperatures in excess of 650 °C. At these temperatures, salt in contact with the cable will quickly decompose, producing NOx and various oxides. The oxides are particularly corrosive, and will corrode the common sheath materials of stainless steel and Inconel. After this happens, the heating elements are exposed to water vapor in the air, and the elements soon fail.

In many commercial projects, the design criteria for the heat trace system often include a provision for only 1 installed redundant cable, regardless of the pipe size and the number of active cables needed to satisfy the preheat requirements. However, if the lifetimes of the cables are measured in, under ideal circumstances, years, then most of the heat trace zones will be forced to switch to the redundant cable in the first years of plant operation. Further, the zones will be unable to meet the heat trace design requirements starting in perhaps year 10 of commercial service. If a salt leak occurs, then the cable lifetimes can be two to three orders of magnitude shorter.

If a zone has only 1 redundant cable, then the loss of 2 cables on a small line (< 10 in.) means that the heat trace can no longer prevent the salt from freezing in a stagnant line. The loss of 2 cables on a large line means that the zone can no longer satisfy the required preheat time from ambient. In both cases, the only solution is to remove the insulation from the lines, replace the failed cables, and reinstall the insulation. Depending on the location of the zone, and the length of the zone, the repair process could require a forced outage lasting between 1 day to 2 weeks. For a nominal 125 MWe project, this could incur a loss in revenue of $150,000 to $2,000,000.

For a specific project, an economic analysis should be conducted to determine the optimum number of installed redundant cables. The analysis should include the following considerations:

- Experience with cable failure rates on commercial projects, rather than projected cable lifetimes offered by the heat trace supplier

- Susceptibility to a salt leak, including the number of valves in the zone, the type of stem seal on the valves (bellows or packing), and the number of instruments in the zone using flanged connections

- Zone location, zone dimension, and access for repair. For example, the riser and downcomer piping in the tower of a central receiver project generally have poor accessibility, and the number of redundant cables is likely to be a higher number than for a short zone consisting of horizontal piping at grade.

- Effect on the plant availability of a failed cable, including longer preheat periods for an empty line, or the thawing time for a frozen pipe

- Installed cost of redundant cables.

In general, the optimum number of installed redundant cables has yet to be identified, and the number is likely to be a function of the characteristics of the zone. Nonetheless, the following values for redundancy may, in the long run, prove be representative:

- 100 percent for zones 1) with valves using conventional stem packings, and 2) with instruments with flanged connections

- 50 percent for zones 1) with valves using bellows stem seals, and 2) without instruments.

9.4 Control Thermocouples

In many commercial projects, 2 thermocouples are installed in each zone for temperature monitoring and control. In some cases, one of the thermocouples is an installed spare. As such, the temperature measured at the thermocouple is taken to be the temperature along the entire length, and around the entire circumference, of the zone.

Clearly, this is a simplified version of the actual conditions. Depending on the pattern of the cables installed in the zone, and depending on the location of the control thermocouple, local zone temperatures can differ from the measured zone temperature by as little as 1 °C to more than 150 °C. These deviations can be above, or below, the zone set point temperature.

Further, if the control thermocouple of Zone 1 is close to Zone 2, then the control of the heat trace circuits in Zone 1 can be determined by the temperature in Zone 2. At one commercial project, this led to a situation in which the heat trace cables, on a section of carbon steel piping, operated with a duty cycle of 100 percent. Within a few weeks, the pipe section failed. A postmortem examination estimated that metal temperatures exceeded 500 °C, which produced rapid oxidation of the steel.

In general, using 1, or in some cases 2, thermocouples for zone temperature control may not be adequate. The number of thermocouples should be based on the following:

- For long zones downstream of isolation valves, vent valves, drain valves, and pressure relief valves, multiple thermocouples are useful for identifying leakage patterns and the potential for frozen plugs

- For long zones with multiple pipe supports and anchors, multiple thermocouples are useful for identifying local areas with low pipe temperatures due to the higher heat losses at the supports and the anchors

- For short zones connected to other short zones, multiple thermocouples are useful for controlling each zone independently of the adjacent zones

- For carbon steel lines, multiple thermocouples are useful for identifying local areas with metal temperatures above the set point value. This, in turn, reduces the potential for overheating and damage due to corrosion.

Adding thermocouples, including the wiring back to the DCS, is not without expense. However, the ability to analyze the temperature profiles throughout a zone has proven to be useful in preventing local freezing, preventing local overheating, and in diagnosing the events leading to an outage.

Thermocouples should be added to a zone until the marginal cost of the thermocouple exceeds the marginal revenue associated with the expected increase in plant availability.

10. Designs for Demonstration Projects

System designs for demonstration projects may have different goals than system designs for commercial projects. For example, the goal for a pumped heat storage concept may be the demonstration of the concept, while the goal of a commercial project may be, in part, an availability of 92 percent. As such, a demonstration project may sacrifice features such as redundancy in what is likely to be a program with tight budget constraints.

Malta is proposing a pump heat storage concept that uses nitrate salt as the high temperature storage media. One potential method to reduce costs is to use the cold salt pump as an emergency backup for the hot salt pump, and to use the hot salt pump as an emergency backup for the cold salt pump. In principle, this would allow 2 pumps to perform the same duty as 4 pumps (i.e., two 100-percent cold salt pumps, and two 100-percent hot salt pumps).

One variation for the design is illustrated in Figure 10-1. Salt from the cold tank flows by gravity to a cold pump sump located below grade. The level in the sump is maintained by a control valve in the line from the tank to the sump. A similar arrangement is used for the hot salt. The two sumps are connected by a jumper line, which is located above the normal liquid levels in the two sumps.

During normal operation, the project is in either charge mode, with the cold salt pump running, or is in discharge mode, with the hot salt pump running. The liquid levels in the two sumps remain below the level of the jumper line.

10.1 Transfer of Pump Operation

If there is a failure of the cold salt pump during a charge period, then the level in the cold sump will rise, and salt will flow from the cold sump to the hot sump through the jumper line. The hot salt pump is started, and acts as a surrogate for the cold salt pump by changing valve positions in the pump discharge lines. Naturally, sending cold salt into the hot sump will cause a decay in the sump temperature, and impose some level of thermal shock on the hot pump. The mass of salt in the hot sump, in combination of the methods selected for mixing within the hot sump, will determine the rate of temperature change for the hot pump. The rate of change in the sump temperature must be consistent with the allowable rate of change specified by the pump vendor. If the rate of change in the sump temperature is greater than the allowable rate, then the pump bowls will thermally contract relative to the shaft, which can lead to rubbing or seizure.

Similarly, if there is a failure of the hot salt pump during a discharge period, the cold salt pump can act as a surrogate for the hot salt pump. The limitations on allowable rate of temperature change for the cold pump also apply.

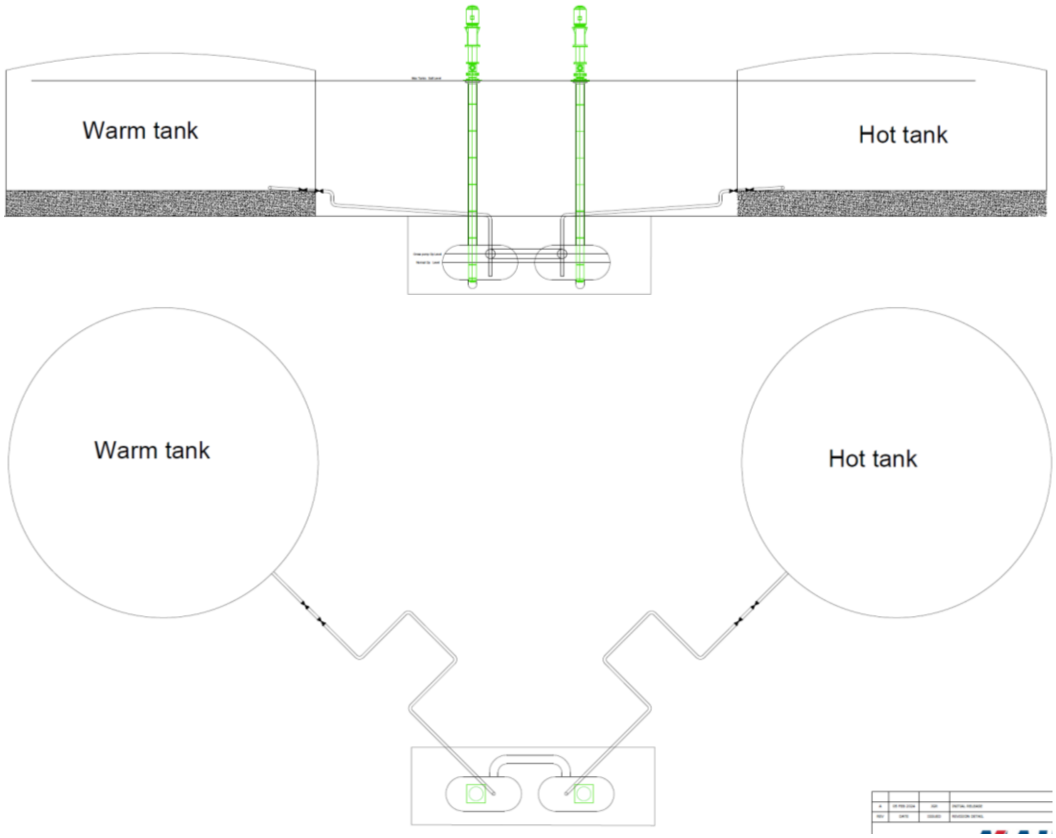

Figure 10-1 Below Grade Pump Sumps with Extended Pumps

10.2 Extended Pumps

The concept of a pump sump, located below grade and fed by gravity from the main storage tanks, was successfully demonstrated at the Solar Two demonstration project. Nonetheless, there was an instance where the level control for the hot sump did not perform as intended and the sump flooded. Salt leaving the sump saturated the mineral wool insulation on the sump, and thermally shocked the concrete in the pit, leading to spalling. In all, the damage was relatively minor. However, had the overflow not been detected and stopped, then the entire concrete pit would have filled with salt. Since there was no method to remove the salt from the pit as a liquid, the only option available would be to allow the salt to freeze, and then remove the solid salt using jackhammers. The time required for the salt to freeze was probably on the order of weeks, and the duration of the forced outage to remove the salt, and make repairs to the pump sump insulation and insulation, may have been on the order of 2 to 3 months.

In a commercial project, the dimensions of the pump sump and pit would be larger, and the time to recover from a sump overflow would certainly be measured in months. Although the probability of this situation would be regarded as low, the financial consequences of a multi-month outage would be significant. To avoid this financial risk, commercial projects use salt pumps supported on structures above the main storage tanks. The pumps have extended shafts and draw suction from locations just above the floor of the tank.

In the conceptual layout shown in Figure 10-1, pumps with extended shafts are shown. The throttle bushing near the top of the pump column is located above the maximum liquid level in the storage tanks. In addition, the design pressure for the pump sump is equal to the maximum static head in the storage tanks. If there is a failure in the level control system for the pump sump, the associated pump will trip, and the static pressure in the sump will rise to the static pressure in the storage tank. However, the idled pump will not overflow due to the elevated location of the throttle bushing. Nonetheless, there are some complexities with this arrangement: a structure will need to be provided to support the pumps; and a comprehensive heat tracing and insulation concept will be required to maintain the required temperatures on the pump columns (particularly the hot pump).

10.3 Conventional Pumps

If extended pumps are replaced with pumps of a more conventional length, some of the complexities associated with structural support and temperature maintenance can be reduced. A potential arrangement is illustrated in Figure 10-2.

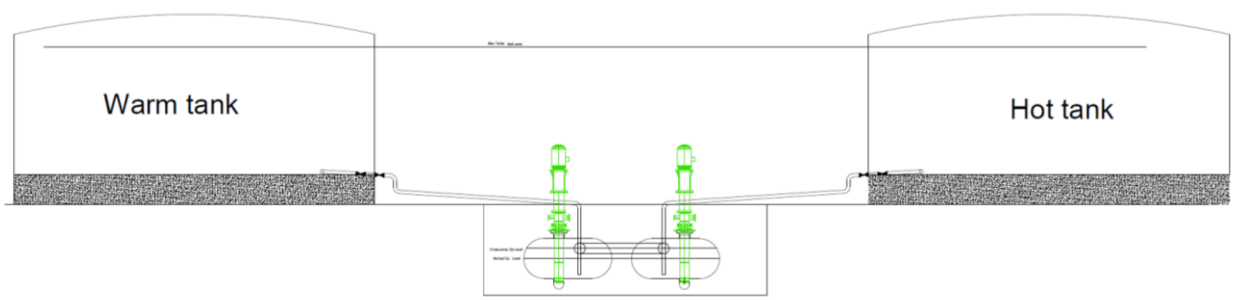

Figure 10-2 Below Grade Pump Sumps with Conventional Pumps

The shorter pumps may also offer a better ability to accommodate transient thermal stresses and a lower capital cost. However, the throttle bushings at the tops of the pumps are located below the maximum liquid level in the tanks. As such, if there is a failure in the sump level control system, it is possible to flood the sumps and flow salt into the sump pit.